



## Copyright Undertaking

This thesis is protected by copyright, with all rights reserved.

**By reading and using the thesis, the reader understands and agrees to the following terms:**

1. The reader will abide by the rules and legal ordinances governing copyright regarding the use of the thesis.
2. The reader will use the thesis for the purpose of research or private study only and not for distribution or further reproduction or any other purpose.
3. The reader agrees to indemnify and hold the University harmless from and against any loss, damage, cost, liability or expenses arising from copyright infringement or unauthorized usage.

### IMPORTANT

If you have reasons to believe that any materials in this thesis are deemed not suitable to be distributed in this form, or a copyright owner having difficulty with the material being included in our database, please contact [lbsys@polyu.edu.hk](mailto:lbsys@polyu.edu.hk) providing details. The Library will look into your claim and consider taking remedial action upon receipt of the written requests.

GAIT REGULATION IN INDIVIDUALS  
WITH UNILATERAL TRANSFEMORAL  
AMPUTATION: FROM NEURAL  
DYNAMICS TO MOVEMENT  
COORDINATION

HU MINGYU

PhD

The Hong Kong Polytechnic University

2024

The Hong Kong Polytechnic University  
Department of Biomedical Engineering

Gait Regulation in Individuals with Unilateral  
Transfemoral Amputation: from Neural  
Dynamics to Movement Coordination

Hu Mingyu

A thesis submitted in partial fulfilment of the requirements for  
the degree of Doctor of Philosophy

October 2023

## **CERTIFICATE OF ORIGINALITY**

I hereby declare that this thesis is my own work and that, to the best of my knowledge and belief, it reproduces no materials previously published or written, nor material that has been accepted for the award of any other degree or diploma, except where due acknowledgement has been made in the text.

\_\_\_\_\_ (Signed)

HU MINGYU (Name of student)

## **ABSTRACT**

Individuals with unilateral transfemoral amputation (uTFA) exhibit asymmetric gait patterns when wearing a prosthesis. Understanding prosthetic gait patterns could benefit prosthetic gait rehabilitation and the development of prostheses. However, the current methods of gait analysis and evaluation rely solely on biomechanics and are primarily focused on assessing the performance of an individual joint. This might lead to two major issues when comprehending the gait patterns of individuals with uTFA. Firstly, prosthetic gait is the result of changes in movement regulation from the central nervous system (CNS) driven by neural plasticity. Focusing on biomechanics solely might neglect the contribution of neural dynamics. Secondly, the movement of the prosthetic limb is commonly compensated by the intact limb or interactions among several segments of the prosthetic limb. Attention on a single joint might overlook the coordination between lower limb segments. Current studies on the gait of individuals with uTFA ignore the two issues, resulting in gaps in understanding gait patterns in individuals with uTFA.

Therefore, the purpose of this project was to understand the gait patterns of individuals with uTFA from neural dynamics to their lower limb coordination. The scopes of this

project included the investigation of (1) Walking coordination wearing a prosthesis in individuals with uTFA; (2) Sprinting coordination wearing a running-specific prosthesis in individuals with uTFA; (3) Connectivity between neural dynamics and coordination during walking in individuals with uTFA.

Before conducting the three studies, continuous relative phase (CRP), the method of evaluating movement coordination was reviewed. A systematic review regarding the application of CRP in competitive movements (running and jumping) was conducted following the preferred reporting items for systematic reviews and meta-analysis (PRISMA) guidelines. In total, 381 studies from 1999 to 2020 were preliminarily found with 26 studies finally included for quality assessment. Results revealed that CRP related tools found significant changes induced by factors such as pathological conditions, gender, age, experience, footwear, treadmill variations, and insoles. According to the reviewed studies, the CRP approach is useful for assessing internal (task-related) and external (environmental/equipment-related) changes in coordination (self-biological). To better comprehend movement coordination, the CRP model might be constructed using segment angles rather than joint angles.

In the first study, fourteen participants with uTFA and their age-matched able-bodied (AB) individuals were included. Segment and joint angles from the participants' lower extremities were obtained and analysed during walking. CRP values were then calculated from segment angles for both the thigh-shank and shank-foot segments. Coordination patterns revealed compensatory strategies in two legs. For CRP in thigh-shank, different coordination features were observed in the stance and swing phases. However, both groups exhibited similar overall coordination throughout the gait cycle (GC). In the shank-foot coupling on the intact limbs of individuals with uTFA, a brief foot-leading pattern was found during mid-stance. This was a distinct contrast to other limbs, likely due to compensating for the reduced force from the prosthetic limbs. The study provides standard coordination patterns for walking in individuals with uTFA, potentially aiding in the rehabilitation of prosthetic gait and prosthesis advancement.

In the second study, a group of seven participants with uTFA sprinted on a 40-metre track. This study measured parameters such as spatial-temporal, segment and joint angles of the participants with uTFA. CRP analysis was applied to shank-foot and thigh-shank couplings. The asymmetry ratios were then calculated for these metrics. The analysis identified notable variances between the intact and prosthetic limbs in terms of

proportion of the stance phase, stance duration, ankle joint angles, and CRP of the shank-foot coupling in uTFA participants. These differences mainly come from the contrasting structures of the prosthetic and intact limbs of participants with uTFA. In terms of coordination, even while noticeable coordination differences were observed in stance and swing phases, the global coordination in the coupling of thigh-shank segments exhibited no marked difference between the lower limbs of uTFA participants. The findings suggest that individuals with uTFA employ diverse adaptive strategies within the coupling of thigh-shank segments throughout the GC, targeting improved limb coordination symmetry.

In the third study, twelve individuals with uTFA and their age-matched AB individuals were recruited. The neural dynamics were recorded using a 64-channel (electroencephalograph) EEG cap. The motion data was collected with the EEG data simultaneously. After removing artifacts and calculating CRP parameters, the correlation between coordination patterns and neural dynamics was investigated. Results showed a strong correlation between neural dynamics and coordination on the intact limb during both stance and swing phases, while no correlation was found in the prosthetic and two limbs of AB individuals. Findings might suggest that the CRP



method is effective in revealing activities from CNS. The intact limb might be dominated by the brain directly, while the central pattern generators (CPGs) control the lower limbs of AB individuals. Forcing the prosthetic limb to mimic the movement of the intact limb might not be reasonable, since the origin of the gait pattern generators is different between the two lower limbs.

In conclusion, the prosthetic and intact limb of individuals with uTFA demonstrated different coordination patterns and neural dynamics during gait compared with the AB individuals. Due to the different origins of the prosthetic and intact limbs' gait pattern generators from the CNS, prosthetic designers should not simply mimic the function of an intact limb when creating a prosthetic limb. The knowledge gained from this research has the potential to greatly benefit prosthetic gait rehabilitation and development, leading to more personalised and effective therapies for individuals with uTFA.

# PUBLICATIONS

## Journal papers from this thesis

**Mingyu Hu**, Toshiki Kobayashi, Jin Zhou, Wing-Kai Lam. (2021) Current application of continuous relative phase in running and jumping studies: a systematic review. **Gait & Posture**, 90, 215-233. [Chapter 2]

**Mingyu Hu**, Yufan He, Genki Hisano, Hiroaki Hobara, Toshiki Kobayashi. (2023) Coordination of Lower Limb During Gait in Individuals With Unilateral Transfemoral Amputation. **IEEE Transactions on Neural Systems and Rehabilitation Engineering**, vol. 31, pp. 3835-3843, 2023, doi: 10.1109/TNSRE.2023.3316749. [Chapter 4]

**Mingyu Hu**, Toshiki Kobayashi, Genki Hisano, Hiroto Murata, Daisuke Ichimura, Hiroaki Hobara. (2023) Sprinting performance of individuals with unilateral transfemoral amputation: compensation strategies for lower limb coordination. **Royal Society Open Science**. 2023;10(3):221198. Published 2023 Mar 8. doi:10.1098/rsos.221198 [Chapter 5]

**Mingyu Hu**, Yufan He, Wing-Kai lam, Hiroaki Hobara, Fan Gao, Toshiki Kobayashi. (2023) Connectivity between neural dynamics and lower-limb coordination during gait in individuals with unilateral transfemoral amputation. **IEEE Transactions on Neural Systems and Rehabilitation Engineering**. (Under review) [Chapter 6]

Yufan He, **Mingyu Hu**, Alpha C.H. Lai, Mark W.P. Koh, Hiroaki Hobara, Fan Gao, and Toshiki Kobayashi. (2023) Gait Classifications in Individuals with Unilateral

Transfemoral Prosthesis: A Hierarchical Cluster Analysis Based on Spatiotemporal Parameters. **IEEE Transactions on Neural Systems and Rehabilitation Engineering**.

(Under review) [Chapter 6]

## **Conference proceedings**

**Mingyu Hu**, Toshiki Kobayashi, Genki Hisano, Daisuke Ichimura, Hiroaki Hobara.

Lower limb coordination during sprinting in individuals with unilateral transfemoral amputation: in the view of continuous relative phase. **(Oral presentation, online mode)**

**The 7th SRC-APOSM22**, Singapore, 8-9 October 2022.

**Mingyu Hu**, Toshiki Kobayashi, Genki Hisano, Daisuke Ichimura, Hiroaki Hobara.

Walking Coordination in Lower Limbs of Individuals with Unilateral Transfemoral Amputation. **(Oral presentation) ISPO 19th World Congress Mexico Guadalajara**,

Mexico 24-27 April 2023

Lau Wing Ki, **Hu Mingyu**, Toshiki Kobayashi. Prediction of the Functionality and Step Activity of Transtibial and Transfemoral Amputees via Telehealth: A Preliminary Study.

**(Oral presentation) ISPO 19th World Congress Mexico Guadalajara, Mexico 24-27**

April 2023

## **Other publications**

Kobayashi, Toshiki, **Mingyu Hu**, Ryo Amma, Genki Hisano, Hiroto Murata, Daisuke

Ichimura, Hiroaki Hobara. (2022) Effects of walking speed on magnitude and

symmetry of ground reaction forces in individuals with transfemoral prosthesis. **Journal of biomechanics** 130 (2022): 110845.

Abu Jor, Mingyu Hu, Mark W.P. Koh, Noelle W.K. Lau, Aliyeh Daryabor, Wing-Kai Lam, Toshiki Kobayashi. (2023) Biomechanical effects of foot orthoses on jump landing performance: a systematic review. **Prosthetics and Orthotics International**. (Under review)

Toshiki Kobayashi, Puiyui Wong, Mingyu Hu, Tsubasa Tashiro, Masanori Morikawa, Noriaki Maeda. (2022) The effects of the tension of figure-8 straps of a soft ankle orthosis on the ankle joint kinematics while walking in healthy young adults: A pilot study. **Gait & Posture** 98 (2022): 210-215.

Kobayashi, Toshiki, Mark WP Koh, Mingyu Hu, Hiroto Murata, Genki Hisano, Daisuke Ichimura, Hiroaki Hobara. (2022) Effects of step frequency during running on the magnitude and symmetry of ground reaction forces in individuals with a transfemoral amputation. **Journal of NeuroEngineering and Rehabilitation** 19, no. 1 (2022): 33.

## ACKNOWLEDGMENTS

First and foremost, I extend my heartfelt gratitude to my supervisor, Dr. Toshiki Kobayashi, for his relentless support, guidance, and mentorship throughout this journey. His insights, expertise, and feedback were invaluable in sculpting this work, and his encouragement kept me inspired at every stage.

I am deeply indebted to my co-supervisor, Prof. Ming Zhang, for his support and encouragement throughout this journey.

Special acknowledgment goes to my colleagues and fellow researchers (Yufan He, Lau Wing Ki, Mark W. P. Koh, Alpha C.H. Lai, Abu Jor) at our prosthetics and orthotics design and performance lab and also other labs (Dr. Duo Wai-Chi Wong, Tony Linwei Chen, Dr. Christina Zonghao Ma, Prof. Yongping Zheng, Celia Mei Dong) at The Hong Kong Polytechnic University.

I would also like to thank Dr. Hiroaki Hobara at The Tokyo University of Science, and Genki Hisano at the Tokyo Institute of Technology, Dr. Wing-Kai Lam at the Hong Kong Sports Institute. Dr. Jin Zhou at Sichuan University for their support on my projects. The stimulating discussions, collaborative efforts, and shared moments of both challenge and celebration added depth and breadth to my academic journey.

My profound appreciation goes out to my girl friend (Echo Shan Liu) and other friends (Wenyu Bao, Hongbing Wang, Qianru Chen, Jianing Zhang, Fuqiang Ye, Sa Zhou, Guoxin Zhang, Yinghu Peng, Fei Chen, Feilong Li) and family. To my parents, your unwavering faith in me has been a source of strength.

To everyone who played a role, directly or indirectly, in this academic endeavour, by offering insights, resources, or simply being there to listen – my sincere thanks.

This doctoral journey, laden with its challenges and triumphs, has been immensely enriched by each individual who stood by me, and for that, I am eternally grateful.

# TABLE OF CONTENTS

<b>CERTIFICATE OF ORIGINALITY.....</b>	<b>I</b>
<b>ABSTRACT.....</b>	<b>II</b>
<b>PUBLICATIONS .....</b>	<b>VII</b>
<b>ACKNOWLEDGMENTS.....</b>	<b>X</b>
<b>TABLE OF CONTENTS.....</b>	<b>XII</b>
<b>LIST OF FIGURES .....</b>	<b>XVII</b>
<b>LIST OF TABLES.....</b>	<b>XIX</b>
<b>LIST OF ABBREVIATIONS.....</b>	<b>XX</b>
<b>1. CHAPTER I INTRODUCTION .....</b>	<b>1</b>
1.1 The development of prostheses.....	1
1.1.1 Better movement performance and gait rehabilitation wearing a prosthesis.....	1
1.1.2 Prosthetic gait: functional asymmetries to compensation mechanisms	2
1.1.3 Biomechanics benefits prosthesis design and prosthetic gait rehabilitation .....	4
1.2 Gait generation in human neuromusculoskeletal system (NMSS) .....	6
1.2.1 Movement generation in human beings .....	6
1.2.2 Normal gait and prosthetic gait generation.....	7

1.2.3	Limitations in biomechanics in investigation NMSS .....	9
1.2.4	Coordination of NMSS from dynamic system theory .....	10
1.2.5	Neuron activities and movement coordination during gait.....	11
1.3	Formulation of the research question.....	12
1.3.1	Gait coordination patterns of individuals with uTFA .....	13
1.3.2	Brain activities of individuals with uTFA during gait.....	14
1.3.3	Connectivity between brain activity and coordination patterns.....	15
1.4	Objectives of the study.....	17
<b>2.</b>	<b>CHAPTER II LITERATURE REVIEW .....</b>	<b>18</b>
2.1	lower limb coordination.....	18
2.1.1	Coordination .....	18
2.1.2	Coordination evaluation.....	19
2.1.3	CRP calculation.....	20
2.1.4	CRP application and interpretation: a systematic review .....	23
2.2	Brain activities .....	57
2.2.1	Brain activities and electroencephalography during walking.....	57
2.2.2	Mobile EEG: Artifacts Removal of EEG during walking .....	58



2.3 Summary and formulation of research scope.....	60
<b>3. CHAPTER III OVERVIEW OF SUB-STUDIES .....</b>	<b>62</b>
<b>4. CHAPTER IV WALKING COORDINATION.....</b>	<b>64</b>
4.1 Summary of the study .....	64
4.2 Introduction.....	65
4.3 Method .....	68
Participants.....	68
Equipment.....	68
Data processing.....	71
Statistical analysis.....	72
4.4 Results.....	73
Kinematics .....	74
Coordination features.....	79
4.5 Discussion.....	81
<b>5. CHAPTER V RUNNING COORDINATION.....</b>	<b>88</b>
5.1 Summary of the study .....	88
5.2 Introduction.....	88
5.3 Method .....	91

Participants.....	91
Experimental procedures .....	94
Data collections and analysis .....	94
Statistics .....	98
5.4 Results.....	98
Basic kinematics and Spatial temporal parameters.....	98
Coordination .....	102
5.5 Discussion.....	103

**6. CHAPTER VI CONNECTIVITY BETWEEN NEURAL DYNAMICS AND COORDINATION.....109**

6.1 Summary of the study .....	109
6.2 Introduction.....	110
6.3 Method .....	113
Participants.....	113
Data collection and experiment protocols.....	114
Data processing.....	119
Statistical analysis.....	124
6.4 Results.....	124

Coordination pattern .....	124
ERSP and connectivity.....	127
6.5 Discussion.....	131
<b>7. CHAPTER VII CONCLUSION .....</b>	<b>136</b>
<b>REFERENCES.....</b>	<b>139</b>

## LIST OF FIGURES

Figure 1-1. Illustration of movement control in human beings and movement coordination. ....	16
Figure 2-1. PRISMA flow diagram.....	27
Figure 2-2. Summary of CRP application.....	30
Figure 3-1. Illustration of the three sub-studies .....	62
Figure 4-1. Retro-reflective marker locations and lower limb model (a) and the definition of the segment angles (b).....	70
Figure 4-2. Results of joint angles and SPM analyses.....	77
Figure 4-3. Results of segment angles and SPM analyses.....	78
Figure 4-4. Results of CRP curves and SPM analyses .....	80
Figure 5-1. Full body markers in this study. ....	95
Figure 5-2. CRP patterns and joint angles. ....	100
Figure 6-1. Channel locations .....	115
Figure 6-2. Marker positions (a) and Model definition (b).....	116
Figure 6-3. Experiment settings and protocol.....	118
Figure 6-4. Data processing flow. ....	122

Figure 6-5. Coordination profiles of the thigh-shank (a) and shank-foot (b) couplings.  
..... 126

Figure 6-6. ERSP for the four limbs.. ..... 128

Figure 6-7. Connectivity between the neural dynamics and the coordination parameters.  
..... 130

## LIST OF TABLES

Table 2-1. National Institutes of Health (NIH) Quality Assessment results .....	28
Table 2-2. Experiment setting and models.....	31
Table 2-3. Outcomes for reviewed running studies .....	33
Table 2-4. Outcomes for reviewed jumping studies .....	46
Table 4-1. Demographic data .....	69
Table 4-2. Results of discrete parameters. ....	76
Table 5-1. Demographic data .....	93
Table 5-2. Mean value, normality, p-value, and asymmetry ratio of the parameters. ....	101
Table 6-1. Demographic data of participants .....	114

## LIST OF ABBREVIATIONS

AB	Able-bodied
RoM	Range of motion
GRFs	Ground reaction forces
GC	Gait cycle
uTFA	Unilateral transfemoral amputation
NMSS	Neuromusculoskeletal system
CNS	Central nervous system
CPGs	Central pattern generators
fMRI	Functional magnetic resonance imaging
DoFs	Degree of freedoms
DST	Dynamic system theory
CRP	Continuous relative phase
PA	Phase angles
MARP	Mean absolute relative phase
DP	Deviation phase
ACLR	Anterior cruciate ligament reconstruction

EEG	Electroencephalography
MRCP	Movement-related cortical potential
ERS/D	Event-related synchronisation/desynchronisation
DCD	Developmental coordination disorders
CRPv	Variability of CRP
SD	Standard deviation
ITBS	Iliotibial band syndrome
LBP	Lower back pain
Q-angles	Quadriceps angles
BSS	Blind source separation
ICA	Independent component analysis
CCA	Canonical correlation analysis
SSA	Singular spectrum analysis
ASR	Artifact subspace separation
AMICA	Adaptive mixture independent component analysis
EEMD	Ensemble empirical mode decomposition



SPM	Statistical parametric mapping
RSPs	Running specific prosthesis
CMC	Cortical muscular coherence
ICs	Independent components
ERSP	Event related spectral perturbation
FDR	False discovery rate

# CHAPTER I INTRODUCTION

## 1.1 The development of prostheses

### 1.1.1 Better movement performance and gait rehabilitation wearing a prosthesis

According to the International Organization for Standardization, prostheses are defined as external devices that replace missing limb segments [1]. Prostheses have also been recognised as priority assistive products that enable individuals with disabilities to enhance their quality of life [2]. Several types of prostheses are used in the community, commonly divided into upper and lower limb prostheses. Based on the levels of amputation, there are six different lower limb prostheses and seven different upper limb prostheses, each with specific classifications [3-5]. Lower limb prostheses focus on basic daily movements, such as walking and running. Given their function and importance, individuals using lower limb prostheses focus more on restoring movement abilities, such as gait, more than individuals using upper limb prostheses.

It is estimated that prostheses will enhance the quality of daily life for around 1.5% of the population around the world (over 0.1 billion) [6]. There are various causes of injuries that can lead to dysfunction or deformities, conditions that may be eased through the use of prosthetic devices. Common causes of dysfunction and deformities include congenital abnormalities, diabetes, burns, and trauma [7]. In such situations, doctors typically prioritize conservative treatment method. However, if conservative treatments are unsuccessful, both reconstruction and amputation methods can be viable solutions [8]. As an example, individuals diagnosed with diabetes frequently face a heightened susceptibility to developing diabetic foot. Ulcers may develop and, if not properly managed through foot care, could lead to lower limb amputation [9]. Once a

patient and their doctor decide to decline conservative treatments, the utilisation of lower limb prostheses can assist in restoring the individual's gait ability [10].

Advancements in prosthetics could enhance both movement performance and prosthetic gait rehabilitation for individuals wearing prostheses. In particular, the optimisation of prosthesis design has the potential to improve movement performance. Lower limb prostheses have developed from simple wooden sticks to complex mechanical structures with multiple joints [11]. To enhance the restoration of biological limbs, they imitate the structures of biological limbs. The quality of a prosthetic design is measured by how much it improves movement performance. Regarding the rehabilitation of gait in individuals who have undergone amputation, there is a period of prosthetic gait rehabilitation [12]. During this period, they learn and refine a prosthetic gait pattern, ultimately enabling independent walking using prostheses. Advancements in prosthetics could offer users a high-quality prosthetic gait rehabilitation experience.

### **1.1.2 Prosthetic gait: functional asymmetries to compensation mechanisms**

Gait in individuals with unilateral amputation is restored using prostheses. However, prostheses cannot fully replicate the physiological function of intact limbs. In comparison to able-bodied (AB) individuals, those who use prostheses exhibit a decrease in walking speed and an increase in limb asymmetry regarding spatiotemporal parameters, kinematics, and joint kinetics [13-17]. Concerning spatiotemporal parameters, individuals with a lower limb amputation often have reduced walking speed and stride length when compared to AB individuals [18]. Among individuals with a unilateral amputation, the prosthetic limb exhibits a shorter step length and swing phase, and a prolonged stance and double support phase compared to the intact limb [19].

Kinematic differences can be observed in the lower limbs, from the proximal to the distal segments. The prosthetic limb commonly exhibits greater hip flexion during the swing phase in comparison to the intact limb [20]. With regards to the knee joint, intact limbs typically demonstrate normal knee flexion and extension patterns, similar to AB individuals. Conversely, the prosthetic limb frequently exhibits reduced knee flexion during the swing phase, especially for individuals with transfemoral amputations [21]. For the ankle joint, the intact limb exhibits normal ankle motion, while the prosthetic limb typically exhibits a constrained range of motion (RoM) due to the passive nature of prosthetic feet [22].

Concerning kinetics, the primary focus of research has been on ground reaction forces (GRFs) and impulses. Individuals with unilateral lower limb amputation typically produce lower vertical and mediolateral GRFs on the prosthetic side during the stance phase [23]. This likely results from adaptations to reduce the load on the prosthesis, showing instability and lateral swing during the gait, and the generation of reduced anteroposterior GRF in the early stance phase [24-26]. Regarding impulses, lower vertical impulses are produced on the prosthetic side, which may indicate an attempt to reduce the load on the prosthesis [23]. The prosthetic side may experience higher mediolateral impulses due to increased lateral sway, suggesting instability during the gait cycle (GC). The prosthetic side commonly exhibits a decrease in both braking and propulsive anteroposterior impulses, which has the potential to impact forward momentum control during gait [27]. Variations in these adaptations can be attributed to factors such as walking speed, level of amputation, and type of prosthesis [23, 28].

In summary, prostheses restore the movement abilities of individuals with amputations.

However, their walking pattern often shows imbalances in the lower extremities, unlike those of AB persons [15, 17]. The observed gait imbalances include differences in force, joint angles, and the stance phase duration of the legs [13-16]. Imbalances are primarily caused by compensatory strategies resulting from the loss of essential bones and muscles on the prosthetic side. Consequently, there is a decreased capacity for force generation, which exerts a negative impact on the kinetics of the prosthetic limb [29]. Moreover, the residual limb may not be able to withstand the heightened pressures associated with walking when connected to the prosthetic socket [30]. To counterbalance the diminished force output of the prosthetic limb, increased progression forces and impulses are generated by the intact limb when walking [15]. From a kinematic perspective, the restricted knee flexion of the prosthetic limb during its swing phase is compensated for by an enhanced hip movement in the intact limb, thus extending the duration of the stance phase for the prosthetic limb [16]. The overall duration of prosthetic gait training and the degree of ease in prosthesis utilisation have a significant impact on the life quality of those with unilateral transfemoral amputation (uTFA) [14]. Gaining insight into prosthetic gait patterns can enhance both prosthesis design and prosthetic gait rehabilitation, ultimately improving the lives of individuals with amputation.

### **1.1.3 Biomechanics benefits prosthesis design and prosthetic gait rehabilitation**

Biomechanics, a field of study focusing on the mechanics of a living body, has contributed to improvement of the design and development of prosthetics and programs for rehabilitating walkers [31]. Understanding human movement through biomechanics is crucial for prosthesis design. Utilising biomechanical principles to study and simulate

human locomotion allows researchers and developers to design prosthetic devices that closely emulate natural human movements. Additionally, examining the forces and movements in human locomotion helps in creating more durable and comfortable prosthetics. As a result, highly personalised prosthetics are created to meet the distinct needs of individuals with amputation, significantly enhancing their mobility and quality of life [32, 33].

Formulating personalised rehabilitation programs involves the use of biomechanics. By studying how someone walks, biomechanics can find determine viable improvements and create better rehabilitation plans. As a result, individuals with amputation can regain their mobility and independence through an improved and more natural walking pattern. Additionally, comprehension of biomechanics can aid in the prevention of secondary complications commonly linked to amputations, including musculoskeletal disorders resulting from abnormal gait patterns. This understanding enables the implementation of early interventions, which in turn leads to improved overall health outcomes for individuals who have undergone amputation [34, 35]. Lastly, biomechanics offers valuable quantitative tools for assessing the efficacy of prosthetics and rehabilitation approaches. The use of these tools allows for the evaluation of objective measures such as stride length, gait speed, and joint movements, thereby facilitating a more accurate assessment and benefiting advancement of prosthetics design and rehabilitation strategies [36]. The application of biomechanics thus covers a broad spectrum, from design to rehabilitation, and evaluation, continually enhancing the quality of life for individuals with amputation.

In conclusion, biomechanics plays a substantial role in the advancement of prosthetic

design and gait rehabilitation. Through the enhancement of the comprehension of human locomotion, the improvement of prosthetic design, the facilitation of personalised rehabilitation programs, the prevention of secondary complications, and the provision of quantitative assessment tools, the field of biomechanics has the potential to consistently advance the care and treatment outcomes for individuals with amputation.

## **1.2 Gait generation in human neuromusculoskeletal system (NMSS)**

### **1.2.1 Movement generation in human beings**

Movement generation in humans is a complex and well-coordinated activity facilitated by the NMSS [37]. This system comprises the nervous system, muscles, and skeletal system, each playing a critical role in generating and controlling motion. The sensory feedback from proprioceptors in muscles, tendons, and joints provides the nervous system with information about the body's position and movement [38]. This information is integrated with motor commands to adjust and fine-tune movements in real-time, ensuring smooth and coordinated movements [39].

The central nervous system (CNS) acts as the command and control centre for human movement, encompassing the brain, spinal cord, and peripheral nerves [40]. The cerebral cortex, particularly the motor cortex, is responsible for initiating voluntary movements. This is accomplished through the transmission of signals via the corticospinal tract to the peripheral nerves that innervate the muscles [41]. The cerebellum and basal ganglia are other critical structures within the brain that contribute to movement control [42]. The cerebellum coordinates voluntary movements, balance,

and muscle tone, while the basal ganglia control movement initiation and intensity. Moreover, the spinal cord is home to central pattern generators (CPGs), which are neural circuits that can generate repetitive motor patterns (such as swimming, walking, and running), even without input from the brain. Gait is among the automatic and repetitive movements controlled by CPGs [43].

Neural commands are converted into physical movement by the musculoskeletal system. The activation of a motor neuron leads to muscle contraction in each innervated muscle fibre. The coordination of multiple muscle contractions allows for smooth and controlled movement [44]. By recruiting motor units and adjusting their firing rate, the contraction's type, intensity, and duration are regulated. The skeletal system provides the mechanical structure needed for movement [45]. Bones are connected through joints, which allow for different ranges of movement depending on the type of joint (hinge, ball-and-socket, pivot, etc). The tendons connect muscle fibres to bones, causing joint movement when muscles contract.

### **1.2.2 Normal gait and prosthetic gait generation**

Gait is a complex neuromuscular activity coordinated by multiple physiological systems that allow us to walk and run. This process involves a combination of motor command transmission, sensorimotor integration, and muscle activity [46]. The CPG, a neural circuit within the spinal cord, plays a critical role in gait generation, producing rhythmic motor patterns like walking or swimming when activated. The existence and role of the CPG in locomotion have been robustly validated in several animal models, including cats and lampreys [47].

When considering humans, the lack of direct evidence for CPGs can be attributed to



ethical and practical limitations; however, the increasing indirect evidence strongly indicates their presence. This evidence was found in studies observing individuals with complete spinal cord injuries who were able to generate rhythmic stepping movements when their body was supported by external devices [48]. However, sensory feedback plays a role in influencing gait control through modulation. Gait is not just an automated process governed by CPGs; it also relies heavily on afferent information, starting with the peripheral and ending with the CNS [49]. In particular, the dynamics of gait generation are influenced by factors such as limb position, surface conditions, and body orientation.

Biomechanical changes in individuals with amputation are visibly apparent in their gait, while underlying neural changes also play a significant role in altering gait patterns. After amputation, the brain significantly reorganises to adapt to limb loss and altered sensory inputs [50]. Neural plasticity is the driving force behind this reorganisation, as it enables the brain to dynamically adjust its structure and interconnections to accommodate learning or damage.

In the somatosensory and motor cortices of the brain, a specific area referred to as a 'cortical map' is allocated to each body part. Research utilising functional Magnetic Resonance Imaging (fMRI) suggests that following amputation, the cortical representation of the amputated limb undergoes a size reduction, while neighbouring regions expand into the unutilised area, referred to as 'cortical remapping' [51]. For example, in the case of individuals who have experienced lower limb amputations the cortical area that was once responsible for the amputated foot's representation may now process sensory inputs from either the remaining limb or the foot on the opposite side,

thereby potentially contributing to the occurrence of phantom limb sensations [52]. This phenomenon is attributed to "cortical remapping". In certain cases, these sensations can sometimes result in severe and chronic phantom limb pain, which is a result of continuous neuron firing caused by maladaptive neural plasticity [53].

Prosthetic gait rehabilitation can be improved by recognising these neural changes. The principle of neuroplasticity is utilised in post-amputation gait training to improve prosthesis integration and control through repetitive and targeted movements [54].

### **1.2.3 Limitations in biomechanics in investigation NMSS**

After amputation, global changes occur throughout the NMSS in individuals with amputations. While biomechanics aids in the understanding of the gait of individuals with amputation, it does not fully capture global changes in the NMSS.

A primary limitation is that biomechanical analyses often focus on individual joints or segments in isolation. This implies that the "coupling effects" or interactions between different parts of the NMSS may not be fully represented or understood. Human movement is a sophisticated process where various joints and muscles collaborate to achieve smooth and efficient motion [55]. Another limitation is that many biomechanical models view the body purely as a mechanical system, often overlooking the neural components of movement. The limitations become more pronounced when investigating changes in NMSS function in cases like limb loss or neurological disorders.

To overcome these limitations and acquire a comprehensive understanding of the NMSS, interdisciplinary approaches combining biomechanics and neuroscience are recommended.

#### **1.2.4 Coordination of NMSS from dynamic system theory**

The optimal coordination of degrees of freedoms (DoFs) indicates that the CNS governs functional movement coordination patterns [56, 57]. A total of 244 DoFs are needed to establish a sophisticated system for describing human body movement [58]. The coordination of all DoFs is managed by the NMSS. The accurate and succinct assessment of this intricate system poses a frequent challenge in biomechanical research [59]. Recently, the utilisation of the Dynamic System Theory (DST) method has become increasingly common, to explain the coordination of segmental movements and DoFs [60]. The fundamental principle of DST proposes that all movements are governed by the neuromuscular system, which sends signals to specific muscles and motor neurons [59, 61, 62].

During gait, the human NMSS acts as a cohesive system, enabling energy transfer. The lower limb movement dynamics, marked by pendulum-like structures oscillating sinusoidally, demonstrate consistent energy flow, resembling a dynamic system. The characterisation of the lower-limb DST can be achieved by considering only its present state and the rate of change [59]. DST offers a numerical approach to describe the coordination of movement, termed the continuous relative phase (CRP) by subtracting the two phase angles (PA) of two body parts [63]. The present condition of the lower limbs and their alteration rate can be represented by the angle deviation and the angle deviation speed at a specific moment, respectively [59]. Modelling lower extremities as components like the thigh, shank, and foot and assessing their angles in relation to a universal coordinate framework, provides a more precise evaluation approach than relying solely on joint angles [63]. The CRP measurements offer a way to describe coordination dynamics among segments. The patterns observed in CRP and the

fluctuations in coordination during a specific gait phase can be measured using the mean absolute relative phase (MARP) and the deviation phase (DP), respectively [63].

CRP is employed to evaluate movement proficiency and identify shortcomings in coordination. Patients with Parkinson's disease exhibited reduced regression coefficients in the relative phase for arm-leg coordination compared to those not on medication [64]. Research has indicated notable adaptations in relative phase during walking and running in individuals after anterior cruciate ligament recovery (ACLR) [65]. The presence of developmental coordination problems is associated with reduced coordination skills involving both hands and the coordination between vision and hand movements [66]. A few studies across different sports have suggested the potential of CRP methods in evaluating performance in running, jumping, and swimming [67-70].

### **1.2.5 Neuron activities and movement coordination during gait**

The CRP method provides tools to gather insights into movement regulation from the NMSS. CRP employs kinematics to depict coordination patterns originating from the CNS. This approach offers novel insights into gait generation from the NMSS. However, this method lacks intuitiveness as it describes movement coordination in the phase space. Since movements originate from the CNS and CRP gathers insights into movement regulation, it's natural to question if there's an association between coordination patterns and neural activities. To comprehend the neuronal activity associated with gait coordination, it is imperative to examine the complex interactions between the brain, spinal cord, and peripheral nervous system.

The investigation of the relationship between movement coordination and neuronal activities can provide valuable insights. This research could deepen our understanding

of the effects of limb loss and adaptations of prosthetic gait to CNS in persons with uTFA. For instance, insights into neural activity changes wearing prosthetic use could guide the development of better rehabilitation protocols or advanced prosthetic designs. On the other hand, the analysis of modifications in dynamic system coordination can deepen our comprehension of gait adaptations in individuals with amputation, thereby enhancing rehabilitation and prosthesis design. Therefore, the integration of neuroscience and biomechanics analysis presents a potential avenue for promising research. This could lead to practical solutions that significantly improve the well-being of individuals with uTFA wearing prosthesis.

### **1.3 Formulation of the research question**

Comprehending the adaptation of the entire NMSS for limb loss can lead to a comprehensive understanding of neural plasticity and movement coordination adaptation [71]. In addition, the examination of the correlation between neural dynamics and movement coordination may illuminate the decoding of neural to movement pathways. This breakthrough holds promise for the improvement of rehabilitation exercises and the design of prosthetic limbs [72].

Among the various types of lower limb amputations, transfemoral amputation has the most significant impact on the lower limb. Therefore, the focus of this study was on individuals with uTFA. By adopting a comprehensive, interdisciplinary approach to the study of gait in individuals with uTFA, we have the opportunity to significantly enhance our understanding and improve patient outcomes.

### **1.3.1 Gait coordination patterns of individuals with uTFA**

Individuals with uTFA implement compensatory strategies to coordinate the asymmetries in their gait. These strategies are evident in different regions of the body [19]. However, a substantial amount of recent research has focused on analysing individual joints. It is crucial to recognise the equal importance of studying the interaction and coordination of lower extremities in individuals with uTFA. However, there is limited research investigating the coordination patterns of those with uTFA [73-75]. One study observed increased DP in knee-ankle coupling for a prosthetic limb during standing, but reported decreased DP during walking [75]. Two separate studies employed CRP to assess prosthetic gait design and rehabilitation, and found changes in coordination [73, 74]. However, the models constructed in these studies were dependent on joint angles, which may be misaligned with DST [59]. The preferred model is constructed based on segment angles, incorporating a dynamic system derived from the concept of a pendulum [76, 77]. Notably, the angle of the joint is defined as the relative angle of neighbouring segments. On the other hand, the pendulum model requires the use of an external standard, such as a horizontal surface, rather than relying on a relative reference segment [77, 78]. Moreover, a study that utilised the CRP model concluded that the segment angles demonstrated a higher level of sensitivity in comparison to the joint angles [79].

The coordination of lower limb segments, particularly those involving uTFA, plays a crucial role in gait training while wearing a prosthesis, as well as in the development of new prosthetic designs. The full comprehension of coordination dynamics, when examined in terms of segment angles during ambulation, is still lacking. Therefore, it is imperative to examine the coordination patterns in those with uTFA during various

gait activities, including walking and running.

### **1.3.2 Brain activities of individuals with uTFA during gait**

Recording the activities of the brain during gait is difficult. Numerous brain imaging modalities are involved in capturing neural activities in static tasks [80-83]. These modalities offer detailed insights into the brain's structural and functional aspects during stationary conditions. However, their limitation becomes apparent during dynamic tasks, as they require the subject to maintain a stationary position during imaging. In contrast, Electroencephalography (EEG) exhibits remarkable effectiveness in the assessment of brain activities during mobile tasks [84, 85]. EEG is capable of capturing the brain activities of participants engaged in activities such as walking or running. EEG can be considered a valuable tool for investigating physical activity. In addition, the aptitude of EEG to monitor rapid changes in brain activity in real-time makes it particularly suitable for complex and continuous tasks such as gait analysis [85]. The unique characteristics of EEG make it particularly helpful for studying gait and related brain activities, providing real-time insights into dynamic brain activity patterns during motion.

A restricted number of studies have explored brain activities during gait. The identification of movement-related cortical potential (MRCP) preceding voluntary movement underscores the proactive function of the brain in generating gait patterns. [86]. The implementation of EEG has made it possible to investigate cognitive demands while walking, particularly in complex scenarios. Evidence from variations in alpha and beta band activities under different cognitive loads supports the significant role of cognitive resources in gait regulation [87].

Furthermore, fluctuations in beta band power across the GC emphasise the association between sensorimotor rhythms and locomotion regulation [88]. Research using EEG has provided insights into the concept of neuroplasticity in the context of gait rehabilitation. This research has demonstrated the brain's ability to reorganise itself in response to motor function deficits caused by injuries or diseases [89]. For individuals with uTFA, only a single study has reported MRCP during gait. The study found that individuals with uTFA needed increased attention when ambulating wearing the specific active prosthesis, compared to using a passive prosthetic device or when compared to AB individuals [90]. The limitation of the findings of the study was that it was limited in time domain. However, brain activity encompasses various aspects, including event-related synchronisation/desynchronisation (ERS/D) in the time-frequency domain and functional connectivity between different regions [90].

It is crucial to comprehend the brain activity during gait in individuals with uTFA, as it has significant implications for cognitive load, prosthetic development, rehabilitation, and pain management [53, 91]. Therefore, it is imperative to investigate brain activities during gait among individuals with uTFA via EEG.

### **1.3.3 Connectivity between brain activity and coordination patterns**

The NMSS exhibits connectivities between the cortical and muscles (Figure 1-1). Human motor cortical areas exhibit distinct features that enable them to access and coordinate various muscle synergies, allowing for the execution of functional tasks through different brain networks [92]. Multiple methods that detect connectivity between time series in signal analysis have been employed to identify functional connectivities associated with brain activities [93-95]. Considering the characteristics of biomechanical signals, the Pearson correlation could potentially be used as an



effective tool to determine directional connectivity between biomechanical signals and neural signals [96].

Movement is generated by the NMSS. Coordination patterns collect clues about movement regulation from the CNS. Techniques, such as EEG, capture brain activity during gait. It is natural for one to question the connection between coordination patterns and brain activity. Considering that the dynamic system mirrors the control mechanism of the CNS and EEG directly captures brain activity, it is reasonable to assume that coordination patterns emerge from brain activity (Figure 1-1). Therefore, it is imperative to understand the correlation between brain activity and coordination patterns.

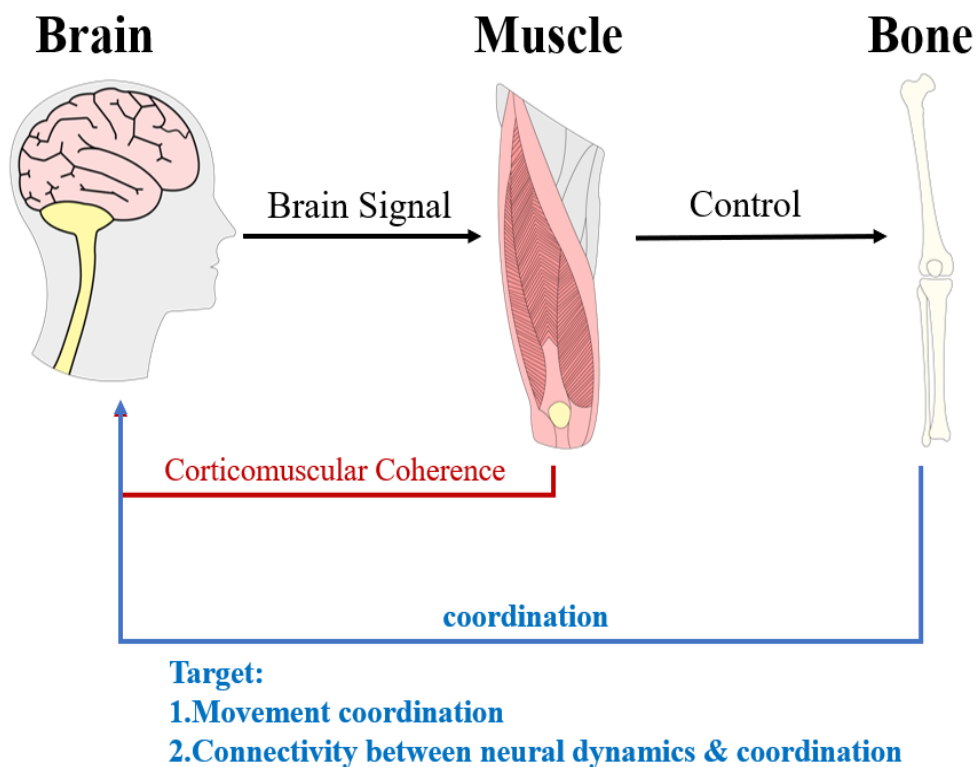


Figure 1-1. Illustration of movement control in human beings and movement coordination.

## **1.4 Objectives of the study**

Based on the research questions, two objectives were proposed in this study.

1. The first objective is to explore coordination patterns in individuals with uTFA during walking and running (or sprinting) using CRP. This study will observe and compare these patterns with those of AB individuals to enhance our understanding of gait in individuals with uTFA. This will be investigated in two separate studies.

2. The second objective is to examine the relationship between the coordination patterns derived from kinematics and the brain activity recorded by EEG. This study aims to bridge the gap between biomechanics and neuroscience by investigating the functional connectivity between the coordination time series and EEG signals.

## **CHAPTER II LITERATURE REVIEW**

### **2.1 lower limb coordination**

#### **2.1.1 Coordination**

Coordination involves the organisation and control of multiple DoFs within a motor system to enable deliberate and controlled movements [57]. The CNS commonly governs functional movement patterns by effectively managing the DoFs [56, 57]. In order to accurately depict the motion of the human body and establish a sophisticated coordination system, a total of 244 DoFs are required [58]. This system ensures the control of all DoFs by the neuromuscular system. The existence of multiple mechanical DoFs, such as joints and muscles, offers significant flexibility, but at the same time, poses a control challenge for the nervous system [57]. An obstacle frequently encountered in biomechanical studies is the accurate and straightforward evaluation of this intricate system [59]. For this purpose, tools like joint kinematics, joint moments, and electromyography are employed in biomechanical investigations of the system [59, 60]. Recently, the DST method has become more popular, aiding in the comprehension of the coordination of segmental movements and DoFs [60]. The DST theory posits that the neuromuscular system is responsible for governing all motions through the generation of signals to specific muscles and motor neurons [59, 61, 62]. Coordination involves creating connections and synergies among DoFs, thereby reducing control dimensionality by integrating mechanical components into operational units [97]. This coordination promotes the stable generation of complex spatiotemporal patterns through the dynamic interaction between the neuromuscular system, environment, and specific tasks [98]. In general, coordination tackles the problem of redundancy through

the utilisation of self-organisation, directing DoFs towards adaptable groupings that showcase synergy.

### **2.1.2 Coordination evaluation**

The CRP method provides a measurable indicator for the human dynamic system, specifically for segmental movements. The neuromuscular system exhibits a tendency towards achieving new equilibrium state, which is in accordance with the principles of DST. [99]. During the transition to this new state, the movements of the relative segments of the dynamic system change [60, 99-102]. Changes in motion consistently coincide with variations in the velocity and displacement of segments or joints. In order to observe changes intuitively, the phase portrait is obtained by plotting the normalised angle deviation and the angular deviation speed of a joint/segment within a polar coordinate system [77]. The PA (phase angle), which reflects a joint's position in a phase space, is calculated by taking the arctangent of the ratio of the joint's displacement to its velocity.

CRP is frequently employed as a robust metric for assessing movement proficiency and detecting coordination changes. People with Parkinson's disease were observed to have a significant alteration in the CRP in arm-leg coordination compared to people without Parkinson's disease [64]. Studies suggest that individuals who have had an ACLR significantly display adaptations in CRP during their recovery period, observable in both their walking and running patterns [65]. Developmental coordination disorders (DCD) can also be diagnosed in children as the health control group exhibited more consistent CRP patterns in hand movements compared with DCD children [66]. While the majority of these studies primarily examine walking coordination, there is limited research on high-intensity activities like running and jumping. In high-intensity actions,

the correlation between joint angle and speed can exhibit variations, resulting in distinctive coordination patterns. In addition, the amount of research conducted on CRP tools in other sports has been limited, thereby substantiating the plausibility of employing this alternative approach to evaluate performances in running, jumping, and swimming [67-70].

### **2.1.3 CRP calculation**

CRP quantifies the interaction of linked segments, providing insight into coordination during a specific motion phase. Initially, the PA is calculated by utilising the data obtained from the associated angle deviation and the angular deviation speed. Subsequently, CRP is determined by subtracting the PA of the proximal segment from the PA of the distal segment. In RP,  $0^\circ$  represents an in-phase condition, moving away from  $0^\circ$  suggests a transition to out-of-phase, and a CRP of  $180^\circ$  ( $-180^\circ$ ) signifies a situation of anti-phase relationship. Two approaches were used approaches for computing CRP. The initial method relies on phase portraits to calculate PA [103, 104]. The other approach calculates the PA through the Hilbert transformation [105]. This method might provide a solution for signals that are not sinusoidal.

The CRP curve acts as a visual tool for analysing the phase relationship between two coupling segments. For plotting, the "X" axis represents normalised time, while the "Y" axis depicts the relative phase angle. Consequently, the angle values at each time point are graphed to form the CRP profile. The CRP profile includes inclines and declines, along with local peaks and troughs. A positive incline signifies the distal segment taking the lead, whereas a negative incline implies it trails the proximal segment. The local

peak value indicates a transition in segment dominance, signalling the conclusion of the distal segment's lead and the commencement of the proximal segment taking precedence. Conversely, the local minimum indicates the opposite.

The variability of CRP (CRP<sub>v</sub>) denotes the fluctuation within the continuous relative phase angle [65, 106-126]. The derivation comes from the average of the standard deviation (SD) of CRP values across all time points. It reflects the NMSS's ability to produce consistent movements. A lower CRP<sub>v</sub> suggests stable movement coordination, while a higher value indicates instability.

MARP is used to evaluate the linkage or interrelation between two segments. Specifically, a lower MARP value signifies an in-phase relationship, whereas a higher value denotes an out-of-phase connection [65, 67, 117, 127-129]. The DP gauges coordination consistency, where a diminished DP value signifies lesser variability and heightened stability in coordination [67, 103, 117, 124, 127-130].

Two distinct methods exist for CRP calculation. One prevalent method follows the approach outlined [103]. The researchers introduced particular equations for computing CRP based on phase portraits. In this context,  $\omega$  and  $\theta$  represent the filtered angle deviation speed and the angular deviation, respectively;  $\bar{\theta}$  and  $\bar{\omega}$  denote the normalised angle deviation speed and the angular deviation (*eq 1* and *eq 2*); The PA, represented by  $\phi_{rp}$  was derived from the normalised angle deviation and the angular

deviation speed (eq 3); CRP ( $\theta_{crp}$ ) was obtained by subtracting the proximal one from the distal one of the PA of the two segments (eq 4).

An alternative method employs the Hilbert transformation for calculation. To start, the

$$\bar{\theta} = 2 \left[ \frac{\theta - \min(\theta)}{\max(\theta) - \min(\theta)} \right] - 1 \quad (eq 1)$$

$$\bar{\omega} = \left[ \frac{\omega}{\max(|\omega|)} \right] \quad (eq 2)$$

$$\phi_{rp} = \arctan \left[ \frac{\bar{\omega}_{(i)}}{\bar{\theta}_{(i)}} \right], \quad i=1,2,\dots,n \quad (eq 3)$$

$$\theta_{crp} = \phi_{distal-rp} - \phi_{proximal-rp} \quad (eq 4)$$

OR

$$\theta_{crp} = \arctan \left( \frac{\bar{\omega}_{distal-rp} \bar{\theta}_{proximal-rp} - \bar{\omega}_{proximal-rp} \bar{\theta}_{distal-rp}}{\bar{\theta}_{distal-rp} \bar{\theta}_{proximal-rp} + \bar{\omega}_{distal-rp} \bar{\omega}_{proximal-rp}} \right)$$

angle deviation data  $\theta_{(i)}$ , is interpreted as an ongoing signal and is expressed as  $\theta(t)$  in equation 5 (eq 5). Subsequently, the Hilbert transformation,  $H(\theta(t))$  is performed as per equation 6 (eq 6).  $H(t)$  is obtained via the Hilbert function in software, such as Origin. Subsequently, a new time series, represented by  $\zeta(t)$ , is introduced. Here,  $j$  denotes the imaginary unit (eq 7) [131]. The phase angle is then calculated (eq 8). The final procedure reflects the phase portrait method outlined in equation 4. The process is operated using the “unwarp” tool available in platforms like MATLAB, Python, or Origin. This function, same as in equation 3 (eq 3), aids in computing the PA from real and imaginary components of a time series.

$$\theta(t) = \theta_{(i)}, i = 1, 2, \dots, n \quad (eq\ 5)$$

$$H(t) = H(\theta(t)) = \theta(t) * \frac{1}{\pi t} \quad (eq\ 6)$$

$$\zeta(t) = \theta(t) + jH(t) \quad (eq\ 7)$$

$$\phi_{rp} = \arctan \left[ \frac{H(t_i)}{\theta(t_i)} \right], i = 1, 2, \dots, n \quad (eq\ 8)$$

MARP and DP are obtained through the equations 9 (eq 9) and 10 (eq 10), respectively. Within these formulas, "n" denotes the count of time length within the normalised length., such as stance-phase.  $\phi_{i\ th-cr p}$ , and  $SD_i$  represent the CRP and SD of the  $i_{th}$  point, respectively.

$$MARP = \sum_{i=1}^n \frac{|\phi_{i\ th-cr p}|}{n}, i=1, 2, \dots, n \quad (eq\ 9)$$

$$DP = \frac{\sum_{i=1}^n |SD_i|}{n}, i = 1, 2, \dots, n \quad (eq\ 10)$$

## 2.1.4 CRP application and interpretation: a systematic review

### 2.1.4.1 Introduction

Currently, the CRP model encompasses various segments including the trunk, pelvis, thigh, and shank, as well as the relationships between joints such as the hip, knee, and ankle. The diverse movement planes and chosen filtering methods have led to varied interpretations across different movement tasks. Properly defined protocols for filtering



techniques and the formulation of the CRP model are essential for simplifying its utilisation and understanding in tasks of significant intensity. To dig deeper into the utilisation and understanding of CRP, a systematic review was conducted. The aim of this study was to unify the use and interpretation of CRP in the analysis of movement. Tasks involving running and jumping were selected due to their fundamental attributes and their high-intensity features. Running, a prevalent daily exercise, is characterised by forward linear motion. In contrast, jumping, often seen in various sports, is typified by vertical motion. The study's results aim to provide recommendations for the current application, encompassing variable selection, filtering methods, and the interpretation of the CRP method.

#### ***2.1.4.2 Methods***

##### ***Search strategy***

The Preferred Reporting Items for Systematic Reviews and Meta-Analyses (PRISMA) guidelines were first referred to and used to guide the subsequent article search strategy

(

Figure 2-1). A search was conducted for articles using the following keyword combinations: “jump OR jumping OR run OR running OR runners” [All fields] AND "continuous relative phase" [All fields] to specifically focus on running and jumping in five databases (Science Direct, Web of Science, Springer, EBSCO, PubMed), spanning from January 1999 to December 2020.

### ***Selection Criteria***

An initial search yielded 381 studies. After excluding duplicates (number =178) and studies (number = 37) such as books, conference abstracts, review papers those without full-text, and non-peer-reviewed articles, 166 studies remained for eligibility assessment. Titles, abstracts, and full text of the studies were then screened using two inclusion criteria: (1) the study's involvement in CRP analysis, and (2) the use of running and/or jumping in test protocols. Of these, only 26 studies were relevant (19 on running and 7 on jumping). Their data were then compiled in Excel for further qualitative analysis (Figure 2-1). Information on every reviewed records, including the publication year, author name, study design components (participant characteristics, CRP model, protocols, and test conditions), and results after statistical analysis, were included. The categorisation of the training level of participants derived from a previous study on running [132], with the categories of the runners' playing levels as novice, recreational, or high-calibre. Furthermore, participants who were described merely being "runners" and, individuals who were physically active or had experience with running (even in other sports) were categorised as "recreational" runners in the reviewed articles. In the context of the CRP model, terms such as "tibia" and "leg" were collectively classified as "shank."

Each reviewed article underwent qualitative analysis using the National Institutes of Health (NIH) Quality Assessment list. Two independent evaluators, Mingyu Hu and Toshiki Kobayashi, assessed the quality of all articles. Their consensus on the findings was 97.1% across 12 questions for the 26 articles, as detailed in Table 2-1. When discrepancies arose between the two assessors, a third evaluator, Wing-kai Lam, made the final call after discussions with all involved. Studies were rated as "Good" if they

received fewer than three "No" responses, "Fair" with fewer than five "No" responses, and "Poor" if they garnered more than five "No" responses post-analysis. All 26 studies met the criteria in the qualitative analysis and were subsequently incorporated into the review (Table 2-1).

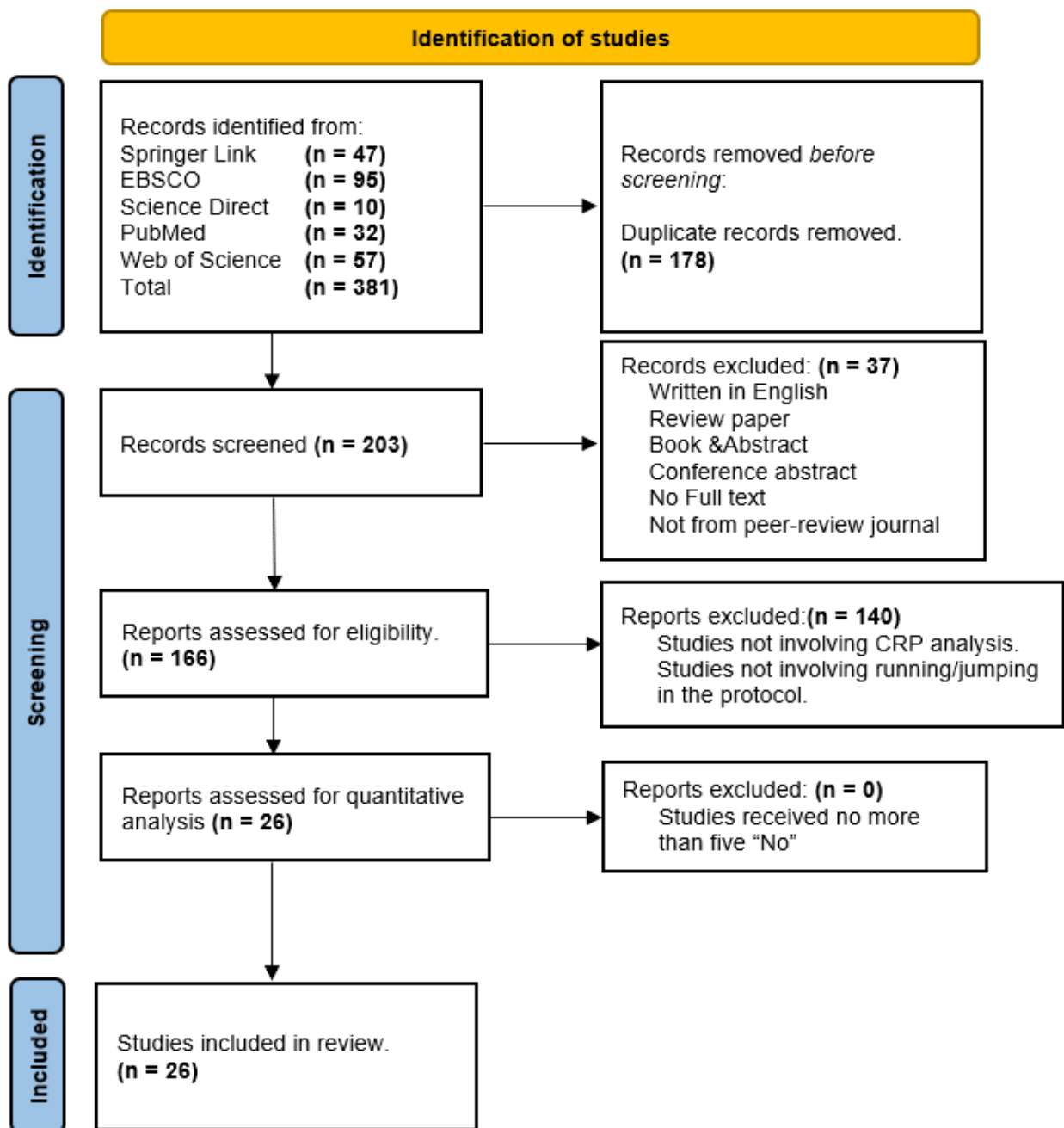


Figure 2-1. PRISMA flow diagram

Table 2-1. National Institutes of Health (NIH) Quality Assessment results

Studies	1	2	3	4	5	6	7	8	9	10	11	12	“N” sum
Abbasi et al.2020	Y	Y	N	N	NA	NA	NR	N	NA	NA	NA	N	4
Argaud et al.2019	Y	Y	N	Y	Y	Y	NR	NR	NA	NA	NA	N	2
Bailey et al.2018 (a)	Y	Y	N	N	Y	NA	NR	N	NA	NA	NA	N	4
Bailey et al.2018 (b)	Y	Y	N	N	Y	NA	NR	N	NA	NA	NA	N	4
Blache et al.2017	Y	Y	N	Y	N	Y	NR	NR	NA	NA	NA	N	3
Castro et al.2017	Y	Y	N	N	NA	NA	NR	N	NA	NA	NA	N	4
Dierks et al. 2007	Y	Y	N	N	NA	NA	NR	N	NA	NA	NA	N	4
Floria et al.2018	Y	Y	N	Y	N	Y	NR	NR	NA	NA	NA	N	3
Frank et al.2013	Y	Y	N	N	NA	NA	NR	N	NA	NA	NA	N	4
Gheller et al.2015	Y	Y	N	N	NA	NA	NR	N	NA	NA	NA	N	4
Gidley et al. 2020	Y	Y	N	N	NA	NA	NR	N	NA	NA	NA	N	4
Gittoes et al.2010	Y	Y	N	N	NA	NA	NR	N	NA	NA	NA	N	4
Hannigan et al.2019	Y	Y	N	Y	N	Y	NR	NR	NA	NA	NA	N	3
Heiderscheit et al.1999	Y	Y	N	Y	Y	Y	NR	NR	NA	NA	NA	N	2
Hein et al.2012	Y	Y	N	Y	Y	Y	NR	NR	NA	NA	NA	N	2
Krajewski et al.2020	Y	Y	N	N	NA	NA	NR	N	NA	NA	NA	N	4
Kurz et al.2005	Y	Y	N	Y	N	Y	NR	NR	NA	NA	NA	N	3
Miller et al.2008	Y	Y	N	Y	N	Y	NR	NR	NA	NA	NA	N	3
Morgan et al.2019	Y	Y	N	Y	Y	Y	NR	NR	NA	NA	NA	N	2
Prejean et al.2019	Y	Y	N	N	NA	NA	NR	NR	NA	NA	NA	N	4
Pupo et al.2013	Y	Y	N	N	NA	NA	NR	N	NA	NA	NA	N	4
Raffalt et al.2016	Y	Y	N	Y	N	Y	NR	NR	NA	NA	NA	N	3
Raffalt et al.2020	Y	Y	N	Y	N	Y	NR	NR	NA	NA	NA	N	3
Seay et al.2011	Y	Y	N	Y	N	Y	NR	NR	NA	NA	NA	N	3
Seay et al.2014	Y	Y	N	Y	N	Y	NR	NR	NA	NA	NA	N	3
Stergiou et al.2001	Y	Y	N	N	NA	NA	NR	N	NA	NA	NA	N	4

Y: yes; N: no; NR: not reported; NA: not applicable.

### 2.1.4.3 Results

Reviewed studies captured kinematic data using digital or infrared cameras. This

dataset covered single movement planes, including the sagittal plane (16 records), the transverse plane (4 records), and the frontal plane (2 records), as well as interactions involving multiple movement planes (9 records). The sampling frequency varied between 60 Hz [65, 126] and 500 Hz [113]. Three distinct filtering algorithms were employed across these studies. Notably, one study did not specify its filtering method [113]. The majority of studies utilised their filtering method through a low pass Butterworth method. There were 18 studies on the fourth order, 2 on the second, 2 on the norm, and 1 on the unknown. Conversely, two studies utilised the Quintic spline method, which yielded a standard error of the mean of 2 mm<sup>2</sup> [110] and a residual analysis [111]. Commonly, the cut off frequencies spanned from 6 Hz to 20 Hz (Table 2-2, Figure 2-2. Summary of CRP application ).

The reviewed studies utilised various CRP variables. These variables included CRP (26 records), CRPv (22 records, [65, 106-126]), MARP (4 records,, [65, 67, 117, 128]) and DP (3 records,, [67, 128, 133]). CRP measures two coupled segments/joints' coordination, by using the PA of the distal portion subtracting the proximal portion. The CRP profiles were generally reported during the stance phase (16 records, [65, 67, 109, 110, 112, 116-118, 120-122, 124-126, 128, 134]) or the whole GC (2 records, [111, 123]) (Figure 2-2. Summary of CRP application) to simplify the assessment of CRP.

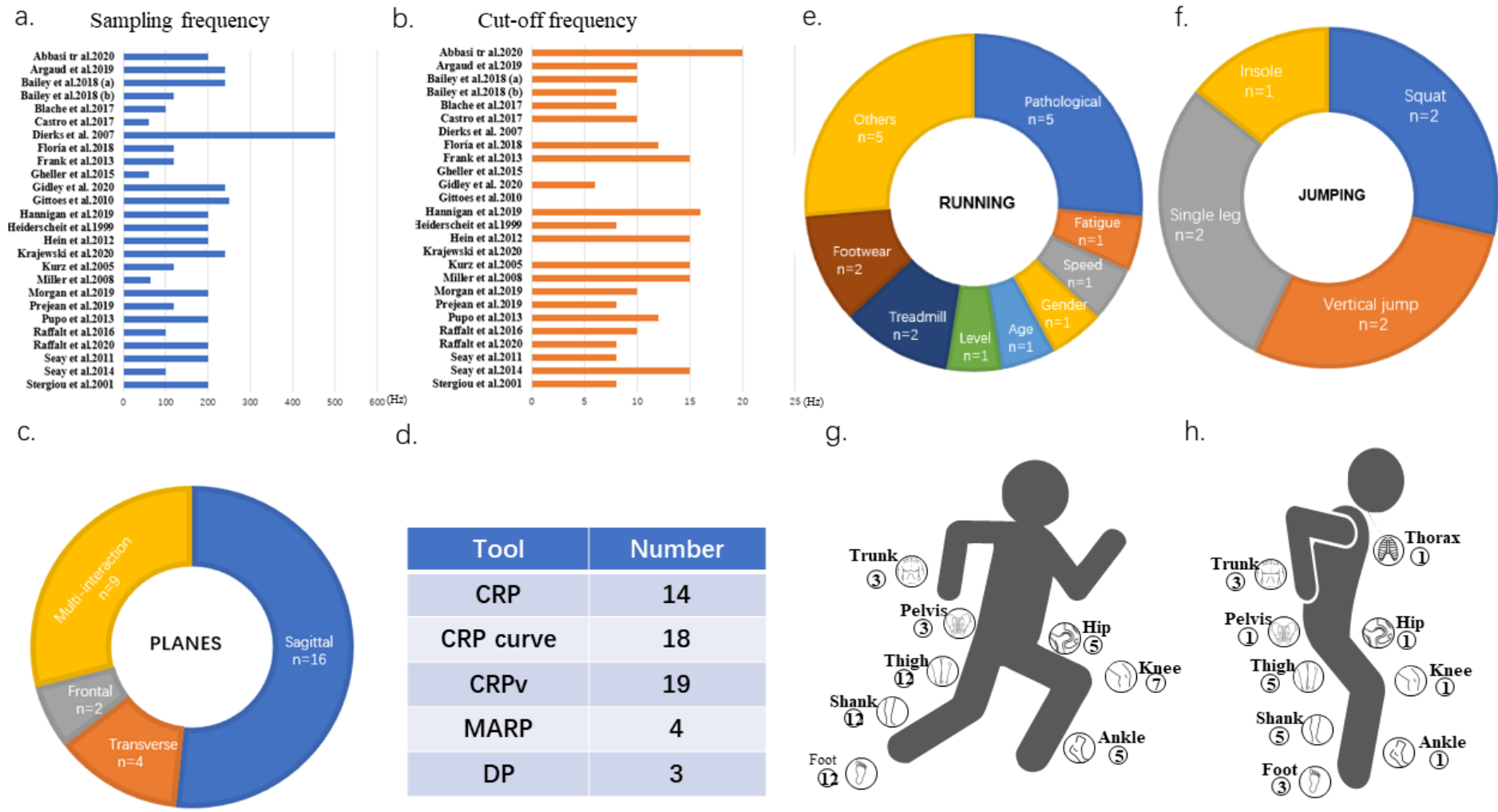


Figure 2-2. Summary of CRP application

Table 2-2. Experiment setting and models

Studies	Sampling frequency (Hz), Equipment	Cut off frequency (Hz), Filtering algorithm	Planes	Model
Abbasi et al.2020	200, (Noraxon, Scottsdale, AZ, USA)	8,4th order low-pass Butterworth	Multi-interaction	Foot, Shank, Thigh
Argaud et al.2019	100, (Ueye, IDS UI2220SE-M-GL; IDS Imaging Development System GmbH, Obersulm, Germany)	15,4th order low-pass Butterworth	Sagittal	Foot, Shank, Thigh, Head/Arms/Trunk (HAT)
Bailey et al.2018 (a)	200, (Bonita; Vicon Motion Systems Ltd., Oxford, UK)	8,4th order low-pass Butterworth	Multi-interaction	Thigh, Shank, Foot
Bailey et al.2018 (b)	200, (Bonita; Vicon Motion Systems, Centennial, CO, USA)	8,4th order low-pass Butterworth	Multi-interaction	Thigh, Shank, Foot, Knee
Blache et al.2017	100, (Ueye, IDS UI-2220SE-M-GL; IDS Imaging Development Systems GmbH, Obersulm, Germany)	10,4th order low-pass Butterworth	Sagittal	Ankle, Knee, Hip
Castro et al.2017	200, (Oqus 300, Qualisys, and Gothenburg, Sweden)	12,4th order low-pass Butterworth	Sagittal	Thigh, Shank, Foot
Dierks et al. 2007	120, (model 370, VICON, Oxford, UK)	8,4th order low-pass Butterworth	Multi-interaction	Foot, Shank, Thigh
Floria et al.2018	200, (Bonita-3, Vicon Motion Systems, Oxford, UK)	10,2nd order low-pass Butterworth	Multi-interaction	Hip, Knee, Ankle, Foot
Frank et al.2013	64, (NDI, Waterloo, ON)	15,4th order low-pass Butterworth	Sagittal	Hip, Knee, Ankle
Gheller et al.2015	120, (ELPH 500HS Canon)	15,4th order low-pass Butterworth	Sagittal	Trunk, Thigh, Shank
Gidley et al. 2020	240, high-speed digital camera.	NR,2nd order low-pass Butterworth	sagittal	Head/Arms/Trunk (HAT), Thigh, Shank, Foot.
Gittoes et al.2010	200, (CODA, 6.30B-CX1)	15,4th order low-pass Butterworth	sagittal	Ankle, Knee, Hip
Hannigan et al.2019	200, (Motion Analysis Corp., Santa Rosa CA)	8,4th order low-pass Butterworth	Transverse, sagittal	Pelvis, Thigh Shank;
Heiderscheit et al.1999	200, (NAC, Burbank, CA)	16,4th order low-pass Butterworth	Multi-interaction	Thigh, Shank, Foot



Hein et al.2012	250, (Vicon peak, MCAM M1, Oxford, UK)	NR, Quintic spline algorithm, mean square error of 2 mm <sup>2</sup>	Multi-interaction	Hip, Knee, Ankle
Krajewski et al.2020	240, (ProReflex, Qualisys AB., Gothenburg, Sweden)	6,4th order low-pass Butterworth	Transverse	Thorax, pelvis
Kurz et al.2005	60, one camera	NR, low-pass Butterworth, NR	sagittal	Foot, Shank, Thigh
Miller et al.2008	120, (Vicon Peak, Centennial, CO)	15, residual analysis	Multi-interaction	Thigh, Shank, Foot, Knee
Morgan et al.2019	120, (Qualisys AB, Gothenburg, Sweden)	12,4th order low-pass Butterworth	Sagittal	Hip, Knee, Ankle
Prejean et al.2019	500, (T40s; Vicon Motion Systems Lt., UK)	NR, NR	Multi-interaction	Thigh, Shank, Foot
Pupo et al.2013	60, (VPC-HD2000 Xacti, Sanyo Electric Co., Moriguchi, Osaka, Japan)	10,4th order low-pass Butterworth	Sagittal	Trunk, Thigh, Shank
Raffalt et al.2016	100, (Gazelle, Point Grey, Richmond, Canada)	8,4th order low-pass Butterworth	Sagittal	Thigh, Shank, Foot
Raffalt et al.2020	120, (Motion Analysis Corp., Santa Rosa, CA, USA)	8,4th order low-pass Butterworth	Sagittal	Thigh, Shank, Foot
Seay et al.2011	240, (Motion Analysis Corp., Santa Rosa, CA)	10,4th order low-pass Butterworth	Transverse, sagittal, frontal	Trunk, pelvis
Seay et al.2014	240, (Motion Analysis Corp., SantaRosa, CA).	10, low pass Butterworth	Sagittal, transverse	Trunk, pelvis
Stergiou et al.2001	200, (NEC, USA, Nashville, TN,USA)	13-16 sagittal& 16-20 frontal, low pass Butterworth, 13-16Hz sagittal& 16-20 Hz frontal	Frontal, sagittal	Foot, Shank, Thigh

---

NR: not reported.

Table 2-3. Outcomes for reviewed running studies

Studies	Participants; Level;shod;warm-up; Test protocol	Outcome
Abbasi et al.2020	13 F &7 M;  Recreational; yes; NR;  Ran for 10 m overground and on a treadmill at 20% slower and 20% faster than the preferred speed.	CRP Treadmill ↓ overground in Thigh fle/ex -Shank fle/ex both IN fast & slow conditions during entire stance phase Fast ↓ slow in Thigh fle/ex -Shank fle/ex in both treadmill & overground during late swing phase  Treadmill ↓ overground in Thigh ab/ad - Shank fle/ex in fast & slow conditions during midstance phase Fast ↑ slow in Thigh ab/ad - Shank fle/ex in treadmill & overground conditions during late stance phase  Treadmill ↑overground in Shank fle/ex - Foot fle/ex in fast & slow conditions during heel contact & midstance phase Fast ↑ slow in Shank fle/ex - Foot fle/ex in treadmill & overground conditions during late stance phase & entire swing phase  Treadmill ↑overground in Shank fle/ex - Foot ir/er in fast & slow conditions during midstance phase Fast ↓slow in Shank fle/ex - Foot ir/er in treadmill & overground conditions during mid stance& entire swing phases  CRPv Treadmill ↔ overground in fast & slow conditions Fast ↔ slow in treadmill & overground conditions Higher velocities↑ lower velocities in stride frequency Higher velocities↓ lower velocities in CM-drop & CM-rise PRV ↑PRV +0.5 & PRV+1.0 in CM-rise ↔ Knee fle/ex in all velocities at Foot contact& toe-off
Bailey et al .2018 (a)	14 (9 M & 5 F);  Recreational; NR; yes;	

Running for five velocity conditions included: preferred running velocity (PRV),  $PRV - 0.25 \text{ m}\cdot\text{s}^{-1}$ ,  $PRV + 0.25 \text{ m}\cdot\text{s}^{-1}$ ,  $PRV + 0.5 \text{ m}\cdot\text{s}^{-1}$ , and  $PRV + 1.0 \text{ m}\cdot\text{s}^{-1}$ .

↔Peak Knee flexion in all velocities during stance.

CRP

Thigh ir/er-Shank ab/ad during loading phase, ↑ or ↓NM

↔ for other couplings and velocities.

CRPv

Fastest condition ( $PRV + 1$ ) ↓  $PRV$  &  $PRV - 0.25$  in Thigh fle/ex -Shank fle/ex during loading phase

Higher velocities ↓ lower velocities in Thigh fle/ex -Shank fle/ex during propulsive phase & mid stance & toe-off & peak Knee flexion

Higher velocities ↓ lower velocities in Thigh fle/ex-Foot pf/df during toe-off & loading phase & propulsive phase & peak Knee flexion

Shank ab/ad-Foot in/ev significantly different at toe-off, ↑ or ↓ NM

↔All other couplings.

CRP

10K2min ↔10K4min in Thigh fle/ex- Shank ir/er in high-PF in all intervals during terminal swing phase

10K2min ↓ 10K4min in Thigh fle/ex- Shank ir/er in low-PF in T2 T4 intervals during terminal swing phase

10K2min ↓ 10K4min in Thigh fle/ex- Shank ir/er in low-PF in T4 intervals during early stance

10K2min ↔10K4min in Thigh ab/ad-Shank ir/er in high-PF in all intervals at Foot contact

10K2min ↑ 10K4min in Thigh ab/ad-Shank ir/er in low-PF in T4 interval at Foot contact

10K2min ↓ 10K4min in Knee fle/ex—Foot pf/df in high-PF in T3 intervals during Last stance

10K2min ↔10K4min in Knee fle/ex—Foot pf/df in low-PF in all intervals during Last stance

10K2min ↔10K4min in Knee fle/ex-Foot in/ev in high-PF in all intervals at Foot contact

Bailey et al. 2018 (b) High-PF (6 M & 3 F): Low-PF (5 M & 6 F);

Recreational; NR; yes;

1-hour run with velocity intervals at 75% of estimated 10 k race pace (5 minutes) and estimated 10 k race pace (1 minute).;

Dierks et al. 2007	20 M & 20 F;  Recreational; yes; NR;  Ran along a 25 m runway at a speed of 3.65 m/s (SD 5%).	10K2min ↓ 10K4min in Knee fle/ex-Foot in/ev in Low-PF in T3 interval at Foot contact Low-PF ↑ High-PF in Knee fle/ex-Foot in/ev at the start of the intervals at Toe-off 10K2min ↔ 10K4min in Knee fle/ex-Foot in/ev in high-PF in all intervals at Toe-off 10K2min ↑ 10K4min in Knee fle/ex-Foot in/ev in Low-PF in T2interval at Toe-off No significant results CRP Out of phase relationship at heel-strike & toe-off In phase relationship beyond maximum loading of the Leg.  CRPv Greatest at the periods around heel-strike& toe-off Smallest just beyond maximum loading.
Floria et al. 2018	10 F athlete runners: 12 F non-runners;  High calibre/Recreational; yes; yes;  Ran at a self-selected speed on treadmill for 30 s.	Runner ↑ control in speed for comfortable pace CRP Runner ↔ control of all couplings during stance Runners ↓ control in Hip ab/ad – Knee flex/ex during midstance Runners ↑ control in Knee flex/ex – Ankle flex/ex during pre-swing CRPv Runner ↔ control of all couplings during stance Runners ↓ control in Knee flex/ex – Ankle flex/ex during midstance Runners ↓ Hip ab/ad – Knee flex/ex control during terminal Runners ↓ Knee flex/ex – Ankle in/ev control during pre-swing
Frank et al. 2013	10 healthy M;  Recreational; yes; yes;  Trial one in own shoe (Pre), trail two in minimal shoe (Minimal), trail three in own shoe (Post)	Minimal ↔ Pre & Post in RPE scores in 5 & 10 min ↔ Foot, Ankle, Knee, Hip Angles at Heel Contact for First 100 & Last 100 strides in 3 shoe condition CRPv ↔ for First100, Middle100& Last100 strides in 3 shoe conditions in Foot-Shank & Shank-Thigh during stance phase
Gidley et al. 2020	11 heel-strikers (6 M & 5 F);  Recreational; yes; yes;	RT ↑ CT in oxygen consumption & stride frequency RT ↓ CT in Contact time RT deck at Foot strike, CT deck throughout the contact phase RT ↑ CT in KLeg (Leg stiffness) & dorsiflexed ankle & flexed Knee

	Ran on two treadmills: compliant deck treadmill (CT) (NordicTrack® X11i Incline Trainer) & rigid deck treadmill (RT) (FreeMotion® i11.9 Incline Trainer)	RT ↔ CT in global center of mass height CT touch down & first half contact phase CRP RT ↑CT in segments (Shank-Thigh& Foot-Thigh), joints (Knee-Hip, Ankle-Hip) during push-off phase RT ↓CT in Thigh-HAT& Ankle-Knee during push-off phase CRP <sub>v</sub> RT ↓CT in Shank-Thigh& Foot-Thigh& Shank-Foot& Ankle-Hip during push-off phase RT ↓CT in Shank-Thigh& Foot-Thigh& Ankle-Hip during extension phase CRP Knee-Ankle ↑Hip-Knee out of phase coordination in step phase in sagittal plane Touch down ↑ toe off out of phase relationship
Gittoes et al.2010	6 M athletes; High-calibre; yes; yes; Four sprint running trials.	CRP <sub>v</sub> Knee-Ankle ↓ Hip-Knee in step phase in sagittal plane
Hannigan et al.2019	30 (15 M& 15 F); Recreational; yes; yes; Ran at preferred pace for 20 continuous laps of approximately 40-meters in the laboratory.	CRP <sub>v</sub> Male ↔ female Pelvis-Thigh for all phases in frontal plane. Male↓ female Pelvis-Thigh Loading response in transverse plane Male ↔ female Pelvis-Thigh for other phases in transverse plane Male↓ female in Thigh-Shank in Loading Response in sagittal plane Male↓ female in Thigh-Shank in Pre-Swing in sagittal plane Male ↔ female in Thigh-Shank for all phases in frontal plane ↔ genders Divided group by LQ (Low Q-angle) & HQ (High Q-angle)
Heiderscheit et al.1999	16 M & 16 F; NR; yes; NR; Male ran at a velocity of 3.83 m·s <sup>-1</sup> ± 5.0%, Female ran at a velocity of 3.6 m·s <sup>-1</sup> ± 5.0%.	CRP <sub>v</sub> LQ ↔ HQ all couplings during stance phase

Hein al.2012	et	18 healthy F& 18 ITBS F; Recreational; yes; NR;	CRP <sub>v</sub> ITBS ↔ control during stance phase. ITBS ↑ control in Hip ab/ad–Knee flex/ex during the 4th sub-stance phase.
Kurz al.2005	et	7 valid trials on a 13 m EVA foam runway at speed of 3.3 m/s (±5%). 7F, 3 M ACL; 10 healthy matched as control; Recreational; NR; yes; Walked and ran on treadmill.	ACL ↔ control in walking & running speed MARF ACL ↑ control in Foot-Shank in walking ACL ↓ control in Shank-Thigh in walking
Miller al.2008	et	8 health:8 ITBS; Recreational; yes; yes; Ran on treadmill with pace exhaust them within 20 min	ACL ↓ control in Foot-Shank in running ITBS ↔ control in fatigue time CRP <sub>v</sub> ITBS ↑ control in Knee flex/ex -Foot ad/ab in GC at the start of the run ITBS ↓ control in Thigh ad/ab–Foot in/ev& Thigh ad/ab–tibia ir/er in GC at the end of the run  ITBS ↑ control in Knee flex/ex–Foot ad/ab at the start of swing phase ITBS ↓ control in Thigh ad/ab–tibia ir/er at the start of swing phase ITBS ↑ control in Knee fle/ex–Foot ad/ab at the end of swing phase ITBS ↓ control in Thigh ad/ab–tibia ir/er & Thigh ad/ab at the end of swing phase  ITBS ↑ control in Knee fle/ex–Foot ad/ab at the start of stance phase ITBS ↑ control in Knee fle/ex–Foot ad/ab at the end of stance phase
Hannigan al.2019	et	30 (15 M& 15 F); Recreational; yes; yes; Ran at preferred pace for 20 continuous laps of	ITBS ↓ control in Tibia ir/er–Foot in/ev at start of heel strike CRP <sub>v</sub> Male ↔ female Pelvis-Thigh for all phases in frontal plane. Male ↓ female Pelvis-Thigh Loading response in transverse plane Male ↔ female Pelvis-Thigh for other phases in transverse plane

		approximately 40-meters in the laboratory.	Male↓ female in Thigh-Shank in Loading Response in sagittal plane Male↓ female in Thigh-Shank in Pre-Swing in sagittal plane Male ↔ female in Thigh-Shank for all phases in frontal plane
Prejean al.2019	et	10 MF & 10 RF distance runners;  Recreational; yes; yes;  Ran on a treadmill at 5 and 7 mph (2.24 and 3.13 m/s) in each Footwear, high cushioning (HI; Hoka Stinson One One), low cushioning (LW; New Balance Minimums), and no cushioning (barefoot) (NO).	Subjects' foot strike (RF for rear foot runner, MF for mid foot runner), shod cushioning factors (HI, LW, NO) ↔ speeds for all factors, then results focused on 5 mph (2.24 m/s) ↔ foot strike patterns for shod conditions CRPv ↔ Footwear conditions ↔ FS patterns (RF MF)
Raffalt al.2020	et	5 M & 6 F;  Recreational; yes; yes;  8 trials of 3 min walking at 0.89, 1.12, 1.34, 1.56, 1.79, 2.01, 2.24 and 2.46 m. s <sup>-1</sup> & 8 trials of 3 min running at 1.79, 2.01, 2.24, 2.46, 2.68, 2.91, 3.13 and 3.35 m. s <sup>-1</sup> in randomized order of both speed & gait mode.	CRP plot visibly altered between the Footwear conditions in both groups CRP Low & high ↑ intermediate walking speeds in Thigh-Shank Low ↑ high & intermediate running speeds in Thigh-Shank  Walking ↓ running (means in phase)  Higher ↓ lower speed in walking & running in Thigh-Foot DP Intermediate ↓ high & low walking speeds in Thigh-Shank & Thigh-Foot. Higher ↓ lower running speeds in Thigh-Shank & Thigh-Foot
Seay al.2011	et	low back pain (LBP 14): resolved low back pain (RES 14): control 14;  Recreational/ LBP; NR; yes;  Walking at 0.8 m/s, speed increments of 0.5 m/s to 3.8 m/s. Transition from a walk to a run at comfortable speed.	LBP ↔ control & RES in preferred running speed CRP LBP ↓ RES & control in pelvis-trunk (more in phase) in walking in Frontal plane (p=.064, es=0.74 for RES group) LBP ↓ RES & control in pelvis-trunk (more in phase) in running in Transverse plane CRPv LBP ↓ control in pelvis-trunk

Seay al.2014	et	LBP 14; RES 14; control 14; Recreational; NR; NR; Ran at 2.3 m/s, speed increments of 0.5 m/s to 3.8 m/s.	LBP ↔ RES& control in preferred running speed CRP LBP ↓ control in pelvis-trunk (more in phase) in running in sagittal & transverse planes CRPv ↔for all
Stergiou al.2001	et	10 healthy M & 3 F runner; Recreational; NR; yes; Ran at baseline pace under four conditions.: level, obstacle of 5%,10%and15% height of the standing height. Impact (from the contact to minimum force) and active period (from minimum force to the 2nd maximum force)	NO (no obstacle)-5%Obstacle-10%Obstacle-15%Obstacle larger obstacle ↑ no obstacle in impact force MARP NO ↑ 10%Obstacle during impact period in sagittal plane 10%Obstacle ↓15%Obstacle during impact period in sagittal plane ↔for all groups during active period in sagittal plane NO ↑10%Obstacle& 15%Obstacle during impact period in frontal plane ↔for all groups during active period in frontal plane DP ↔for all groups during impact & active periods in sagittal & frontal planes

In participants, NR: not reported; M (F): male (Female); ITBS: iliotibial band syndrome; LBP: low back pain; RES: resolved pain group; ACL: anterior cruciate ligament; MF(RF): mid foot (rear foot) runner; Low (High)-PF: low (High) perceived fatigue; LQ (HQ): low (high) quadriceps angle; SP(1,2,3,4,5): Sub-phase (1,2,3,4,5). For outcomes. Abbreviation for couplings' movements (ab/ad: abduction/adduction; flex/ex: flexion/extension; in/ev: inversion/eversion; ir/er: internal rotation/ external rotation/df: plantarflexion/dorsiflexion). CM-drop: enter of mass vertical position at initial foot contact to the lowest vertical position during stance; CM-rise: the rise of center of mass from the lowest vertical position to toe-off. For those symbols (↓, ↑ & ↔), A "↓ (↑)" B represents "A" is significantly smaller (larger) than "B". "A" ↔ "B" represents that there is no significant difference among "A" and "B", single "↔" symbol represents there is no significant difference among all groups (groups number ≥3).



### *Application in running studies*

Table 2-3. Outcomes for reviewed running studies and Figure 2-2. Summary of CRP application depict the attributes of CRP during running. Of the 19 studies reviewed that utilised CRP variables in running, the focus areas included pathological conditions (5 records), gender and age differences (2 records), and running related factors: speed (1 record), footwear (2 records), level and fatigue (2 records), conditions (2 records), and other test conditions (5 records). The majority of the studies under review examined the thigh, shank, and foot segments (12 records each). Subsequently, there were seven instances focused on the knee, five instances on the ankle, five instances on the hip joints, and three instances on other body parts (three on the trunk and three on the pelvis). (Table 2-2, Table 2-3. Outcomes for reviewed running studies, Figure 2-2. Summary of CRP application).

### *Comparison between healthy and patient*

Among the 19 reviewed articles, 5 conducted comparisons between patient groups and healthy populations to identify differences. The examined medical conditions, contained iliotibial band syndrome (ITBS, 2 records), lower back pain (LBP, 2 records), and ACLR ( 1 record). ITBS is commonly acknowledged as an injury from excessive use impacting the outer knee, and it is believed to interfere with the leg CRP profile. In one study, ITBS-afflicted runners displayed decreased and increased CRPv in the thigh and knee respectively, when compared to their healthy counterparts [111]. In a separate investigation, there were no changes in CRPv observed between female ITBS runners and healthy runners [110].

Trunk-pelvis coordination is frequently impacted by LBP [114, 115]. In a study,

participants from three groups: the LBP group, reduced pain group, and normal control group, participated in running trials. The findings reported the LBP participants exhibited higher in-phase coordination patterns in the transverse and frontal planes and decreased variability in CRP than the other two groups [114]. In a subsequent study that assessed the influence across multiple movement planes, it was observed individuals with LBP exhibited increased in-phase features in coordination patterns compared to the control group. However, CRPv revealed no changes across all couplings [115].

ACLR is believed to affect the coordination during movement [65]. In an early study focusing on gait, it was observed that individuals who underwent ACLR demonstrated a decrease in MARP within the shank-thigh coupling during walking. Conversely, they displayed an increase in MARP within the shank-foot pair during gait than the health individuals [65].

### *Footwear effects*

Two studies examined the impact of footwear types on CRP [108, 113]. In a study where participants ran in minimalist shoes versus their regular footwear, the perceived workload, joint angles, and variability of CRP showed no changes during the stance phase [108]. While focusing on the impact of mid-foot padding effects on running on a treadmill in the two types of runners in other studies, it was observed that the foot drop profiles of the two groups remained unchanged by variations in midsole cushioning. Concerning CRP measurements, although alterations were evident in CRP plots across different mid-foot padding conditions for the two groups, the variability of CRP values exhibited statistical consistency [113].

### *Influence of running speed*

The kinematics and kinetics of running are significantly influenced by running speed. In an experimental setting, participants engaged in treadmill running at five different speeds, it was observed that while the lower limb CRP value remained consistent across speeds, the CRPv notably decreased with increased speed [107]. Although CRP appears to be insensitive to variations in running speed, employing CRPv is more appropriate in these contexts.

### *Effects of gender and age*

Two studies were included in this category, focusing on the impact of age and gender on CRP [109, 112]. In the first record [109], changes in the variability of CRP were observed when comparing females to males. In the second record, an older demographic was found to have reduced habitual running speeds, horizontal GRFs, vertical GRFs, and CRPv values in lower limb couplings in several phases [112].

### *Running level and fatigue*

Running performance is frequently influenced by factors such as running experience and fatigue [106, 121]. In a study, it was noted that experienced runners exhibited larger CRP and its variability at different gait speeds. In contrast, the control group exhibited stable CRP and CRPv values regardless of speed [121]. In terms of fatigue, there were

notable shifts in CRP and CRPv corresponding to varying fatigue levels [106]. Thus, fatigue emerges as a crucial factor influencing running coordination.

### *Effects of treadmill*

Two studies examined the impact of treadmill usage on coordination [116, 122]. When contrasted with overground running, treadmill use modified the lower limb's CRP, though CRPv remained largely unchanged [116]. When comparing running on a treadmill with a stiffer surface to a softer surface treadmill, it resulted in increased oxygen intake, cadence, and stiffness of the leg. Furthermore, a decrease in lower limb CRPv was observed during both the push-off and extension phases [122].

### *Others*

Five studies examined coordination patterns across various activities: walking vs. running, healthy running, sprinting, obstacle crossing, and among individuals with varying quadriceps angles [120, 123, 124, 130, 133]. Two of these studies [120, 123] outlined the typical coordination patterns observed in healthy runners. In running, the study observed that the majority of out-of-phase patterns appeared during the heel strike and toe off events, whereas in-phase patterns were more prevalent after the leg's maximum loading event [120]. In comparison to running, walking exhibited reduced CRP in healthy individuals [133]. The study on sprinting highlighted shifts in intralimb coordination, as evidenced due to alterations in CRP and its variability within lower limb couplings [123]. Stergiou et al. (2001) studied 13 runners navigating an obstacle

crossing task and posited that observed coordination alterations could serve as compensatory mechanisms to minimize injuries [130]. One record reported the effects of quadriceps angles (Q-angles) on CRP and found that there were no significant variations in coordination patterns between individuals with low and high Q-angles [124].

### ***Summary of running studies***

Of the 19 records analyzed, 13 reported the CRP curve for the entire GC or just the stance time. Additionally, 10 studies reported on CRP, while 15 focused on CRPv. The MARP (2 records) and DP (2 records) were only reported by limited records (Table 3). It's worth noting that no changes in the variability of CRP were observed in relation to footwear or Q-angle effects. However, various factors, including medical conditions, gender, age, running speed and proficiency, perceived workload, and treadmill usage, notably influenced overment coordination, as indicated by the findings of CRP tools.

### ***Applications in jumping studies***

Table 2-4. Outcomes for reviewed jumping studies and Figure 2-2. Summary of CRP application present the utilisation of CRP in jumping, encompassing jumping types (6 records) and insoles (1 records). The predominant focus in the analysed jumping studies was on the thigh (5 records) and shank (5 records) segments. Additionally, there were investigations involving the trunk (3 records), foot (3 records) segments, as well as other body parts such as the thorax (1 record), pelvis (1 record), hip (1 record), knee (1

record), and ankle (1 record).

Table 2-4. Outcomes for reviewed jumping studies

Studies	Participants; level; shod; warm-up; Test protocol	Outcomes
Argaud al.2019	et 20M young; 21M older;  Recreational; NR; yes;  3 maximal squat jumps	Young ↑ older in jump height MARF Young ↔ older in Ankle-Hip Young ↓ older in Ankle-Knee & Knee-Hip CRP <sub>v</sub> Young ↓ older in Ankle-Knee & Ankle-Hip & Knee-Hip
Blache al.2017	et 12M ACL; 12M healthy;  High-calibre; no; yes;  3 barefoot single-Leg squat jumps. Healthy (DL, NDL) ACL (IL, NIL)	DL ↔ NDL in vertical jump height IL ↓ NIL in vertical jump height CRP DL ↔ NDL in each coupling IL ↓ NIL in Ankle-Knee & Ankle-Hip CRP <sub>v</sub> DL ↔ NDL each coupling IL ↑ NIL Ankle-Knee and Knee-Hip
Castro al.2017	et 20 university students (10 M & 10 F);  High-calibre; yes; yes;  Five successful jump-landing trials. insole stiffness: Asker C-40 (soft), Asker C-65 (stiff), and non-insole	↔ for shoe conditions in Foot-Shank CRP & CRP <sub>v</sub> CRP & CRP <sub>v</sub> Women ↓ men in Foot-Shank in non-insole condition, Women ↔ men in Foot-Shank in stiff & soft conditions. ↔ in Shank-Thigh shoe condition & gender
Gheller al.2015	et 20M volleyball & basketball players;  High-calibre; NR; yes;	CMJ test in three angles: CMJ<90 & CMJPREF ↑ CMJ>90 in jump height & relative vertical net impulse CMJ>90 ↑ CMJ<90 & CMJPREF in peak power & maximum force ↔ Rate of force development CRP

Krajewski et al.2020	14 M;	High-calibre; no; yes;	<p>SJs (squat jump): maximum Knee-flexion angle at 70° (SJ70), 90°(SJ90), 110° (SJ110);</p> <p>CMJs (counter movement jumps): relative Knee flexion at the end of the countermovement phase smaller than 90°(CMJ&lt;90); greater than 90° (CMJ&gt;90); &amp; a preferred position (CMJPREF)</p>	<p>↔ Thigh–Trunk &amp; Leg–Thigh during descent phase</p> <p>CMJ&lt;90 ↓ CMJPREF &amp; CMJ&gt;90 in Thigh–Trunk during ascent phase;</p> <p>CMJ&gt;90 ↓ CMJPREF &amp; CMJ&lt;90 in Leg–Thigh during ascent phase</p> <p>CMJ&lt;90 ↑ CMJPREF in Leg–Thigh during ascent phase</p> <p>SJ test in four angles:</p> <p>SJ70 &amp; SJPREF ↑ SJ90 &amp; SJ110 in jump height</p> <p>↔ Relative vertical net impulse</p> <p>SJ110 &amp; SJPREF ↑ SJ70 &amp; SJ90 in Peak power &amp; maximum force</p> <p>SJ110 ↑ SJ70 &amp; SJ90 &amp; SJPREF in rate of force development</p> <p>CRP</p> <p>SJ70 ↓ SJ90 &amp; SJ110 &amp; SJPREF in Thigh–Trunk</p> <p>SJ90 ↓ SJ110 in Thigh–Trunk</p> <p>SJ70 ↑ SJ90 &amp; SJ110 &amp; SJPREF in Leg–Thigh</p> <p>↔ (SJ90 &amp; SJ110 &amp; SJPREF) in Leg–Thigh</p> <p>CRP</p> <p>Pelvis/thorax only plot, no quantified results.</p>
Pupo et al.2013	20M athletes;	High-calibre; NR; yes;	<p>Jump in a clockwise direction from their right Leg and counterclockwise from their left Leg.</p> <p>30 s of maximal countermovement vertical jumps. Jumps were divided into ten deciles.</p>	<p>Larger deciles ↓ smaller deciles in jump height (second, seventh, ninth, tenth decile)</p> <p>Larger deciles ↓ smaller deciles in power output (third, seventh, eighth, ninth, tenth decile)</p> <p>↔ vertical stiffness (beginning-sixth decile);</p> <p>Larger deciles ↓ smaller deciles in vertical stiffness (seventh-final decile)</p> <p>Larger deciles ↑ smaller deciles in ground contact time (third decile, seventh decile)</p> <p>Larger deciles ↓ smaller deciles in maximum Knee flexion (final decile)</p> <p>Larger deciles ↓ smaller deciles in maximum Hip flexion (second decile)</p> <p>CRP</p> <p>↔ in Trunk–Thigh during eccentric phase</p> <p>Larger deciles ↓ smaller deciles in Trunk–Thigh during concentric phase</p> <p>↔ in Thigh–Leg during eccentric &amp; concentric phase</p>



Raffalt al.2016	et	10 healthy men; 10 healthy boys;  Recreational, yes; NR;  9 maximal countermovement jumps (own sport shoes)	<p>CRPv Larger deciles ↑ smaller deciles in Trunk–Thigh in eccentric &amp; concentric phases ↔ in Thigh–Leg during eccentric phase Larger deciles ↑ smaller deciles in Thigh–Leg during concentric phase Adult ↑ Children in jumping height &amp; mean vertical force &amp; mean power during concentric phase.</p> <p>Adult ↔ Children in take-off time, duration of the eccentric phase &amp; duration of the concentric phase, rate of power development &amp; rate of force development</p> <p>Adult ↓ Children in variation in jumping height, take-off time, duration of the concentric phase &amp; duration of the eccentric phase, mean vertical force &amp; mean power during the concentric phase.</p> <p>Adult ↔ Children in the variation of the rate of power development &amp; rate of force development</p> <p>MARP Adult ↔ Children in Thigh–Shank &amp; Shank–Foot &amp; Foot–Foot coordination pattern throughout take-off phase. Adult ↓ Children in Thigh–Thigh &amp; Shank–Shank</p> <p>Adult ↓ Children for Intra-subject variability in Thigh–Shank &amp; Shank–Foot, Thigh–Thigh &amp; Shank–Shank couplings. Adult ↔ Children for Intra-subject variability in Shank–Shank coupling Adult ↓ Children for Inter-subject variability in Thigh–Shank &amp; Shank–Foot for both left &amp; right sides.</p>
--------------------	----	--	--

---

In participants, NR: not reported; M (F): male (Female); ACL: anterior cruciate ligament. For outcomes, DL: dominant limb; NDL: non dominant limb; IL: injured limb; NIL: non injured limb. For those symbols (↓, ↑ & ↔), A “↓ (↑)” B represents “A” is significantly smaller (larger) than “B”. “A” ↔ “B” represents that there is no significant difference among “A” and “B”, single “↔” symbol represents there is no significant difference among all groups (groups number ≥3).

### *Influence of jump types*

Among the seven reviewed studies, six delved into various jump types. These studies encompassed various jumping types, including single-leg jump (2 records), vertical jump (2 records), and squat jump (2 records). Investigations focused on the effects of knee take-off angles and age on the coordination during squat jump [117, 134]. In a comparison between younger and older adults [117], it was observed that younger adults jumped higher and displayed reduced MARP, variability of CRP in the knee-hip, and ankle-knee couplings. When analysing CRP, it was noted that smaller take off angles resulted in out-of-phase between the leg-thigh coupling when considering coordination aspects [134].

Two studies on vertical jumps investigated the effects of fatigue and age. In the context of fatigue conditions, the coordination between the thigh-leg segment remained unchanged, the trunk-thigh coupling showed an enhanced in-phase pattern [126]. Another study [128], a notable increment in the variability of CRP was observed, particularly in the shank-foot and thigh-shank couplings on two lower limbs, when comparing children to adults. This finding aligns with a previous [117] that revealed older adults exhibited greater coordination variability in squat jumps.

Two additional studies included in the review focused on individuals who had undergone ACLR and their performance in single-leg jumps, specifically the unilateral 180° jump [118, 125]. In the ACLR group, the injured leg demonstrated reduced CRP and increased variability of CRP in knee-ankle and hip-ankle, but the control group

showed no changes in any of these couplings [118]. In another study that focused on jump coordination, CRP tools were used to assess the pelvis-thorax coupling during the unilateral 180° jump. While different patterns were noticeable in the profile, these alterations did not attain statistical significance [125].

### *Insole*

One of the reviewed studies investigated the effects of different insole types on landing movement [135]. Findings revealed that there were no changes in foot-shank CRP and its variability among the various foot orthoses types. In the non-insole condition as well as the stiff and soft insole conditions, women exhibited a decrease (or no change) in CRP and CRPv within their foot-shank couplings. Across all three insole conditions (non-insole, stiff insole, and soft insole), the shank-thigh coupling exhibited stability in both male and female groups.

### ***Summary for jumping studies***

Of the studies examined, seven depicted the CRP curve throughout the GC or during the stance phase, and five of the studies employed CRP (4 studies) and CRPv (4 studies) as their main metrics. Also, two of the studies integrated MARP (2 studies) and DP (1 study). Footwear's effect was not statistically significant on the assessed CRP metrics (Table 2-4. Outcomes for reviewed jumping studies ). Effects like age, ACLR, angles of knee starting position, and fatigue notably alter coordination during jumping.

#### ***2.1.4.4 Discussion***

This research delivers an exhaustive overview of current literature related to CRP methods applied to running and jumping activities. Findings suggest that CRP metrics can adeptly identify shifts in coordination patterns caused by various interventions. Our investigation highlights the criteria and analytical procedures for CRP metrics. Additionally, it offers a thorough review of interpretations concerning two major movement activities.

#### ***Selection of CRP model and filtering method***

Utilisation of the model of CRP varied on the choice of segments, joints, and the application of different filtering methods at varying frequencies and algorithms, which is influenced by the specific task and movement plane under investigation. Pertaining to the development of the CRP model, the reviewed studies predominantly centred on segmental angles including the thigh, shank, and foot, and they also included joints such as the ankle, knee, and hip. Additionally, the findings often covered several planes or integrated multiple plane interactions. Thus, it becomes imperative to elucidate the criteria for selecting the models and plane for in various research. The initial method was introduced where they utilised angles of lower limb segments, to construct the foot-shank coupling and shank-thigh couplings [103]. Following research employed joint angle to compute CRP, and effectively demonstrated alterations of the coordination in the joints [108, 110, 121]. However, using the joint angle to develop the CRP model appears to deviate from the foundational idea that advocates for modelling segments as pendulums [59]. Considering the need for data from the shank segment for CRP in

knee-ankle across both angles, this could influence the accuracy of single joint angle estimates. Moreover, two studies [77, 78] emphasised the necessity of employing an external reference frame to facilitate more logical and interpretable results. They provided evidence supporting the superiority of establishing the CRP model through segments rather than joint angles.

Concerning the choice of movement plane, 26 of the reviewed studies constructed their models within one plane (e.g., transverse plane), while others incorporated interactions between several planes. In the initial research, multiple high-velocity cameras were employed to study sagittal plane motion while running [103]. This approach is intuitively comprehensible for understanding movements; consequently, subsequent studies primarily focused on projecting their movements within a single plane. Nevertheless, nine of the reviewed studies opted for the use of multiplane interactions [106, 107, 110, 111, 113, 116, 120, 121, 124]. Four of these nine studies selected this method due to the belief that the examined multiplane couplings held greater significance within their respective activities or participant populations [111, 113, 121, 124]. The remaining two studies did not provide a specific rationale [110, 120], while three studies based their choice of multiplane interaction on prior research [106, 107, 116]. Upon further examination of the aforementioned studies (excluding one citation for which only an abstract is available), it was observed that all studies made reference to two previous studies [103, 111]. It's worth noting that in these two studies, the first study exclusively focused on the sagittal plane in their study, whereas the other study justified their selection of multiplanes coupling by emphasising the relevance to the individuals with ITBS. Consequently, facts regarding the benefits of either approach remains uncertain. Therefore, upcoming studies should carefully consider their research

objectives and the specific activities involved to make informed decisions regarding the selection of movement planes, ultimately yielding more precise results.

In terms of the filtering approach, most studies utilised the Butterworth technique. The preference for this algorithm stems from its enhanced signal rise time capability, making it a popular option in human movement studies [136]. In the studies examined, the cut off frequency often varied between 6 Hz and 20 Hz. No single ideal frequency suits every test scenario, including diverse movement tasks and planes. As an example, a study under review highlighted the use of distinct frequencies for both sagittal and frontal planes [67]. In the future, researchers can determine the adequate cut off frequency by referring to factors, including experimental conditions, equipment, and planes of movement, to ensure the precision of signal processing.

### **Effectiveness of CRP**

Studies examined suggest that CRP instruments are proficient in detecting changes in coordination influenced by various biological factors (e.g., pathology, gender, age, running level) [65, 109-112, 114, 115, 121], task-related factors (such as fatigue and jump type) [106, 117, 126, 128, 134] and environmental conditions (e.g., treadmill surface and overground running) [116, 122]. Nevertheless, CRP tools seemed inadequate for assessing changes in coordination associated with footwear and insole effects [108, 113, 119].

As per the CRP definition [59], sensitivity was demonstrated for both global factors (such as environment and task) and local factors (pertaining to an individual's biology).

Changes in these factors prompt adjustments in the human NMSS as it strives to achieve a new state of equilibrium [60, 101]. It is evident that biological, task-related, and environmental factors can significantly impact individuals' coordination. Nevertheless, research on footwear and insoles indicated that the applied tools detected only minor changes, suggesting a similarity in lower limb coordination amidst varying footwear and insole scenarios [108, 113, 135]. Such phenomenon might be clarified by considering factors such as the participants' jump-landing proficiency [135], individual variations in response to midsole alterations and the relatively brief period available for footwear adaptation [108]. These investigations imply that the influence of footwear and insoles on coordination changes is minimal to negligible. Even though statistically significant changes were absent, the CRP plot allowed for the visual observation of trends in coordination among different footwear conditions [113].

A potential approach to enhance CRP sensitivity is to subdivide the target phase into several small phases [110, 121], or by analysing every specific point throughout the entire GC [116]. As an illustration, when considering ITBS, both CRP and its variability demonstrate consistent results across the full GC. But, alterations were reported in certain sub-phases [110, 121].

### ***Limitations and Recommendations***

A common suggestion for using the CRP method is to first compute it in the adequate model. Subsequently, these computed values aid in plotting the CRP profile. Additionally, the MARP for the specified phases could be calculated, which could cover the complete GC or solely the stance phase. Following this, researchers evaluate CRPv

across strides, requiring the computation of the SD of CRP for every time percent of the GC, and the DP is the averaged CRPv for the chosen time period. Yet, before classifying the in or out-of phase interactions between segments in the examined research, a vital detail demands elucidation. In other studies, the average CRP value was used to define the in or out-of-phase connection between segments, which differs from the application of MARP [120, 123, 128]. This way of calculation could potentially give rise to misinterpretations since the  $0^\circ$  value signifies an in-phase relationship, and any deviation from  $0^\circ$ , whether positive or negative, indicates an out-of-phase relationship. Categorising the negative and positive CRP values as "out-of-phase" might lead to misconceptions. In cases where the CRP values span from negative to positive, it's important to note that the mean CRP value in such circumstances may differ from the MARP, as the latter represents the mean of absolute values. As an example, in certain reviewed studies, the CRP coincided with the MARP because their CRP calculations fell within the range of  $0$ - $180^\circ$  [114, 115, 133]. Conversely, in additional reviewed studies, the CRP exhibited a broader range, spanning from  $-180^\circ$  to  $180^\circ$  [116, 118, 120-123, 126, 128, 134]. In the majority of these cases, the focus was primarily on tracking the increments or decrements in CRP [116, 118, 121, 122, 126, 134]. Hence, it becomes imperative to question the interpretability of relationships between couplings when they are quantified solely based on mean CRP values [120, 123, 128].

To the best of our knowledge, the interpretation of CRP tools is often regarded as challenging due to the complexity of their calculation and the non-intuitive nature of their interpretation [110]. CRP instruments integrate several biomechanical factors into an advanced variable, deriving knowledge from the central nervous system via phase



space exploration [59]. When employing CRP tools, it is imperative to establish a control group as a reference standard to ensure a valid interpretation of coordination across different conditions, including those involving pathological factors [103, 114, 115]. Alternatively, researchers may opt to focus solely on acquiring coordination features specific to particular groups [120] or activities [123, 125, 130].

In the context of utilising CRP tools, it is advisable to employ CRP curves as they facilitate the intuitive observation of dynamic changes in CRP. Additionally, MARP serves as a quantitative descriptor of the “in-phase” or “out-of-phase” nature, while CRPv and DP aid in clarifying the consistency of coordination schemes. Additionally, segmenting the examined phase into various sub-phases can potentially improve differentiation skills and allow a more detailed analysis of coordination dynamics during running and jumping.

#### ***2.1.4.5 Conclusion***

The CRP approach demonstrates efficacy in evaluating performances in running and jumping. CRP instruments facilitate observation of changes in control strategies and reactions to overarching elements (such as the environment and task) and local factors (pertaining to the individual's biology). Employing a modeling approach that relies on segment-based representation within a single movement plane and incorporating precise sub-phase analysis has the potential to enhance the sensitivity and interpretive capacity of CRP tools.

## **2.2 Brain activities**

### **2.2.1 Brain activities and electroencephalography during walking**

The brain, being a complex organ, generates its own electrical signals. The source of these signals can be attributed to the synchronised electrical activity of neurons, cells capable of electrical excitation. Neurons transmit messages through electrochemical signalling, generating measurable electric currents when electrodes are placed on the scalp [137]. EEG operates on this principle, enabling the non-invasive recording of brain activity.

EEG records voltage fluctuations caused by ionic currents in neurons of the brain [138]. Specifically, EEG identifies synchronised neuronal activity with a similar spatial orientation. Signals detected on the scalp reflect the collective activity of thousands to millions of neurons [137]. The EEG technique possesses a significant temporal resolution, measured in milliseconds, allowing for the real-time observation of neural activity.

EEG recordings reveal various patterns of rhythmic brain activity. Notable frequency bands in EEG studies are delta (1-4 Hz), theta (4-8 Hz), alpha (8-12 Hz), beta (12-30 Hz), and gamma (>30 Hz) [138]. These waves indicate synchronised neuronal network activity. Alpha waves manifest during quiet rest, whereas beta waves relate to active thinking and attention [137].

EEG demonstrates distinct advantages in the analysis of cognitive processes during gait, as compared to slower techniques [139]. EEG is a method that can capture the rapid neural dynamics responsible for cognition, perception, and behaviour, occurring within milliseconds. This follows the temporal scale at which our mind operates, such as visual

processing happening within a range of 50-100ms. EEG, measuring cortical activity via voltage fluctuations, offers greater precision in neural processing than fMRI's indirect blood flow signals. EEG oscillations mirror the rhythmic patterns of neural firing, with mechanisms revealed in invasive animal studies [140]. The multidimensionality of EEG data allows for hypothesis testing based on neurophysiology, connecting findings with invasive animal research and computational models. The cognitive functions are suitably mapped to the neural spaces by the multidimensionality of EEG, given the brain's multidimensional neural representations. EEG's temporal precision, direct cortical measurement, neural oscillation capture, and multidimensional analysis collectively make it potent for understanding intricate neural mechanisms behind cognition and behaviour. The capacity of EEG to directly and precisely probe mind dynamics with multidimensional neural data provides insights that cannot be achieved by slower, indirect methods [139].

### **2.2.2 Mobile EEG: Artifacts Removal of EEG during walking**

EEG captures a time series of voltages at electrode locations. It directly reflects voltage fluctuations due to brain activity [141]. Walking introduces multiple physiological and mechanical artifacts that affect EEG readings [142]. Cable movements or device interferences can lead to electrical artifacts [143]. Muscle activity, eye movements, and cardiac signals are sources of physiological artifacts [144]. Faster walking speeds amplify the artifacts' intensity and complexity [143]. Research on EEG during treadmill walking reveals artifacts spanning various frequencies, aligned with the stepping rhythm. Walking at an increased pace leads to the emergence of higher frequency artifacts and intricate harmonic patterns, presenting obstacles in their identification and

removal [142]. In conclusion, the occurrence of substantial EEG artifacts during walking makes it problematic to isolate cortical signals [143].

Several techniques aim to eliminate walking artifacts from EEG [145]. Low and high-pass filtering, although basic, often proves insufficient when used in isolation artefacts [145]. Advanced techniques encompass blind source separation (BSS) with tools like independent component analysis (ICA), canonical correlation analysis (CCA), singular spectrum analysis (SSA), and newer methods such as artifact subspace separation (ASR) [146]. Among them, ICA-based algorithms, notably adaptive mixture independent component analysis (AMICA), are predominantly used [143]. Yet, the ideal parameters remain undefined. Research suggests using high-pass filtering over 1.5 Hz before ICA decomposition and employing more electrodes (minimum 64) for faster walking to effectively isolate artifacts [146]. While ASR supports real-time applications, it demands parameter adjustments for peak performance. CCA effectively addresses muscle artifacts, but combining it with other techniques enhances its efficacy [145]. In essence, while current techniques are promising, their efficacy during walking remains to be fully assessed.

Combining the artifact removal techniques tend to improve performance over individual techniques. Effective combinations like ICA + ASR, CCA + ICA, CCA + ensemble empirical mode decomposition (EEMD), and CCA + SSA utilise complementary methods [145]. Yet, clear guidelines on choosing techniques based on walking speed and specific EEG features remain elusive [147]. There's a need for more research to methodically assess techniques for locomotion EEG data. Thoughtful experimental design, combined with integrated hardware and software, promises better

removal of intricate walking artifacts in EEG [148].

### **2.3 Summary and formulation of research scope**

Gait coordination profiles, especially in the context of prosthetic gait rehabilitation, are of great interest in the fields of rehabilitation science and neurology. This process involves learning a new gait post-amputation, often coupled with NMSS adaptations. After an amputation, individuals face the challenge of adopting a distinct gait pattern from their previous walking style [149]. This is not just about a new walking technique; it is a deep relearning process requiring specialised training and physiotherapy [150]. Regarding the adaptations of NMSS, the human body undergoes significant NMSS changes post-amputation [151]. This process of adaptation is driven by neuroplasticity, which is the brain's capacity to reorganise and establish new neural connections [152]. Neuroplasticity plays a crucial role in the establishment of new control pathways, thereby aiding the body in achieving balance during gait [153]. Studies have shown that prosthetic gait modifications lead to immediate alterations in gait parameters, along with observable power modulations in cortical rhythms during the adaptation process [154]. The brain's central role in gait adjustments is highlighted by modulations, particularly during the heel strike and swing phase [155]. These findings highlight the necessity for a comprehensive rehabilitation approach that encompasses both the physical and neurological dimensions of gait relearning [156].

Traditional gait rehabilitation programs have often emphasised typical gait analysis, but they often overlook coordination evaluation. Historically, these programs centred on individual joint analysis, neglecting the complex coordination of multiple body parts in

human locomotion [157]. A single movement, such as walking, involves the coordinated action of several body parts, from the feet to the trunk [158]. Focusing solely on isolated joints overlooks coupling effects, or how joints and body parts coordinate during motion [151]. In prosthetic gait studies, even if specific kinematic parameters are met with prosthetic joints, overall coordination may vary from natural gait [159]. This emphasises the requirement for an approach that considers both individual joints and their interactions during gait in rehabilitation.

In conclusion, understanding the coordination dynamics of gait in individuals with uTFA is extremely important, especially when it comes to gait rehabilitation and prosthesis design. Firstly, examining coordination patterns in both running and walking for those with uTFA is essential. This analysis can demonstrate the variation in coordination between individuals with uTFA and AB individuals. This insight reveals how the body adjusts its movements post-amputation to approximate natural gait. Emphasis is on the complex interplay of joints and muscles. Secondly, it is crucial to consider the connection between coordination patterns and EEG during gait. Adapting to a prosthetic limb, individuals with uTFA experience brain changes to accommodate new movement dynamics. Analysing EEG patterns during gait offers insights into active neural mechanisms. This sheds light on brain-prosthetic limb coordination, aiming for comfortable walking or running. These insights contribute to the development of prostheses that align with the neural patterns of the user, thereby enhancing a natural and comfortable walking motion.

## CHAPTER III OVERVIEW OF SUB-STUDIES

Based on the literature review and the research questions, this study regarding gait features of individuals with uTFA was segmented into three sub-studies (Figure 3-1) in Chapters four to six.




	Study 1	Study 2	Study 3
<b>Topic</b>	Walking coordination	Sprinting coordination	Neural coordination connectivity
<b>Data type</b>	Motion + Force	Motion + Force	Motion + EEG
<b>Participants</b>	14 uTFA 14 control	7 uTFA	12 uTFA 12 control
<b>Illustration</b>			

Figure 3-1. Illustration of the three sub-studies

The first sub-study assessed the coordination dynamics of individuals with uTFA while walking. This study included 14 individuals with uTFA and their age matched AB individuals.

The second sub-study focused on evaluating coordination dynamics during running. This study included 7 individuals with uTFA to perform maximum speed sprinting. It should be noted that there is a limited number of individuals with uTFA who can perform sprinting.

Both the two sub-studies employed the CRP method on the segment angles of lower limbs to analyse coordination patterns. These coordination patterns may illustrate changes in the NMSS, aiding in understanding prosthetic gait coordination. Identifying coordination dynamics in individuals with uTFA during walking and running can enhance prosthetic gait rehabilitation and prosthesis design.

The third sub-study aligned individuals' EEG during gait with their gait patterns. Brain signals during walking were directly compared to coordination patterns. This study aimed to bridge neuroscience and biomechanics concerning movement control. The origin of movements lies within the CNS, whereby brain signals may serve as potential indicators of movement control. Coordination reflects the NMSS's control strategy. Grasping the link between brain signals and coordination patterns can help to decode movement patterns.



## CHAPTER IV WALKING COORDINATION

### 4.1 Summary of the study

Comprehending the coordination of persons with uTFA when ambulation is pivotal to understanding their gait profile. The CRP evaluation illuminates the coordination dynamics of the NMSS, based on motion joint/segment angles. This research recruited fourteen participants with uTFA and their similar age counterparts without amputations. During walking, segment angles and joint angles from the participants' lower extremities were derived. The the CRP values were then calculated from segment angles for both the thigh-shank segments and shank-foot segments. A statistical parametric mapping (SPM) test was used to compare the curves of the participants' lower limbs. Coordination patterns revealed compensatory strategies in two legs. For CRP in thigh-shank, different coordination features were observed in the two phases of gait. However, although both groups exhibited equivalent coordination throughout the GC, for the shank-foot coupling of individuals with uTFA of intact limbs, a brief foot-leading pattern was found during mid-stance. This differed significantly from other limbs, likely compensating for the reduced force from prosthetic limbs. The study provides standard coordination patterns for walking in individuals with uTFA, potentially aiding in rehabilitation of prosthetic gait and prosthesis advancement.

## 4.2 Introduction

Prostheses typically restore walking ability in people with uTFA. However, their walking patterns frequently show functional disparities in the lower limbs, setting them apart from individuals without impairments [15, 17]. Walking imbalances appear as differences in force production, duration of the stance phase, and angular variations in the lower extremities [13-16]. Compensation mechanisms account for some of these asymmetries. The amputated side, having lost major muscles and bones, exhibits reduced force generation, affecting kinetic parameters [29]. Moreover, the residual limb within the prosthetic socket may struggle to withstand high pressures during walking [30]. As a result, the unaltered limb exerts higher progression forces and impulses to offset the diminished force output of the prosthetic limb while walking [15]. Kinematically, the enhanced hip movement of the intact limb offsets the restricted flexion of the prosthetic knee during swing, leading to an extended stance phase for the unaltered limb [16]. Length of prosthetic gait rehabilitation and comfort with prostheses significantly influence the well-being of people with uTFA [14]. Gaining a thorough understanding of the prosthetic gait characteristics can improve gait therapy as well as prosthesis crafting, resulting in enhanced well-being for those with uTFA utilising prosthetics.

Owing to the absence of a limb, those with uTFA display modified walking patterns. Describing a movement directly is difficult and a practical approach is to build a sophisticated NMSS framework based on dynamic system theory [59]. Within gait analysis, the NMSS framework is perceived as a unified system facilitating energy flow. The movements of lower limbs and energy transfer mimic a dynamic system, characterised by pendulum-like structures moving in a sinusoidal pattern with steady

energy flow. To describe this dynamic system of the lower limb, only its current state and rate of change are required [59]. Dynamic system theory offers a quantitative approach, termed the CRP angle, to describe movement coordination [63]. Angular displacement represents the current state of the lower limbs, while angular velocity indicates its rate of change [59]. Separating the leg into sections like the foot, shank, and thigh and evaluating the angles based on a universal coordinate system, offers more accuracy compared to solely depending on joint angles [63]. CRP values can quantify the coordination dynamics between segments, reflecting the underlying control strategies. MARP and DP measure the CRP dynamics and their fluctuations during particular phases of gait, respectively[63].

Individuals with uTFA exhibit functional asymmetries in their gait profile due to compensatory mechanisms. Compensatory mechanisms manifest in various body parts [19]. While many recent studies have concentrated on individual joints [29], the coordination dynamics and coupling effects in the leg of those with uTFA are crucial. Such coupling effects illuminate the coordination processes steered by the CNS, deepening our understanding of gait traits in uTFA individuals. Few research works have ventured into exploring the coordination dynamics in the legs of people with uTFA [73-75]. Research has suggested that in the stance phase, the prosthetic limb had rises in DP in the knee-ankle coupling, while an inverse was seen in the swing phase [75]. Two additional research works applied CRP in evaluating prosthetic gait therapy and design, observing changes in coordination dynamics [73, 74]. Yet, these studies relied on calculation derived from joint angles, potentially conflicting with dynamic system theory principles [59]. The initial model was constructed using segment angles, favoured due to the pendulum foundation of the dynamic system [76, 77]. Notably, the

angle of the joint is defined relative to the angle of neighbouring segments. On the other hand, the pendulum model necessitates an external standard, such as a horizontal surface, instead of using relative reference points [77, 78]. A study employing the CRP model discerned that the segment angles exhibited greater sensitivity compared to joint angles [79].

Regarding prosthetic gait training and design, there is a considerable focus on the coordination dynamics in the legs of people with uTFA. Yet, when based on segment angles, these coordination patterns during walking remain ambiguous. The coordination profile during the GC represents changes in coordination dynamics at every percentage of gait. The research aims to understand the walking coordination profiles of lower extremities in people with uTFA, by contrasting them with the two limbs of AB individuals. Three hypotheses were proposed. First, in thigh-shank segments, a prosthetic limb will exhibit a greater MARP but reduced DP compared to the other three limbs (intact, left, and right). This is attributed to the prosthetic side's absence in synchronisation with the residual skeletal and body tissues. Second, in shank-foot coupling, a prosthetic limb will display reduced MARP and DP values compared to the other three limbs due to the passive nature and limited RoM of the shank and foot segments on the prosthetic side. The third hypothesis postulates that the right and left limbs of AB individuals will demonstrate similar MARP and DP values in both shank-foot and thigh-shank couplings, owing to functional and anatomical similarities between these limbs.

## **4.3 Method**

### **Participants**

This study included 14 participants with uTFA and 14 AB counterparts. Their mean age was  $32.6 \pm 10.2$  years, with an average height of  $1.65 \pm 0.10$ , weight of  $60.0 \pm 10.6$  kg, and an mean amputation duration of  $14.1 \pm 9.1$  years (Table 4-1. Demographic data). Silicone sleeves were used by all participants.

The inclusion criteria specified that participants must meet the following conditions: 1) be above 18 years old, 2) have uTFA, and 3) be free from CNS or NMSS complications, excluding amputation. Fourteen AB counterparts, chosen from a database, had an average age of  $32.5 \pm 9.5$  years, a weight of  $66.9 \pm 12.5$  kg, and a height of  $1.69 \pm 0.09$  meters [160]. The study received approval from the National Institute of Advanced Industrial Science and Technology (AIST)'s ethical review board and adhered to the guidelines outlined in the Declaration of Helsinki (1983). Before participating, informed consent was obtained, and all individuals were provided with detailed information about the research.

### **Equipment**

Motion data was obtained from motion capturing equipment (MX-T 160, Vicon, Oxford Metrics, UK). The sampling rate was set at 200 Hz and the capturing room contained 15 near infrared cameras. Nine AMTI force plates were embedded within a walkway (AMTI, MA, USA) were employed, and the sampling rate was set at 2000 Hz, to collect GRF data. Following a Helen Hayes marker set [161] (Figure 4-1), markers were labelled on the participants. Following this, they ran on a 10 meter walkway in a straight line at a preferred speed five times.

Table 4-1. Demographic data

Participant	Gender (M/F)	Age (y)	Height (cm)	Mass (kg)	Amputated side	Etiology	Time since amputation (y)	Residual limb length	Prosthetic knee	Prosthetic foot	Prosthetic history(y)	Exercise frequency (times/w)
1	M	24	176	63	Left	Trauma	2.7	Long	3R95	Valiflex	2.5	1
2	M	40	167	57.1	Left	Cancer	4	Long	3R106	Triton	4	1
3	M	52	170	66.6	Left	Trauma	29	KD	Intelligent	Lapoc J-foot	20	6
4	M	44	178.5	63.6	Right	Trauma	28	Short	3R80	Triton	0.1	2
5	F	38	148.5	43.9	Right	Infection	15	Long	Intelligent	Total Concept	12	4
6	M	21	167	56.4	Left	Cancer	18	Short	3R80	Valiflex	1.5	0.3
7	M	43	168	67.7	Left	Trauma	16	Middle	3R80	Valiflex	3	4.5
8	F	19	149	43.3	Right	Sarcoma	7.5	Short	3R106	1H38	4.5	5
9	M	33	167	62	Left	Trauma	16	Long	3R95	J-foot	15	5
10	F	32	156	47.4	Right	Trauma	6.5	Middle	Total knee	Total Concept	5	5
11	F	18	156	58.3	Right	Trauma	3.5	Middle	Total knee	Valiflex xc	1	5
12	M	32	180	83.7	Left	Cancer	24	KD	Genium Xtrem	1D35	5.5	6
13	M	26	175	66	Right	Trauma	5.2	Middle	3R80	Rflex Rotate	0.3	5
14	M	34	161	58.7	Left	Sarcoma	21	Middle	3R95	Valiflex	2.5	2
<b>Mean</b>	—	32.6	165.6	59.8	—	—	14	—	—	—	1.5	—
<b>SD</b>	—	10.2	10.3	10.6	—	—	9.2	—	—	—	1.1	—

Abbreviations: F: female; M: male; KD: knee disarticulation; SD: standard deviation; y: year; w: week. The residual limb length was categorized as: long when it constituted 2/3 or more of the original femur bone length; medium when it ranged from 1/3 to 2/3 of the original length; and short when it was equal to or less than 1/3 of the original length.

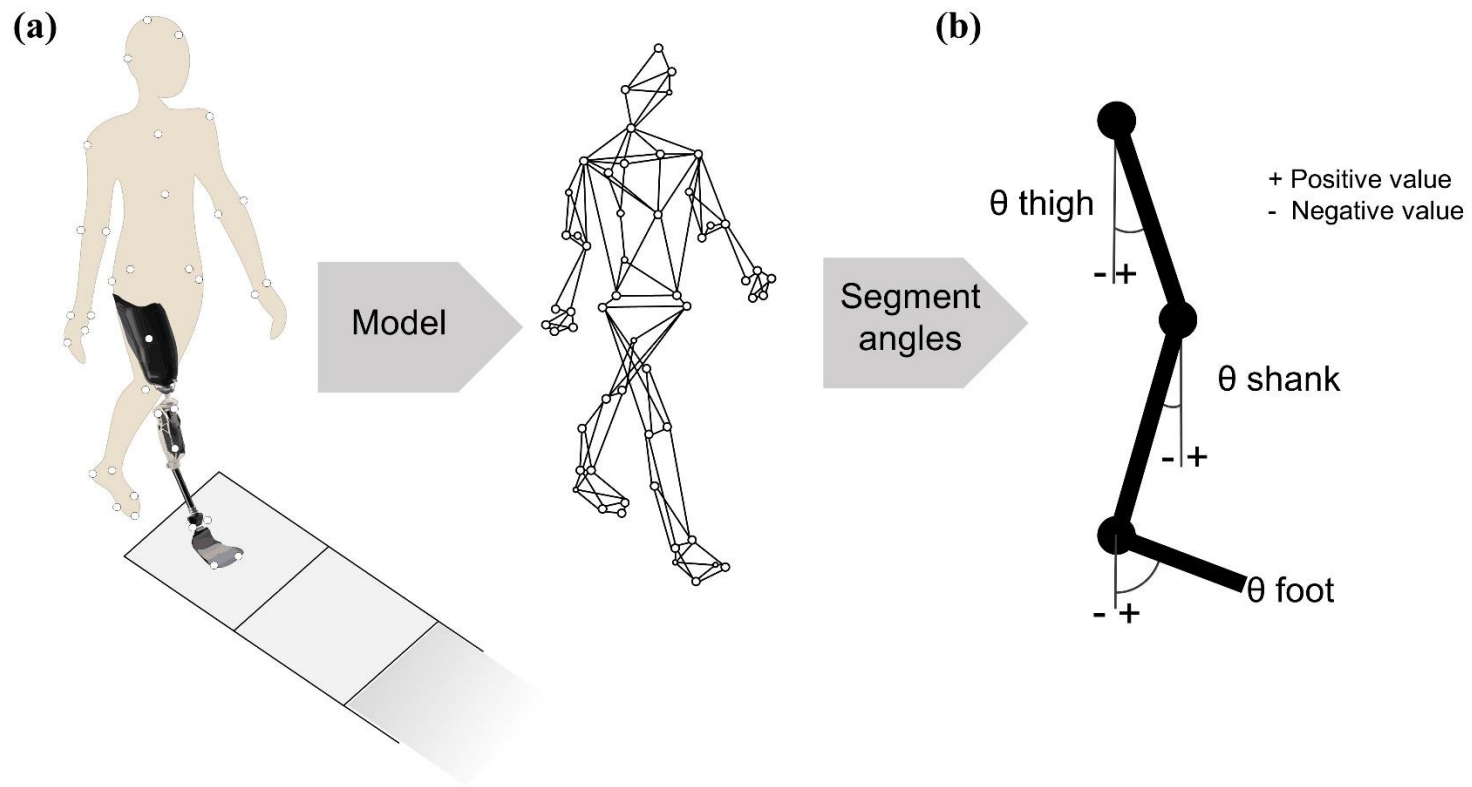


Figure 4-1. Retro-reflective marker locations and lower limb model (a) and the definition of the segment angles (b)

## Data processing

Data processing was carried out using the default software from Vicon Motion Capturing System (Oxford, UK). We applied a 4th order Butterworth filter with 50 Hz cutoff frequency to process the collected GRF data. The moments for initial contact and toe off were identified by setting 16 N as a threshold for vertical GRFs. For the motion data, a 4th order Butterworth low-pass filter with a 10 Hz cutoff frequency was employed. Finally, the time of the whole GC was transformed to 101 points with a linear normalisation.

For statistical analyses, four limbs were considered from both the uTFA and AB groups. For these four sets of limbs, we conducted calculations related to segment angles, CRP related parameters, and joint angles only in the sagittal plane. Segmental angles were acquired for coordination analysis. We defined the positive directions as hip flexion, knee flexion, and ankle dorsiflexion for joint angles. Concerning segment angles, we set 0 degrees with reference to a line perpendicular to the ground, designating the anti-clockwise direction as positive (Figure 4-1). Next, we investigated the CRP profiles in shank-foot and thigh-shank couplings. We calculated the RoM and peak values in the curves of the segment and joint angles..

The Hilbert transform was used to calculate CRP. Segment angles ( $\theta$ ) underwent normalisation (eq1) and were interpreted as a time series signal (eq2), with  $i$  and  $t$  denoting the respective data points. A house written script using MATLAB was utilised to execute the Hilbert transformation on the data in steps (eq3) and (eq4), with  $j$  representing the imaginary component. The phase angle (eq5) was calculated using the MATLAB 'unwarp' function. Although the arctan function produced phase angles within  $\pm 90^\circ$ , a full  $360^\circ$  range was necessary for polarised coordinates. The “unwarp”



tool was utilised to maintain the prior value and to avoid limiting it to the  $\pm 90^\circ$  range. The CRP angles for target coupling were calculated by using the PA of distal segment minus proximal segment (eq6). In cases where CRP angles exceeded  $\pm 180^\circ$ , we adjusted them to fall within this range by  $\pm 360^\circ$ . Then the CRP values obtained were applied to compute the DP and MARP using the equations (eq7) and (eq8). The DP and MARP assess the variability of the coordination and the general coordination patterns, respectively [162]. MARP close to  $0^\circ$  signifies an in-phase coordination pattern, whereas increasing distance from  $0^\circ$  indicates an out-of-phase pattern within the coupled segments. Regarding the DP, a notably big (or small) value of DP suggests inconsistent (or limited) motion coordination [63].

In CRP curves, a positive (negative) slope signifies that the distal (proximal) segment is leading the movement. CRP in shank-foot coupling and thigh-shank coupling were computed using the angles of the foot, shank, and thigh segments.

### **Statistical analysis**

To assess the normal distribution of the parameters, the Shapiro-Wilk test was performed. If the parameters meet normal distribution, we performed a one-way ANOVA to identify distinctions among the four lower limbs. Subsequently, we applied the Bonferroni post-hoc comparison for p-value adjustments and to determine specific differences. In cases of non-normally distributed data, we evaluated the distinctions using the Kruskal-Wallis test. We conducted these statistical analyses in SPSS (IBM SPSS Statistics 22, SPSS Inc., Chicago, IL), with an alpha level of 0.05. For the comparison among the profiles, we employed Statistical Parametric Mapping (SPM). To rectify p-values and assess significant variations among the four limbs, we employed the Bonferroni post-hoc comparison [163].

$$\bar{\theta} = \theta - \min(\theta) - \left( \frac{\max(\theta) - \min(\theta)}{2} \right), \quad (\text{eq1})$$

$$\theta(t) = \bar{\theta}_{(i)}, i = 1, 2, \dots, n, \quad (\text{eq 2})$$

$$H(t) = H(\theta(t)) = \theta(t) * \frac{1}{\pi t^2}, \quad (\text{eq 3})$$

$$\zeta(t) = \theta(t) + jH(t), \quad (\text{eq 4})$$

$$\phi_{rp} = \arctan \left[ \frac{H(t_i)}{\theta(t_i)} \right], i = 1, 2, \dots, n, \quad (\text{eq 5})$$

$$\phi_{CRP} = \phi_{rp-distal} - \phi_{rp-proximal}, \quad (\text{eq 6})$$

$$MARP = \sum_{i=1}^n \frac{|\phi_{i th-crp}|}{n}, i = 1, 2, \dots, n, \quad (\text{eq 7})$$

$$DP = \frac{\sum_{i=1}^n |SD_i|}{n}, i = 1, 2, \dots, n \quad (\text{eq 8})$$

#### 4.4 Results

Table 4-2 shows the outcomes of the parameters included in this study. Using SPM, the angle curves for the four limbs were contrasted. Differences in discrete parameters (DP values) were observed between the right and left limbs. However, based on the SPM outcomes, no distinctions were found between the profiles of the right and left limbs (joints angles and segments angles and CRP curves). Thus, the plots of the joints and

CRP encompass three lower limbs: the right limb of the AB individuals, and the intact and prosthetic limb of the individuals with uTFA (Figure 4-2, Figure 4-3, Figure 4-4).

### **Kinematics**

Table 4-2 displays the outcomes of the included data. No changes were obtained in joint and segment angles between the two lower limbs of AB individuals. However, a notable difference emerged in ankle plantar flexion angle, with the prosthetic limb significantly exhibiting lower values than other groups ( $p < 0.01$ , TI:  $34.76 \pm 7.50^\circ$ , TP:  $9.54 \pm 2.34^\circ$ , AR:  $25.68 \pm 7.65^\circ$ , AL:  $24.83 \pm 6.48^\circ$ ). Furthermore, a substantial reduction in ankle RoM was evident in the prosthetic limb relative to the other limbs ( $p < 0.01$ , TI:  $42.24 \pm 4.70^\circ$ , TP:  $17.74 \pm 3.25^\circ$ , AR:  $33.28 \pm 6.26^\circ$ , AL:  $32.96 \pm 5.80^\circ$ ). Regarding the minimum angle on the segments, no changes were found on the thigh segment among the four limbs ( $p = 0.15$ ). But the prosthetic side exhibited lower value in the shank segment compared to the other limbs ( $p < 0.01$ , TI:  $-54.16 \pm 4.38^\circ$ , TP:  $-60.22 \pm 4.21^\circ$ , AR:  $-55.58 \pm 2.65^\circ$ , AL:  $-55.21 \pm 2.67^\circ$ ). In the foot segment, significant differences were observed, with intact limbs showing smaller minimum segment angles and prosthetic limbs displaying larger value compared to the other limbs ( $p < 0.01$ , AR:  $-7.21 \pm 7.64^\circ$ , AL:  $-6.63 \pm 6.83^\circ$ , TI:  $-18.68 \pm 6.37^\circ$ , TP:  $3.59 \pm 6.80^\circ$ ). Additionally, the thigh segment on the prosthetic side had a higher RoM compared to the left and right limbs ( $p < 0.01$ , TI:  $52.07 \pm 3.76^\circ$ , TP:  $54.67 \pm 4.45^\circ$ , AR:  $49.67 \pm 3.76^\circ$ , AL:  $49.33 \pm 4.30^\circ$ ). Notably, larger RoM of shank in the prosthetic limb than the other three limbs were observed ( $p < 0.01$ , TI:  $77.00 \pm 4.67^\circ$ , TP:  $84.19 \pm 4.66^\circ$ , AR:  $76.94 \pm 3.53^\circ$ , AL:  $75.48 \pm 3.51^\circ$ ). As for the RoM in the foot segment, significant differences were observed between the individuals with uTFA and AB individuals ( $p < 0.01$ , TI:  $112.85 \pm 6.71^\circ$ , TP:  $87.27 \pm 5.14^\circ$ , AR:  $98.35 \pm 7.61^\circ$ , AL:  $96.91 \pm 7.41^\circ$ ).

The joint angles curves are presented in Figure 4-2. Notable variations in the hip angle profile are found within the initial 20% among the gait. During this phase, the multi-comparison test reveals greater flexion in the intact limbs compared to the prosthetic limbs. No significant difference is observed between the lower limbs of individuals with uTFA. In the knee joint profile, differences are apparent during the entire period. During early stance, reduced knee flexion is observed in the prosthetic limbs, a finding supported by the multi-comparison test using SPM. Furthermore, at around 90% GC, the prosthetic limbs reached the limitation on extension earlier than both the right and intact limbs. In the ankle profile, notable differences are evident at the conclusion of the terminal stance phase and the onset of the pre swing phase. The segment angle curves are presented in Figure 4-3. Thigh angle profile exhibits changes during the early stance phase and the swing phase. In the shank curve, significant changes are noted during the swing phase and early stance. The foot curve displays differences during the swing phase and mid-stance.

Table 4-2. Results of discrete parameters

Parameters	Limbs				Normality	p-value (Main)	Post-hoc					
	Intact	Prosthetic	CR	CL			CR-	CR-TI	CR-CL	CL-TI	CL-	TI-TP
<b>Peak Ankle D-flex</b>	7.49 ± 4.11	8.20 ± 2.36	7.60 ±	8.13 ±	N	0.71	—	—	—	—	—	—
<b>Peak Knee Flex</b>	61.02 ±	62.73 ± 8.25	63.02 ±	62.79 ±	Y	0.83	—	—	—	—	—	—
<b>Peak Hip Flex (°)</b>	35.94 ±	34.24 ± 5.42	32.09 ±	30.89 ±	Y	0.07	—	—	—	—	—	—
<b>Peak Ankle P-flex</b>	34.76 ±	9.54 ± 2.34	25.68 ±	24.83 ±	N	<0.01*	1	0.22	<0.01*	0.16	<0.01*	<0.01*
<b>Peak Knee Ext (°)</b>	1.68 ± 2.41	1.84 ± 1.59	-0.61 ±	-0.99 ±	N	0.07	—	—	—	—	—	—
<b>Peak Hip Ext (°)</b>	16.71 ±	18.35 ± 4.84	17.39 ±	17.91 ±	Y	0.89	—	—	—	—	—	—
<b>Ankle RoM (°)</b>	42.24 ±	17.74 ± 3.25	33.28 ±	32.96 ±	N	<0.01*	1	0.12	<0.01*	0.08	<0.01*	<0.01*
<b>Knee RoM (°)</b>	62.70 ±	64.57 ± 8.02	62.41 ±	61.80 ±	Y	0.6	—	—	—	—	—	—
<b>Hip RoM (°)</b>	52.66 ±	52.59 ± 5.51	49.48 ±	48.80 ±	Y	0.1	—	—	—	—	—	—
<b>Min Thigh (°)</b>	-21.79 ±	-22.85 ± 3.67	-20.54 ±	-20.47 ±	Y	0.15	—	—	—	—	—	—
<b>Min Shank (°)</b>	-54.16 ±	-60.22 ± 4.21	-55.58 ±	-55.21 ±	Y	<0.01*	1	1	0.01*	1	<0.01*	<0.01*
<b>Min Foot (°)</b>	-18.68 ±	3.59 ± 6.80	-7.21 ±	-6.63 ±	Y	<0.01*	1	<0.01*	<0.01*	<0.01*	<0.01*	<0.01*
<b>Thigh RoM (°)</b>	52.07 ±	54.67 ± 4.45	49.67 ±	49.33 ±	N	<0.01*	1	1	0.02*	1	0.02*	0.49
<b>Shank RoM (°)</b>	77.00 ±	84.19 ± 4.66	76.94 ±	75.48 ±	Y	<0.01*	1	1	<0.01*	1	<0.01*	<0.01*
<b>Foot RoM (°)</b>	112.85 ±	87.27 ± 5.14	98.35 ±	96.91 ±	Y	<0.01*	1	<0.01*	<0.01*	<0.01*	<0.01*	<0.01*
<b>MARP thigh-</b>	45.53 ±	53.52 ±	46.72 ±	47.58 ±	N	0.11	—	—	—	—	—	—
<b>MARP shank-foot</b>	18.93 ±	10.19 ± 3.40	21.17 ±	21.70 ±	N	<0.01*	1	1	<0.01*	0.67	<0.01*	<0.01*
<b>DP thigh-shank</b>	3.18 ± 1.34	1.73 ± 0.70	2.71 ±	1.77 ±	N	<0.01*	0.04*	1	0.03*	0.01*	1	<0.01*
<b>DP shank-foot (°)</b>	2.35 ± 0.94	0.71 ± 0.42	1.75 ±	0.99 ±	N	<0.01*	0.05*	1	<0.01*	<0.01*	1	<0.01*

Abbreviations: Y: Yes; N: No; Ext: extension; Flex: flexion; D-Flex: dorsiflexion; P-Flex: plantarflexion; RoM: range of motion; MARP thigh-shank: mean absolute relative phase of thigh-shank coupling; MARP shank-foot: mean absolute relative phase of shank-foot coupling; DP thigh-shank: deviation phase of thigh-shank coupling; DP shank-foot: deviation phase of shank-foot coupling. An asterisk (\*) indicates a statistical significance level at  $p < 0.05$ . CR-CL: post-hoc between control right limb and control left limb; CR-TI: post-hoc between control right limb and uTFA intact limb; CR-TP: post-hoc between control right limb and uTFA prosthetic limb; CL-TI: post-hoc between control left limb and uTFA intact limb; CL-TP: post-hoc between control left limb and uTFA prosthetic limb; TI-TP: post-hoc between uTFA intact limb and uTFA prosthetic limb.

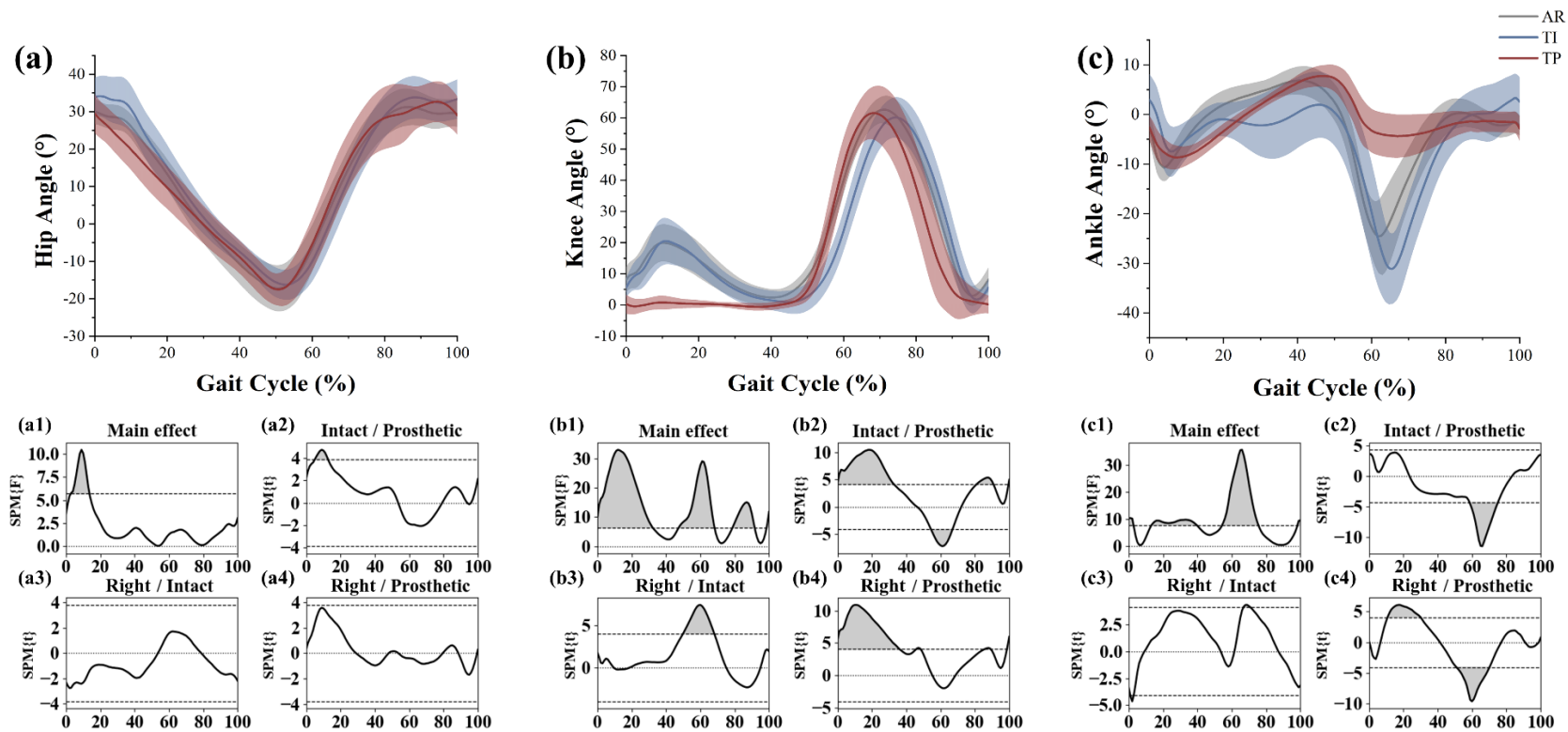


Figure 4-2. Results of joint angles and SPM analyses. The red and blue colors represent prosthetic limbs and intact limbs, respectively. The black color represents the right limbs of the control group. The a, b, and c are results for hip, knee, and ankle joints. In each joint angle, the top plots are the joint angle curves with standard deviations of the three limbs, while the bottom four plots are the SPM results with Bonferroni correction. The shaded parts indicate significant differences. The bottom first plots (a1, b1, c1) show the main effects among the four limbs (prosthetic limbs and intact limbs of the group with uTFA, left limbs, and right limbs of the able-bodied group). The bottom second plots (a2, b2, c2) show the statistical significance between intact and prosthetic limbs. The bottom third plots (a3, b3, c3) show the statistical significance between intact limbs and right limbs. The bottom fourth plots (a4, b4, c4) show the statistical significance between the right limbs of the control group and the prosthetic limbs.

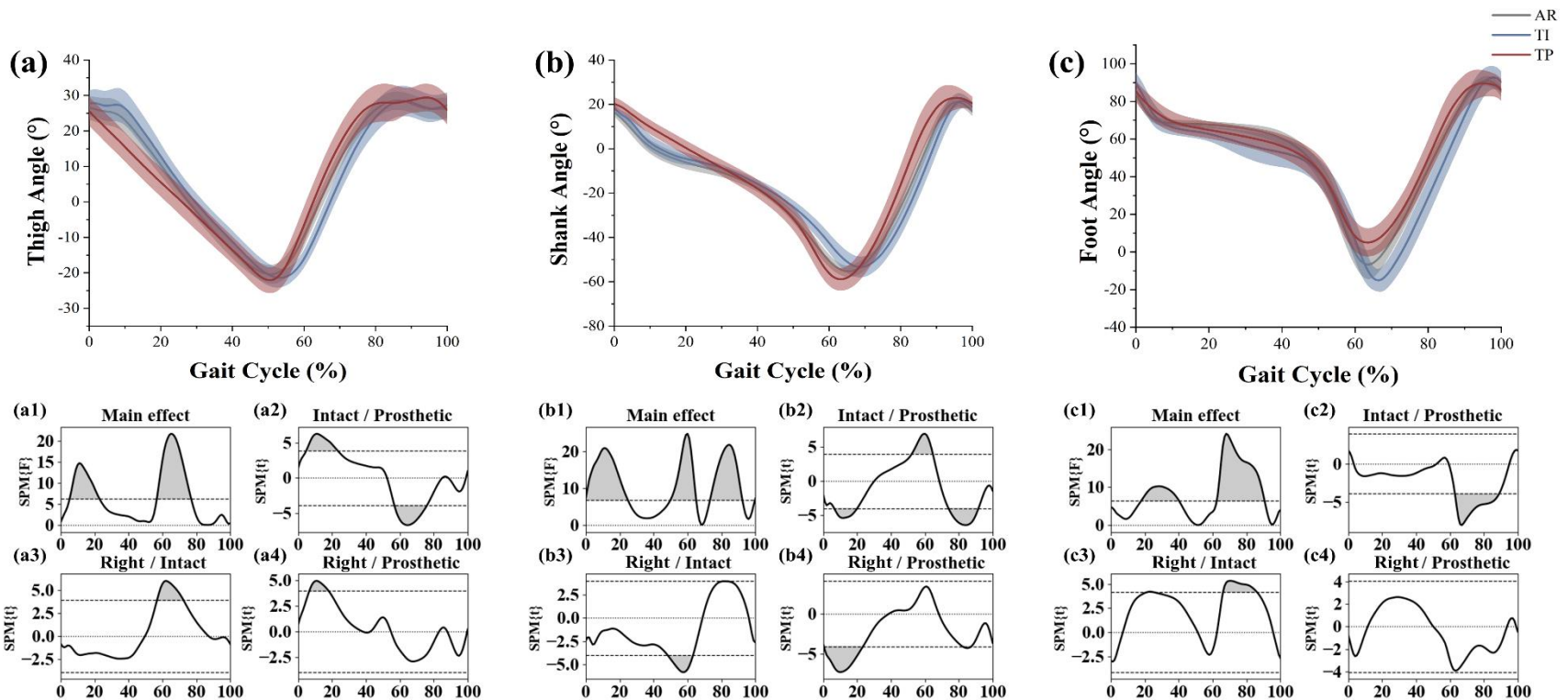


Figure 4-3. Results of segment angles and SPM analyses. The red and blue colors represent prosthetic limbs (TP) and intact limbs (TI), respectively. The black color represents the right limbs (AR). The a, b, and c are results for thigh, shank, and foot segments. In each segment angle, the top plots are the segment angle curves with standard deviations of the three limbs. The bottom four plots are the SPM results with Bonferroni correction. The shaded parts indicate significant differences. The bottom first plots (a1, b1, c1) show the main effects among the four limbs (prosthetic limbs, intact limbs, left limbs, and right limbs). The bottom second plots (a2, b2, c2) show the statistical significance between intact limbs and prosthetic limbs. The bottom third plots (a3, b3, c3) show the statistical significance between intact limbs and right limbs. The bottom third plots (a3, b3, c3) show the statistical significance between intact limbs and right limbs. The bottom fourth plots (a4, b4, c4) show the statistical significance between right limbs and prosthetic limbs.

### **Coordination features**

The MARP of the thigh-shank showed no notable difference among the four limbs (Table 4-2). In shank-foot, a significantly lower MARP was observed on the prosthetic limb than other three limbs ( $p < 0.01$ , TI:  $18.93 \pm 3.84^\circ$ , TP:  $10.19 \pm 3.40^\circ$ , AR:  $21.17 \pm 2.53^\circ$ , AL:  $21.70 \pm 2.87^\circ$ ). For the DP of thigh-shank, the prosthetic limbs and the left limbs showed similar values, as did the intact and right limbs. A significantly lower DP value was observed in the prosthetic and left limbs than in the intact and right limbs. For the DP of shank-foot, the right and intact limbs had no changes, and neither did the left and prosthetic limbs. But, the intact limb demonstrated a higher DP value than the prosthetic limb, and the right limb had a higher DP value than the left limbs ( $p < 0.01$ , TI:  $2.35 \pm 0.94^\circ$ , TP:  $0.71 \pm 0.42^\circ$ , AR:  $1.75 \pm 0.43^\circ$ , AL:  $0.99 \pm 0.49^\circ$ ).

The results of CRP curves are presented in Figure 4-4. Variability in the patterns of CRP thigh-shank profile are primarily observed before 60% of the gait. Between 0% and 25% GC, notable distinctions are evident when comparing both the right and intact limbs with the prosthetic limbs. Between 45% and 60% of the GC, significant changes emerge between lower limbs of individuals with uTFA. Initially, both the intact and right limbs exhibit a shank-leading coordination pattern, which transitions to a thigh-leading coordination pattern near the 10% mark of the GC, persisting until 60%. Subsequently, they return to the shank-leading coordination pattern for the remaining GC. In contrast, the prosthetic limb maintains a thigh-leading coordination pattern until 55% of the GC. They then switch to a shank-leading coordination pattern before 90%, after that they revert to a thigh-leading pattern towards the cycle's end. Importantly, the overall coordination pattern on the thigh-shank coupling had no significant changes



when compared with the right and intact limbs.

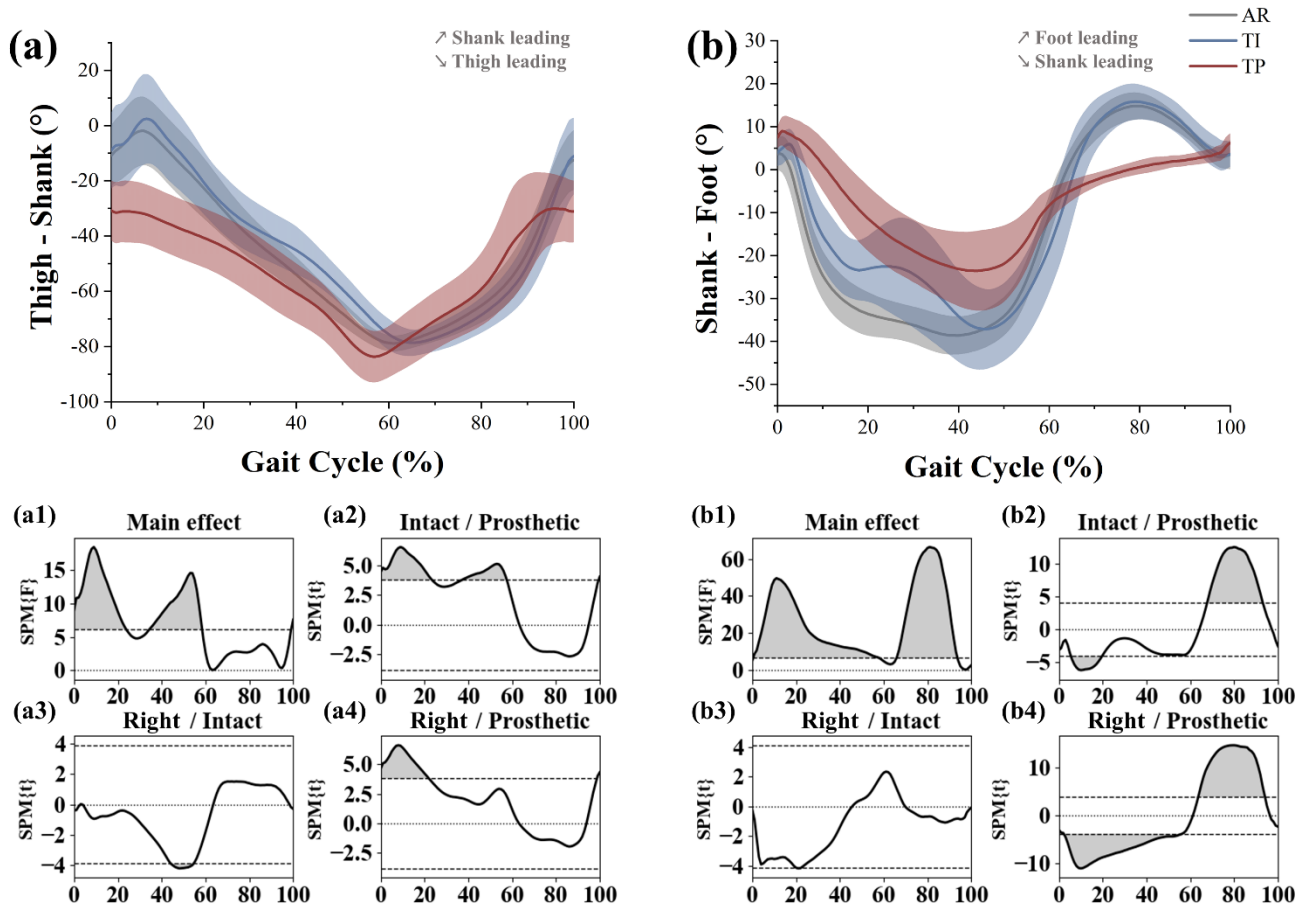


Figure 4-4. Results of CRP curves and SPM analyses. The red and blue colors represent the prosthetic limbs (TP) and intact limbs (TI), respectively. The black color represents the right limbs (AR). The a and b are the CRP curves for thigh-shank and shank-foot couplings. In each CRP curve, the top plots are the CRP curves with standard deviations of the three limbs. The bottom four plots are the SPM results with Bonferroni correction. The shaded parts indicate significant differences. The bottom first plots (a1, b1) show the main effects among the four limbs (prosthetic limbs, intact limbs, left limbs, and right limbs). The bottom second plots (a2, b2) show the statistical significance between intact limbs and prosthetic limbs. The bottom third plots (a3, b3) show the statistical significance between intact limbs and right limbs. The bottom fourth plots (a4, b4, c4) show the statistical significance between right limbs and prosthetic limbs.

Throughout the profile CRP shank-foot, distinct variations are observed. Notable variations between lower limbs are observed from roughly 5% to 20% and again during 70% to 90% of the GC in individuals with uTFA. Between 5% to 60% and 65% to 90% of the GC, marked discrepancies are seen between the right and prosthetic limbs. There are no pronounced variations between the intact and right limbs. During the initial stance, every limb follows a foot-leading coordination pattern, transitioning swiftly to the shank-leading pattern. During mid-stance, the intact limbs display a brief foot-leading coordination pattern at 20% of the GC, in contrast to the other three limbs. During the swing phase, the prosthetic limb maintains the foot-leading coordination pattern. Conversely, the other three limbs transition from foot-leading coordination pattern to shank-leading coordination pattern near 75% of the gait.

## **4.5 Discussion**

This research examined coordination in participants with uTFA and AB during ambulation. Three hypotheses centred on the shank-foot coupling and thigh-shank coupling interactions were proposed. Regarding context of thigh-shank interaction, the initial hypothesis posited that prosthetic limbs would exhibit a greater MARP and reduced DP compared to the other three limbs. Concerning shank-foot interaction, it was hypothesized that prosthetic limbs would display decreased MARP and DP values in comparison to the other three limbs. As for AB participants, it was anticipated that DP and MARP values across the lower limbs would be similar. Contrary to the first hypothesis, there were negligible MARP variations observed among all four limbs. However, the prosthetic and left limbs displayed reduced DP values when compared to

the intact limb and the right limb. The second hypothesis was partly rejected, as prosthetic limb demonstrated more synchronised coordination than other three limbs. Yet, only the prosthetic limb exhibited reduced DP values compared to the intact and right limbs. The third hypothesis received partial confirmation, as significant DP variations were found among the two limbs of AB participants.

Participants with uTFA display distinct gait patterns in the kinematics of their lower limbs, and these patterns are further illuminated through SPM analyses. Segment and joint angle curves observed in this research closely resemble the typical gait of prosthetic described in other researches [164, 165]. Particularly, prosthetic limbs exhibited a significantly restricted RoM and a reduced peak ankle plantar flexion angle compared to the other three limbs. This limitation in motion can be attributed to the passive nature of the prosthetic ankle joint, which lacks ankle plantar flexors for active propulsion [166]. No changes were revealed in the RoM or peak angle values for the knee and hip joints. However, a notable absence of knee flexion in prosthetic limb was observed at the initial stance. This strategy of limited knee flexion in prosthetic limbs helps prevent unintentional buckling due to excessive forces during weight-bearing [167]. Moreover, the analysis of segment angles revealed more disparities between lower limbs than joint angles did. While joint angles determine relation between neighbouring segments, the segment angles assess the rotation related to a environment coordinate. These findings suggest that the segment modelling offer greater sensitivity in identifying variations compared to joint modelling. This observation aligns with earlier research that utilised segment angles for CRP computation [77-79].

CRP tools reveal distinct gait patterns in individuals with uTFA, and the analysis of

MARP values in the thigh-shank coupling indicates consistent coordination patterns across the GC for all four limbs. Upon closer examination of the thigh-shank CRP curves, it is observed that prosthetic limbs do not transition from the shank-leading to the thigh-leading pattern in the stance phase, a feature that becomes evident in the swing phase when compared to intact and right limbs. This characteristic resembles a compensatory strategy seen in the sprinting gait of individuals with uTFA [162]. The thigh-shank coupling appears to employ this compensatory strategy, leveraging distinct coordination patterns in both the stance and swing phases to maintain consistent gait coordination. The passive nature of the prosthetic limb shank requires a reliance on the thigh-leading coordination pattern in the first half of stance to support weight [168]. Regarding variations in the swing phase, both right and intact limbs consistently adopt the shank-leading coordination pattern, preparing for a heel strike. However, as the GC progresses toward 90%, the prosthetic knee's limited extension capacity necessitates a shift to the thigh-leading pattern for support. Individuals with uTFA utilise distinct control mechanisms to maintain consistent thigh-shank coupling's coordination throughout the GC.

In the coupling of shank-foot, the coordination strategies observed in prosthetic limbs significantly differed from the other three limb types. Prosthetic limbs, as indicated by their MARP shank-foot values, adopted a more synchronised coordination profile throughout the gait compared to the other three limbs. Which suggests heightened synchronisation in the coupling of shank-foot segments on the prosthetic side [59]. It's important to note that increased synchronisation does not necessarily equate to superior coordination. The study revealed that the segments of foot and shank on the prosthetic side, being structures without active force generation, primarily rotated in response to

external influences. For instance, while an ambulation force is generated by the intact limb, the prosthetic limb's force deficiency is partially compensated by the force generation on the intact side [165]. In the profile of the CRP shank-foot coupling, the curve for prosthetic limbs approaches zero more consistently than others. The observation aligns with the notably reduced MARP on the shank-foot coupling seen in prosthetic limbs compared to the other limb types. Several distinct features were observed in these curves. Initially, it was observed that prosthetic limbs consistently exhibited foot-leading coordination pattern during the swing phase, in contrast to other limbs that transitioned to shank-leading patterns near the 80% mark of the GC. Prosthetic limbs were primarily influenced by inertial forces resulting from rotation and gravitational pull, leading to synchronised foot-shank coordination. In contrast, during the terminal swing, right and intact limbs preferred a shank progression to start the subsequent GC [169]. Consequently, prosthetic limbs did not exhibit a coordination pattern shift in the shank-foot coupling throughout the swing phase. A notable variation emerged during mid stance: while the coordination profile on the intact limb predominantly followed the shank-leading trend, it showed fluctuations between 20% to 40% of the GC, unlike the consistent shank-leading pattern seen in prosthetic and right limbs. This modulation could be attributed to a heightened foot-leading pattern during that phase, possibly correlated with the observed heel elevation in intact limb from the last two-thirds of stance. As the heel ascends, the intact limb exerts greater forces compared to a typical AB limb, resulting in a brief foot-leading coordination pattern [169].

The study sheds light on coordination pattern variability, offering deeper insights for both uTFA and AB participants. A greater DP could correlate with increased limb

activity, such as force generation, during walking. As per the CRP method's definition, a notably low DP value signifies limited coordination [63]. Earlier research on sprinting indicated greater restrictions in prosthetic limbs compared to intact ones [162]. This study's results imply that a modest DP can be within normal ranges, especially since the DP value aligns with prior research, and AB participants also showed a reduced DP in the left limb. A noteworthy observation is the disparity between the left and right limbs in AB participants. AB participants' limbs generally displayed comparable kinematic parameters and MARP values across two couplings. However, distinctions between the lower limbs became evident in the DP values. DP encapsulates the coordination pattern's variability and is known for its sensitivity in pinpointing coordination changes [63]. The study suggests potential variations between non-dominant and dominant limbs. While the dominant limb wasn't specifically recorded in this research, prior studies indicate that the majority likely favor the right limb [170]. It underscores the efficacy of CRP tools in identifying alterations related to movement.

Outcomes of this research provide valuable insights regarding coordination patterns of gait rehabilitation and prosthetic development. From a clinical perspective in gait rehabilitation using prosthetic, understanding the typical coordination patterns of lower limbs can establish a benchmark for training individuals using prostheses. Utilising the standard profile during gait using prosthetic of experienced persons with uTFA as a reference can help newcomers in mastering walking with prostheses and setting achievable goals. In terms of prosthetic design considerations, expecting a prosthetic limb to perfectly mimic the motion of an intact limb is not always practical, especially with traditional passive prosthetic limbs that lack actuators for segment control [162]. However, with the advancement of technology, including the development of advanced

exoskeletons or powered prostheses, motors can generate forces and torques using various control algorithms [171]. Optimising these control algorithms to align segments and coordinations with those of intact or AB limbs could lead to improved prosthetic designs.

There are multiple limitations to this research. Firstly, participants exhibited a range of amputation causes. Such variations are believed to impact specific gait metrics. As an example, vascular amputations are often associated with reduced walking speeds and briefer stride lengths than traumatic amputations [172]. Secondly, there was an inconsistency in the residual limb lengths among uTFA participants. Gait metrics might be influenced by femoral length, especially as shorter residual limbs correlate with increased hip abduction angles [173]. Thirdly, the research focused solely on kinematic data in the sagittal plane via CRP analysis. Future studies could explore other two planes, to expand our comprehension of walking coordination among uTFA individuals. Finally, the walking velocity is not consistent in this study, which might be a confounding factor. Future studies could consider using a fixed the walking speed.

To conclude, those with uTFA adopt adaptive methods during both the swing and stance phases. This strategy was reflected by the lower limb coordination patterns of the coupling in thigh-shank segments during ambulation. Given the reduced force in the prosthetic shank, it compensates with a thigh dominant pattern throughout the stance phase. Comparing to the intact limb, it transitions from a shank-dominant to thigh-dominant pattern in the same phase. While in swing phase, the prosthetic limbs change from a shank-leading coordination pattern to thigh-leading coordination pattern, while intact limbs consistently maintain a shank-leading coordination pattern. Differences in

the coordination characteristics help in attaining same coordinations during walking. In terms of the coupling of shank-foot segments, the inactivity of a prosthetic limb leads to improved in-phase coordination and alignment, in contrast to an intact limb driven by functional muscles. These observations provide fresh perspectives on prosthetic gait recovery and set the stage for advancements in prosthetic devices, enriching our grasp on lower-limb coordination dynamics.



## **CHAPTER V RUNNING COORDINATION**

### **5.1 Summary of the study**

It's crucial to comprehend the sprinting dynamics of those with uTFA to enhance the development of running specific prosthesis (RSPs) and rehabilitative gait training. Utilising CRP analysis, which stems from movement kinematics, we can dig deeper in the coordination patterns during in persons with uTFA. A group of seven participants with uTFA sprinted on a 40-meters track. This study measured parameters such as spatial-temporal, segment and joint angles of the participants with uTFA. CRP analysis was applied to shank-foot and thigh-shank couplings. Then, the asymmetry ratios were also calculated for these metrics. These parameters underwent statistical evaluation, contrasting the lower limbs. Notable variances were identified between the intact and prosthetic limbs in terms of proportion of the stance phase, stance duration, ankle joint angles, and CRP of the shank-foot coupling ( $p < 0.05$ ) in uTFA participants. Such differences mainly arise from the structural contrasts in the prosthetic and intact limbs of participants with uTFA. Even noticeable coordination differences were observed in stance and swing phases, the global coordination in the coupling of thigh-shank segments exhibited no marked difference between the lower limbs of uTFA participants. The findings suggest that uTFA individuals employ diverse adaptive strategies within coupling of thigh-shank segments throughout both the GC, targeting improved limb coordination symmetry.

### **5.2 Introduction**

Comprehending the profile of sprinting in persons with amputation holds significance

for advancing RSP designs and enhancing gait rehabilitation [174-176]. In sprinting, athletes strive to achieve their peak speed and sustain it throughout the race [177]. Running-specific prostheses enable individuals with amputation to regain some sprinting capability, albeit limited [178]. Yet, inherent differences stemming from limb loss persist between amputees and non-amputees, leading to variations in gait [17]. To bridge this structural gap, individuals with amputation must emulate similar movements using a distinctively different prosthetic limb. Additionally, they need to adjust and adopt novel movement patterns when using prostheses, in contrast to those without amputations [179].

Sprinting reveals disparities between individuals with transfemoral amputation and those without. When juxtaposed with AB counterparts, those with transfemoral amputation exert less force on the prosthetic limb against the starting blocks, resulting in a notably subpar start [180]. Following the initial start, the prosthetic limbs in individuals with transfemoral amputation show reduced horizontal and vertical accelerations during the first two stance phases compared to AB counterparts [181]. Upon reaching peak speed and while maintaining it, the intact limb's vertical GRFs in persons with transfemoral amputation exceed those in the limbs of AB individuals and prosthetic limb[182].

Sprinting in individuals with transfemoral amputation reveals limb asymmetries and variances, especially when considering kinematics and kinetics of daily-use prostheses and knee joints. Sprinting requires people with unilateral amputation to harmonise the asymmetries in the anatomic and function aspects of legs. Observations indicate that the intact limb exhibits greater peak extensor and flexor moments in the joints of knee

and hip and compared to their prosthetic counterpart [183]. Given the prosthetic limb's inefficiency in exerting ground forces during push off, intact limb compensates by producing greater force during stance phase of running [184]. Such forces lead to kinematic alterations, notably in joint angles and angular velocities. Running kinematics reveal unique characteristics between the prosthetic and intact limbs of people with transfemoral amputation. During stance phase, the thigh segment on the prosthetic limb displays limited RoM, and its knee joint remains overextended for an extended duration than the intact side. Additionally, the prosthetic limb's ankle joint exhibits a delay in achieving peak dorsiflexion relative to the intact limb [185]. For those with transfemoral amputation using the Terry Fox jogging prostheses, the prosthetic limb's knee joint consistently hyperextends throughout the stance phase [186].

In addition to the kinematic analysis, angles and angular velocities underwent separate evaluations, but were jointly assessed in coordination studies. Kinematic movement coordination can be measured using the DST through the CRP approach [63]. This gait analysis technique consolidates the angles and angular velocities of two segments into a singular parameter, depicting their coordination. However, few studies have delved into the coordination patterns of amputees. A walking coordination study indicated that individuals with transfemoral amputation exhibit distinct limb coordination patterns, compensating for limb absence and ensuring foot control precision [75]. Two studies explored the risk of lower back pain in amputees. One study highlighted that, in terms of transverse plane CRP values, individuals with transfemoral amputation without lower back pain mirrored the walking coordination of AB counterparts [187]. The second study found no notable link between pelvis-trunk coordination and self-reported lower back pain among those with transfemoral amputation [188]. Balancing the

disparities in lower limbs during sprinting poses challenges for amputees [189]. Nonetheless, research on sprinting coordination in individuals with uTFA remains scant. Prostheses designed specifically for running are commonly employed by those with uTFA to enhance their running capabilities. However, few studies have explored the running kinematics of amputees utilising a running-specific prosthesis. Moreover, the kinematic coordination patterns and their asymmetries in lower limbs using RSP remain uncharted. This research seeks to decipher the sprinting coordination patterns of lower limbs in persons with uTFA. It was posited that distinct coordination features exist between the sprinting gait of the prosthetic and intact limbs. To test hypothesis, a comparison was made among coordination features, asymmetry ratios of fundamental gait metrics of prosthetic and intact limbs.

### **5.3 Method**

#### **Participants**

The study involved seven participants with uTFA (Table 5-1). Participants hold the active level of the K4 or K3 [190], and a mean weight of  $56.5 \pm 7.9$  kg, height of  $1.63 \pm 0.09$  m, age of  $32.7 \pm 11.2$  years,  $11.9 \pm 8.6$  years post-amputation, and a speed during sprinting at  $5.85 \pm 0.45$  m/s. To be eligible, individuals with uTFA had to meet the following criteria: 1. Absence of neuromuscular disorders; 2. No functional restrictions in any lower limb; 3. Engagement in consistent fitness activities higher than once a prior to the research. The local ethics committee approved this study, adhering to the 1983 Declaration of Helsinki's procedures. All participants received information about the test and provided their consent.



Table 5-1. Demographic data

Participant	Gender (M/F)	Age (years)	Height (m)	Mass (kg)	Amputated side	Etiology	Time since amputation (years)	Residual limb length	Footstrike types of the intact limb	Prosthetic knee	Prosthetic foot	Running speed (m/s)
1	M	42	1.67	57.2	Left	Cancer	6	Long TF	Rearfoot	3S80	Sprinter 1E90 (cat.2)	5.68
2	M	52	1.70	66.6	Left	Trauma	29	KD	Forefoot	3S80	Sprinter 1E90 (cat.3)	6.02
3	F	38	1.49	43.9	Right	Infection	15	Long TF	Forefoot	3S80	Sprinter 1E90 (cat.2)	5.63
4	M	21	1.67	56.4	Left	Cancer	18	Short TF	Forefoot	3S80	Sprinter 1E90 (cat.3)	5.34
5	F	32	1.56	47.4	Right	Trauma	6.5	Middle TF	Forefoot	3S80	Sprinter 1E90 (cat.2)	5.59
6	F	18	1.56	58.3	Right	Trauma	3.5	Middle TF	Forefoot	3S80	Sprinter 1E90 (cat.2)	5.89
7	M	26	1.75	66.0	Right	Trauma	5.2	Middle TF	Forefoot	3S80	Sprinter 1E90 (cat.3)	6.83
Mean	—	32.7	1.63	56.5	—	—	11.9	—	—	—	—	5.85
SD	—	11.2	0.09	7.9	—	—	8.6	—	—	—	—	0.45

Abbreviations: F: female; M: male; TF; transfemoral; KD; knee-disarticulation; SD: standard deviation

### **Experimental procedures**

Participants acclimated to the testing environment and underwent adequate warm-up exercises prior to data collection. Next, participants sprinting at their maximum running speed on a runway with 40 meters. The ground where the test conducted contains seven plates which can assess the forces, with dimensions 60 cm x 40 cm were embedded in the ground BP400600-1000 models BP400600-2000, sourced from AMTI, Watertown, MA, USA). This study utilised a movement collection system with 20 cameras (VICON MX system, Oxford Metrics Ltd., UK), capturing effectively up to roughly 22 m from the start line. Data from each trial, encompassing two to three attempts per leg, underwent subsequent analysis. Trials were deemed successful solely if participants' steps remained within the force platform's confines. Adequate rest intervals were ensured between each trial for participants.

### **Data collections and analysis**

Before the experiment, each participant's body was adorned with 58 retro-reflective markers (Figure 5-1). The positions of the reflective markers on the prosthetic limb follow to guidelines from a prior study [183]. Within this method, the "ankle" joint of the prosthetic limb corresponded to the sharpest point midway between the prosthesis's medial and lateral curvatures. The placement of the remaining markers conformed to the a market set named Helen Hayes [190].

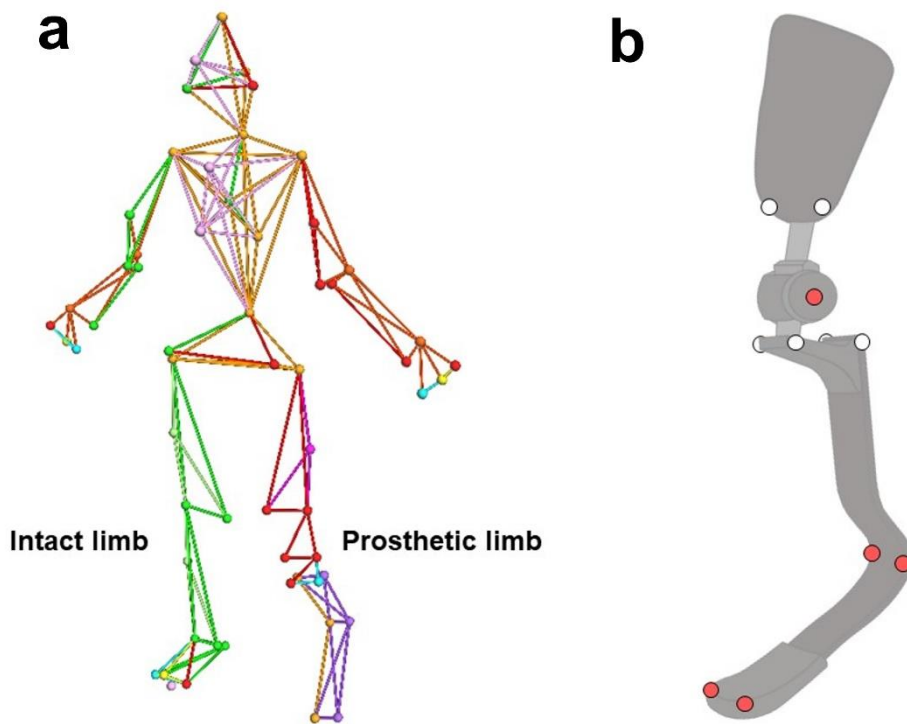


Figure 5-1. Full body markers in this study

Normalisation of the gait was first conducted, and the cycle was divided into 101 points. Data collection frequencies were set at 2000 Hz for GRF and 200 Hz for three-dimensional marker positions. Raw GRF data and motion data underwent filtering using a 4th order Butterworth filter with a cutoff frequency at 75 Hz and 20Hz, respectively. Gait events were delineated using GRF data, with a threshold set at 40 N [23]. Steps not making contact with the force plates had their gait events discerned via a limb-dependent kinematic algorithm. For the intact limb, initial contact identification relied on peak vertical accelerations: the first metatarsal for forefoot strikes and heel markers for rear-foot strikes [191]. Toe-off in both foot strike patterns was determined by the apex of the vertical acceleration observed in the first metatarsal marker [24]. In



parallel, sagittal plane angles for segments like the thigh, shank, and foot were assessed for a more detailed coordination study.

The CRP analysis was conducted using the Hilbert transform technique [63]. Each participant's segment angles ( $\theta$ ) were normalised (eq1) and were subsequently processed as continuous signals (eq 2) where "i" represents the  $i$  th point and "t" represents the  $t$  th point within the analytical dataset. The Hilbert transformation of the prior signal was executed using a tailored MATLAB script (eq 3 and eq4) where  $j$  represents the imaginary part. The phase angle was computed using MATLAB's "unwarp" function (eq 5). By definition, the arctan function's outcomes span between  $\pm 90^\circ$ ; however, a polarised coordinate's phase angle necessitates a complete  $360^\circ$  range. The "unwarp" method maintained the phase angle value, preventing it from jumping to the  $\pm 90^\circ$  range. CRP angles for the shank-foot and thigh-shank were derived by taking the difference between the distal and proximal angles (eq 6). Any CRP angles exceeding the  $\pm 180^\circ$  range were modified to fit within  $\pm 180^\circ$  by either adding or deducting  $360^\circ$ . Based on the previously obtained For each GC, CRP values along with the MARP and DP were calculated. While MARP assesses the overarching coordination, DP signifies the target phase's overall coordination variability. A  $0^\circ$  MARP (or CRP) value signifies in-phase coordination within the coupling. Conversely, values deviating from  $0^\circ$  point to an out-of-phase relationship [63].

$$\bar{\theta} = \theta - \min(\theta) - \left( \frac{\max(\theta) - \min(\theta)}{2} \right), \quad (\text{eq1})$$

$$\theta(t) = \bar{\theta}_{(i)}, i = 1, 2, \dots, n, \quad (\text{eq 2})$$

$$H(t) = H(\theta(t)) = \theta(t) * \frac{1}{\pi t^2} \quad (\text{eq 3})$$

$$\zeta(t) = \theta(t) + jH(t), \quad (\text{eq 4})$$

$$\phi_{rp} = \arctan \left[ \frac{H(t_i)}{\theta(t_i)} \right], i = 1, 2, \dots, n, \quad (\text{eq 5})$$

$$\phi_{CRP} = \phi_{rp-distal} - \phi_{rp-proximal}, \quad (\text{eq 6})$$

$$MARP = \sum_{i=1}^n \frac{|\phi_{i th-crp}|}{n}, i = 1, 2, \dots, n, \quad (\text{eq 7})$$

$$DP = \frac{\sum_{i=1}^n |SD_i|}{n}, i = 1, 2, \dots, n \quad (\text{eq 8})$$

A CRP curve was generated using the values of CRP at each time point during gait. During each trial, the time points of local minima or maxima were selected and averaged for each limb. Regarding the curves, a positive slope indicates the of distal PA leading the proximal PA (vice versa for a negative slope), these identified local minima or maxima may represent moments when there's a shift in coordination patterns [63].

Asymmetry ratio was computed for every gait parameter as a subsequent step [192]. In uTFA individuals, the asymmetry ratios quantify the differences between the lower limbs. An asymmetry ratio value of 1 indicates a balanced gait metric between both lower extremities. A ratio exceeding 1 suggests a greater gait metric in the prosthetic limb, while a ratio between 0 and 1 highlights a diminished metric compared to the natural limb. The study calculated asymmetry ratios concerning spatial-temporal aspects, kinematic features, and MARP metrics.

### **Statistics**

The normal distribution of the data was tested using Shapiro-Wilk test. For normal distributed gait parameters, paired t-test was applied to examine changes between the prosthetic and intact limbs. For non-normal distributed gait parameters, a Wilcoxon signed-rank test was applied to assess changes between the prosthetic and intact limbs. All statistics were carried out in SPSS software (IBM SPSS Statistics 22, SPSS Inc., Chicago, IL), with a predetermined significance threshold set at  $p < 0.05$ .

## **5.4 Results**

### **Basic kinematics and Spatial temporal parameters**

Table 5-2 illustrates that the step length among prosthetic and intact limbs did not show significant differences ( $p = 0.18$ ). Conversely, the intact limb exhibited significantly shorter stance phase duration and time when comparing to the prosthetic limb, with p-values of 0.01 and  $< 0.01$ , respectively.

Table 5-2 and Figure 5-2 (a, b, and c) showed the kinematics of the hip, knee, and ankle joints. No marked differences were observed between lower limbs for peak ankle dorsiflexion, as well as hip flexion and extension. For the ankle joint, large peak values

of plantar-flexion and RoM were revealed in the intact extremity compared to its prosthetic counterpart ( $p < 0.01$ ). Notable disparities were present in the knee joint metrics between the two legs. Among the whole gait, while the intact limb consistently showed knee flexion, the prosthetic limb manifested an extension averaging  $-5.41 \pm 2.35^\circ$ . In terms of the knee's kinematics, the intact limb had considerably larger peak values of flexion and a wider RoM in contrast to the prosthetic limb ( $p < 0.01$  for both flexion and RoM). Hip joint's RoM was larger on the intact limb than the prosthetic limb ( $p < 0.01$ ).

Regarding spatial temporal parameters, the intact limb exhibited a greater step length compared to the prosthetic limb. Conversely, both stance phase duration and time were prolonged in prosthetic limb. Kinematically, peak values of ankle plantar-flexion and its RoM both neared a value of zero. However, the peak ankle dorsiflexion exceeded 1, representing the highest asymmetry ratio among all. All parameters in the knee joint and hip joint are greater in intact limb. Notably, the maximum hip extension neared symmetry.

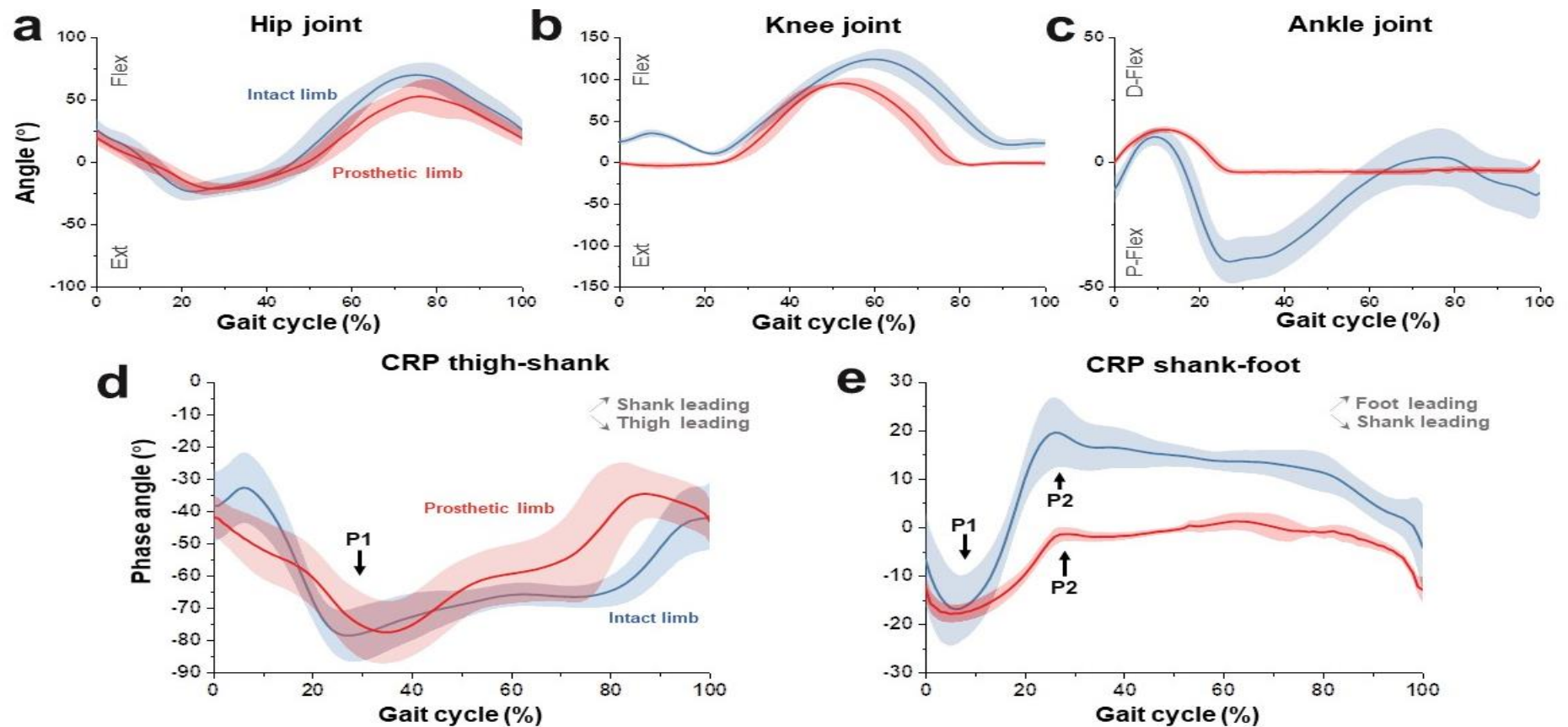


Figure 5-2. CRP patterns and joint angles. Colors red and blue symbolize the prosthetic and intact limbs, respectively. The results for hip, knee, and ankle joints are denoted as a, b, and c, respectively. Within these three diagrams, "D-Flex" stands for dorsiflexion, "P-Flex" indicates plantarflexion, "RoM" refers to the range of motion, and "Ext" represents extension. The diagram labeled as "d" depicts the CRP curve for thigh-shank coupling. The chart labeled as "e" illustrates the CRP curve for the shank-foot coupling.

Table 5-2. Mean value, normality, p-value, and asymmetry ratio of the parameters

Parameters	Intact limb	Prosthetic limb	Normality	p-value	Asymmetry ratio
Step length	1.57 ± 0.06 m	1.46 ± 0.19 m	n	0.18	0.93 ± 0.10
Stance time	0.12 ± 0.01 s	0.13 ± 0.01 s	y	<b>0.01</b>	1.14 ± 0.09
Stance phase	22.33 ± 2.23 %	26.01 ± 1.73 %	y	<b>&lt;0.01</b>	1.17 ± 0.10
Ankle D-Flex	11.39 ± 3.70 °	13.35 ± 1.28 °	y	0.28	1.33 ± 0.49
Ankle P-Flex	-40.98 ± 8.95 °	-4.08 ± 1.28 °	y	<b>&lt;0.01</b>	0.11 ± 0.05
Ankle RoM	52.37 ± 7.25 °	17.43 ± 1.04 °	y	<b>&lt;0.01</b>	0.34 ± 0.03
Knee Flex	127.28 ± 8.96 °	97.37 ± 4.62 °	y	<b>&lt;0.01</b>	0.77 ± 0.06
Knee Ext	—	-5.41 ± 2.35 °	—	—	—
Knee RoM	118.27 ± 7.34 °	102.78 ± 3.86 °	y	<b>0.01</b>	0.87 ± 0.07
Hip Flex	73.39 ± 6.16 °	54.00 ± 12.75 °	y	0.43	0.73 ± 0.15
Hip Ext	-24.41 ± 6.89 °	-22.54 ± 4.26 °	n	0.61	0.99 ± 0.29
Hip RoM	97.80 ± 4.04 °	76.54 ± 10.31 °	y	<b>&lt;0.01</b>	0.78 ± 0.10
MARP <sub>thigh-shank</sub>	61.07 ± 6.03 °	55.55 ± 9.61 °	y	0.33	0.92 ± 0.22
MARP <sub>shank-foot</sub>	12.73 ± 1.44 °	5.15 ± 0.67 °	y	<b>&lt;0.01</b>	0.92 ± 0.61
DP <sub>thigh-shank</sub>	1.97 ± 0.75 °	1.51 ± 0.58 °	y	0.34	—
DP <sub>shank-foot</sub>	1.26 ± 0.41 °	0.79 ± 0.40 °	y	0.10	—
TP1 <sub>thigh-shank</sub>	27.86 ± 1.81 %)	35.00 ± 2.88 %	y	<b>0.01</b>	—
TP1 <sub>shank-foot</sub>	5.43 ± 1.68 %	6.00 ± 1.31 %	n	0.50	—
TP2 <sub>shank-foot</sub>	27.71 ± 1.16 %	25.57 ± 1.99 %	y	<b>0.04</b>	—

Abbreviations: y: Yes; n: No; Ext: extension; Flex: flexion; D-Flex: dorsiflexion; P-Flex: plantarflexion; RoM: range of motion; MARP<sub>thigh-shank</sub>: mean absolute relative phase of thigh-shank coupling; MARP<sub>shank-foot</sub>: mean absolute relative phase of shank-foot coupling; DP<sub>thigh-shank</sub>: deviation phase of thigh-shank coupling; DP<sub>shank-foot</sub>: deviation phase of shank-foot coupling; TP1<sub>thigh-shank</sub>: time (percent of GC) to the first peak (P1) of thigh-shank coupling CRP curve in Figure 3(d); TP1<sub>shank-foot</sub>: time (percent of GC) to the first peak (P1) of shank-foot coupling CRP curve; TP2<sub>shank-foot</sub>: time (percent of GC) to the second peak (P2) of shank-foot coupling CRP curve.

Regarding spatial-temporal parameters, the intact limb exhibited a greater step length than the prosthetic side. In contrast, the prosthetic extremity showed longer durations for both time and phase of the stance. Asymmetry ratios were recorded as step length is 0.93 , stance time is 1.14, and stance phase duration is 1.17. Kinematically, both the peak value of ankle plantar-flexion and its RoM trended towards zero. Yet, the peak value of ankle dorsiflexion is close to one, marking it as the most prominent among all recorded asymmetry ratios. Precisely, the ratios for asymmetry stood at the peak value of ankle dorsiflexion is 1.33, RoM is 0.34, and ankle plantar-flexion is 0.11. All metrics pertaining to the knee and hip joints displayed higher values in the intact limb. Significantly, the peak value for hip extension closely aligned with symmetry. As for the asymmetry ratios the peak value of knee flexion is 0.77, knee's RoM is 0.87, peak values of hip extension is 0.99, peak value of hip flexion is 0.73, and hip's RoM is 0.78.

### **Coordination**

MARP of the shank-foot in the intact limb showed a notably higher ( $p < 0.01$ ) value compared to the prosthetic limb. Between intact and prosthetic limbs, there were no marked disparities concerning the MARP value of the coupling of thigh-shank segments or the DP for the couplings of thigh-shank and shank-foot segments. The asymmetry ratios were  $0.92 \pm 0.22$  for the MARP value of the coupling of thigh-shank segments and  $0.41 \pm 0.08$  for the coupling of shank-foot segments.

Figure 5-2 showcases the CRP curves in panels (d) and (e). In the phase space, positive values signify the distal one leading the proximal one among two segments, and the opposite for negative values. For the slopes, A positive one suggests the distal segment leads, while a negative one indicates the proximal segment is ahead [59, 63]. For the

coupling of thigh-shank segments, the throughout negative values of the whole gait indicate the shank consistently leading the thigh in both limbs. In the prosthetic limb, up to about 35% (P1) of the gait, the thigh led the shank, reverting to a thigh leading feature till the end of the gait (Table 5-2). The intact limb transitioned from a coordination pattern of thigh-leading to a coordination pattern of shank-leading earlier than the prosthetic limb. This plot reveals two distinct features. First, before 10% of during the GC, intact limb displayed a coordination pattern of shank-leading, in contrast to the prosthetic limb which maintained a coordination pattern of thigh-leading during the whole stance. Second, intact limb consistently showed a coordination pattern of shank-leading during the swing phase. In contrast, the prosthetic limb followed this pattern for about 80% GC before transitioning to a coordination pattern of thigh-leading.

Figure 5-2 shows the results of the coupling of the shank-foot segments, where both lower limbs transition from a coordination pattern of shank-leading to a pattern of foot-leading at approximately 6% of the GC. The time of this transition did not significantly differ between the limbs ( $p=0.50$ ). The intact limb concluded its coordination pattern of foot-leading later than the prosthetic limb ( $p=0.04$ ). Subsequently, the intact limb maintained a coordination pattern of shank-leading during the whole GC, while the prosthetic limb varied around  $0^\circ$  up to the swing phase's end, transitioning to a coordination pattern of shank-leading for the remaining of the GC.

## **5.5 Discussion**

We explored lower limb coordination in people with uTFA while sprinting. The coupling of thigh-shank segments showed consistent overall coordination, consistent with distinct characteristics during GC. The shank-foot couplings between the lower



limbs exhibited varied coordination. The results partially validate the study's hypothesis.

While sprinting, there were notable disparities in basic kinematics and spatial-temporal metrics between the prosthetic and intact limbs of uTFA individuals. For spatial temporal parameters, longer phase duration and time of stance were observed on the prosthetic limb when compared with the intact limb. Likewise, those with transtibial amputation had an extended time of stance on their prosthetic limb than intact limb [193]. This could be attributed to the strategy on the cost-effective force production approach [194]. The extension of the time of stance on the prosthetic limb could serve as a compensatory mechanism, allowing for corresponding vertical force response impulse generation and offsetting reduced force production [184]. In terms of joint kinematics, the prosthetic limb displayed a significantly limited RoM relative to the intact limb. For the joint angle of ankle, similar dorsiflexion levels were observed between prosthetic and intact limbs, with the prosthetic limb's restricted RoM mainly due to diminished peak ankle plantar-flexion. The pronounced asymmetry ratio in ankle plantar-flexion further supports this observation. Due to the absence of ankle plantar flexors [195], the prosthetic ankle couldn't achieve the same plantar-flexion movement and also the RoM as its intact counterpart. The restricted RoM in the prosthetic limb's knee joint mainly stemmed from its peak values in the knee flexion curve. While there are muscles left on the residual limb, particularly the hamstrings, they might lack the strength to regulate prosthetic knee flexion [168]. The prosthetic knee flexion during swing might be contributed by the forward movement for the residual limb and the backward swing inertia of the prosthetic structure. However, the prosthetic limb's flexion aligned with that of the intact limb, given that active muscles primarily govern the intact limb's knee flexion. As for the hip joint on the prosthetic limb showed a RoM

similar to that observed during walking [196]. Reduced hip RoM could result from lesser hip moments and muscle strength in the prosthetic limb compared to the intact one. Mechanical constraints arising from pelvis-socket interference [198] could be another contributing factor [197].

Individuals with uTFA attained symmetrical coordination, with the coupling of thigh-shank segments preserving the MARP at a near-balanced level between the lower limbs. MARP in the coupling of thigh-shank segments, DP in the coupling of thigh-shank and shank-foot segments, indicating a consistent out-of phase relationship in the coupling of thigh-shank segments of both limbs throughout the GC [59]. The coupling of shank-foot segments in the prosthetic limb had greater in-phase coordination compared to the intact limb. Finding implies a higher synchronisation in the coupling of shank-foot segments of the prosthetic limb, with both segments moving concurrently [63]. This observation aligns with expectations, given that the coupling of shank-foot segments of the prosthetic limb is shaped as a blade. Consequently, the prosthetic limb's segments of foot and shank inherently exhibit greater synchronisation compared to the intact limb. However, increased synchronisation doesn't necessarily equate to improved coordination. A previous study indicated that patients with LBP exhibited a greater in-phase state than their healthy counterparts [198]. Regarding coordination variability (DP), earlier research indicated elevated DP values in older individuals and children compared to young adults during activities like squat jumping and vertical jumping [128, 199]. While this study lacked a control group, findings suggest comparable coordination levels in the couplings of thigh-shank and shank-foot segments of both lower limbs, indicating that individuals with uTFA can effectively coordinate their limb movements.

Individuals with uTFA exhibited symmetrical coordination (evidenced by symmetrical MARP) despite having asymmetrical basic kinematics and spatial-temporal parameters. While the prosthetic and intact limbs showed consistent overall coordination, distinct coordination features emerged between the prosthetic and intact limbs during gait. In the coupling of thigh-shank segments, the intact limb initiated with a coordination pattern of shank-leading up to 10% of the GC, transitioning to a coordination pattern of thigh-leading during the phase of stance. In contrast, the prosthetic limb consistently exhibited a coordination pattern of thigh-leading throughout the stance. The variation may arise from the prosthetic limb's inability to actively produce force in the shank, necessitating reliance on the coordination pattern of thigh-leading during stance. The intact limb sustained a coordination pattern of shank-leading up to the end of the GC covering the whole swing phase. Conversely, the prosthetic limb began with a coordination pattern of shank-leading, transitioning to a coordination pattern of thigh-leading around 80% of the GC, and persisted with this pattern until the cycle's end. The prosthetic knee achieved maximum extension at 80% of the GC, earlier than the biological knee. This could account for the shift back to a coordination pattern of thigh-leading in the prosthetic limb. At this time in the GC, the shank lacks room for the knee extension angle. Therefore, the thigh segment compensates for this extension, and leading the shank segment back to its starting position to finalise the swing phase. As a result, amputees preserved symmetrical coordination in the thigh-shank coupling across both prosthetic and intact limbs.

Notable differences in the MARP (shank-foot) indicate a variation in the overall coordination pattern of the coupling of shank-foot segments. In the shank-foot coupling, both limbs demonstrated a consistent pattern that transitioning from coordination

pattern of shank-leading to foot-leading at about 6% of the GC. At the GC's starting postin, both limbs exhibited a coordination pattern of shank-leading, transitioning to a coordination pattern of foot-leading at the middle of the stance phase. Then the prosthetic limb predominantly showed in-phase coordination during the swing phase. In contrast, the intact limb followed a coordination pattern of shank-leading, reverting to its initial phase position. The prosthetic limb's in-phase coordination pattern during the swing phase can be attributed to its design: the shank and foot segments merge into a single rigid blade, preventing flexion when not grounded.

Several limitations should be noted to understand the findings of this study. Firstly, the participants had varied reasons for amputation, and prior research indicates that these causes can impact lower limb biomechanics. Specifically, traumatic versus vascular amputations can lead to variations in preferred speeds and stride lengths [172]. Secondly, there was a variation in the residual limb lengths among participants. As documented in earlier studies, femoral length plays a crucial role in determining gait parameters [173, 200]. Thirdly, the sprinting protocol limited the number of participants, given the challenge of finding uTFA individuals with adept sprinting abilities. Finally, the research focused solely on basic kinematics through CRP evaluation in the sagittal plane. Future research could encompass other planes, to enhance comprehension of sprinting coordination in those with transfemoral amputation. Integrating CRP with kinetics or electromyography could further elucidate control strategies in amputees. Finally, the sprinting velocity is not consistent in this study, which might be a confounding factor.

In conclusion, people with uTFA manage sprinting by compensation strategies

between the lower limbs during every phase of GC to maintain a symmetrical coordination pattern. To attain this symmetrical coordination, varied coordination techniques were utilised to counterbalance the asymmetries in the coupling of thigh-shank segments between limbs. The absence of the ankle joint in such prosthetic limbs means that coordination disparities between the lower limb segments of the lower limbs persist. While compensation techniques have harmonised coordination in the coupling of thigh-shank segments, discrepancies in the coupling of shank-foot segments between limbs remain.

# CHAPTER VI CONNECTIVITY BETWEEN NEURAL DYNAMICS AND COORDINATION

## 6.1 Summary of the study

Ambulation is a fundamental skill that is dominated by the CPGs in the spinal cord in human beings. However, after amputation, the individuals with uTFA show more varied gait patterns than AB individuals. Coordination patterns derived from CRP collect changes in CNS. Understanding the connectivity between neural dynamics and coordination patterns might shed some light on the gait generation in individuals with uTFA and advance the prosthetic gait rehabilitation. Twelve individuals with uTFA and their age-matched AB individuals were included in this study. The neural activities were recorded using a 64 channel EEG cap. The motion data were collected together with the EEG data. After artifact removal and calculation of the CRP parameters, the correlations between coordination patterns and neural dynamics were investigated. Results show a strong correlation in the intact limb during both stance and swing phases, while no correlations were found in the prosthetic and two limbs of AB individuals. Findings might suggest the CRP method is effective in revealing activities from CNS. The intact limb might be dominated by the brain directly, while the CPG controls the lower limbs of AB individuals. Forcing the prosthetic limb to mimic the movement of the intact limb might not be reasonable, since the origins of the gait pattern generators are different between the two lower limbs.

## 6.2 Introduction

Prosthetic gait rehabilitation training is crucial for individuals with uTFA [201, 202]. A wide range of difficulties may arise in the day-to-day walking activities of these individuals due to changes in their gait patterns and possible physical discomfort [203]. The complexities of their newly adopted gait patterns may hinder their ability to attain a quality of life equivalent to their previous state prior to amputation [204]. Consequently, there is a pressing need for a comprehensive understanding of their gait patterns [201]. By studying their walking patterns, we can create better prosthetic training programs that address their unique challenges [202]. Clinicians can build training programs that not just enhance mobility but also elevate the comprehensive well-being of individuals with uTFA, by fostering a more refined comprehension of the gait patterns [204]

Conventional gait analysis has the limitation of overlooking crucial coupling effects that are important in understanding human locomotion due to its focus on single joint movements[205]. This narrow focus can potentially overlook the interactions between various joints and muscles during gait, thereby limiting the depth of analysis and understanding of gait patterns [206, 207].The notion of dynamic systems arises as a promising approach to address this limitation. This approach facilitates a more comprehensive analysis by considering the synergistic interactions between different body segments during movement [59] .

A crucial element of this methodology is the concept of CRP, which is a mathematical tool utilised to quantify the synchronisation between two oscillating joints or segments [63]. CRP serves as a significant metric in understanding the lower limb coordination

and compensation strategies adopted during gait. It provides insights into the phase relationship between joint movements, thereby offering a nuanced perspective on the adaptive and compensation strategies employed by individuals during gait [207]. CRP has shed light on the altered gait patterns, facilitating the development of targeted interventions to enhance mobility and reduce the risk of secondary complications [208]. Through the application of CRP, researchers have been able to understand the complex inter-joint coordination strategies adopted by individuals with uTFA, creating more effective rehabilitation programs [207].

EEG has been applied to reveal the complex neural processes underlying various cognitive functions [209, 210]. It has been combined with other tools to investigate the synergistic relationship between neural activity and physical movements. High-density EEG investigated the cortical muscular coherence (CMC) networks in stroke patients and found a significant correlation with upper limb motor control [211]. Its application extends to the gait analysis in deciphering the neural correlations to gait. Facilitating a deeper understanding of the brain's role in coordinating complex walking patterns [212]. For example, by analysing the coherence between cortical and muscular activities, the functional connectivity and synchronisation between the brain and muscles during human locomotion were obtained [213]. Two neural pathways of the cortical muscular and intermuscular coherence were revealed to reflect the direct corticospinal projection and coordination of multiple muscles during movement [214]. Specifically, coordinated cortical and spinal inputs were found during the double support phase of GC [215]. However, to the best of our knowledge, no study investigated the EEG during locomotion in individuals with uTFA. Understanding gait patterns and their underlying neural process is crucial in prosthetic gait rehabilitation.



Through the integration of EEG data with gait analysis, the neuro pathways between the brain and locomotion system could foster advancements in both neuroscience and rehabilitation science.

Gait dynamics in individuals with uTFA has traditionally been approached from isolated perspectives, such as focusing on kinematics or kinetics [165, 216]. However, the potential of integrating coordination envelopes with EEG offers a promising avenue for a more comprehensive understanding of gait dynamics in this population. CRP quantifies the coordination between two segments and, provides insights into the movement patterns and compensatory strategies employed by amputees[63]. On the other hand, EEG captures the real-time neural activity associated with motor control and coordination during walking. Combining CRP and EEG data can bridge the gap between the biomechanical and neural aspects of gait. Such an integrated approach can elucidate how the brain adapts and reorganises its neural pathways in response to the altered biomechanics post-amputation. This holistic view can potentially reveal the intricate interplay between neural activity and biomechanical coordination, offering a deeper understanding of the challenges faced by individuals with lower limb amputation and paving the way for the development of targeted interventions to enhance their gait training and rehabilitation.

Understanding the association between coordination patterns and EEG signals in individuals with uTFA could potentially benefit prosthetic gait rehabilitation. The aim of this interdisciplinary study is to unveil the intricate dynamics of gait, bridging the gap between biomechanical adaptations and neural reorganisation that occurs post-amputation. The motion control follows the contralateral control mechanism[217].

Thus, a limb is controlled by the contralateral side of the brain hemisphere. Based on the facts, this study hypothesised that the brain activity from the contralateral side of the intact limb would have a significant association with the coordination patterns. The brain activity from the contralateral side of the prosthetic limb would have limited association with the coordination patterns, since the prosthetic limb has a loss of muscles and skeletal bones.

## **6.3 Method**

### **Participants**

Twelve individuals with uTFA (ten male and two female individuals; mean  $\pm$  standard deviation age,  $53.92 \pm 6.81$  years; amputation time,  $18.17 \pm 16.45$  years; height,  $1.74 \pm 0.07$  m; weight,  $74.42 \pm 15.38$  kg) participated in this study (Table 6-1). All individuals were able to use their prostheses proficiently. The inclusion criteria were as follows: 1) younger than 65 years old, 2) with uTFA, 3) able to walk on a treadmill without using assistive devices, and 4) no NMSS complications other than amputation. A group of AB individuals with matched age of the uTFA group were also recruited. The AB group was recruited as follows: 1) matched age with the uTFA group, 2) able to walk on a treadmill without using assistive devices, and 3) no NMSS complications. This study was approved by the ethical commitment of the Hong Kong Polytechnic University (HSEARS20220719001) All subjects were informed of the study, and consent was obtained before participation.

Table 6-1. Demographic data of participants

Participants	Gender (M/F)	Age (year)	Height (m)	Mass (kg)	Time since amputation (year)	Walking speed (km/h)	Amputated side	Etiology	Prosthetic knee	Prosthetic foot	Socket type	Suspension	Liner
1	F	55	1.56	53	5	1.7	R	Trauma	KX06	Pro-Flex XC	IRC	Suction	Polyurethane
2	M	52	1.76	78	6	1.8	L	Infection	Mauch	Pro-Flex LP Torsion	IC	Suction	Urethane
3	M	43	1.74	100	7	1.4	L	Trauma	Paso	Rush Foot	IC	Suction	N.A.
4	M	66	1.79	71	53	2.8	L	Trauma	RHEO	Pro-Flex XC	IC	Suction	Silicone
5	F	56	1.75	93	7	1.7	L	Trauma	3R-106 PRO	Pro-Flex XC	IC	Locking	Silicone
6	M	49	1.76	74	11	2.1	R	Trauma	Paso	Pro-Flex XC	IRC	Suction	Urethane
7	M	44	1.78	101	4	1.5	L	Trauma	Jiguang	Multiflex Foot	IRC	Locking	Silicone
8	M	61	1.63	54	12	1.7	L	Infection	3R78	Single-axis Foot	IC	Suction	Urethane
9	M	54	1.85	71	34	1.2	L	Tumor	3R80	1C60 Triton	IRC	Suction	Urethane
10	M	62	1.78	65	45	2.0	R	Trauma	TSA	TSA	QL	Belt	N.A.
11	M	57	1.77	65	7	1.8	L	Tumor	Paso	Pro-Flex XC	IRC	Locking	Silicone
12	M	48	1.69	68	27	1.7	L	Trauma	Covered	Covered	QL	Suction	N.A.
<b>Mean</b>	—	53.92	1.74	74.42	18.17	1.78	—	—	—	—	—	—	—
<b>SD</b>	—	6.81	0.07	15.38	16.45	0.38	—	—	—	—	—	—	—

Abbreviations: M: male; F: female; R: right; L: left; IRC: ischial-ramal containment; IC: ischial containment; QL: quadrilateral; N.A.: not applicable; TSA: traditional single axis. Prosthetic knee: KX06 is from Endolite, India; Mauch knee, Paso knee, RHEO knee are from Ossur, Iceland; 3R-106 PRO, 3R78, 3R80 are from Ottobock, Germany; Jiguang knee is from Zeanso, China. Prosthetic foot: Pro-Flex XC, Pro-Flex LP Torsion are from Ossur, Iceland; Rush foot is from PROSTTEK, Australia; Multiflex is from Endolite, India; 1C60 Triton is from Ottobock, Germany.

### Data collection and experiment protocols

EEG was captured using ANT Neuro systems (ANT Neuro, Hengelo, Netherlands).

The non-magnetic and comfortable ANT WaveGuard cap was used, with a 64 Ag/AgCl sintered electrode configuration, and the cap was connected with eego™ amplifier.

Electrode caps were placed by the 10–5 electrode placement system (Figure 6-1). EEG was collected with a sampling rate of 2000 Hz. Electrode impedances were kept below 5 kΩ before the experiment and kept below 20 kΩ throughout the walking experiment.

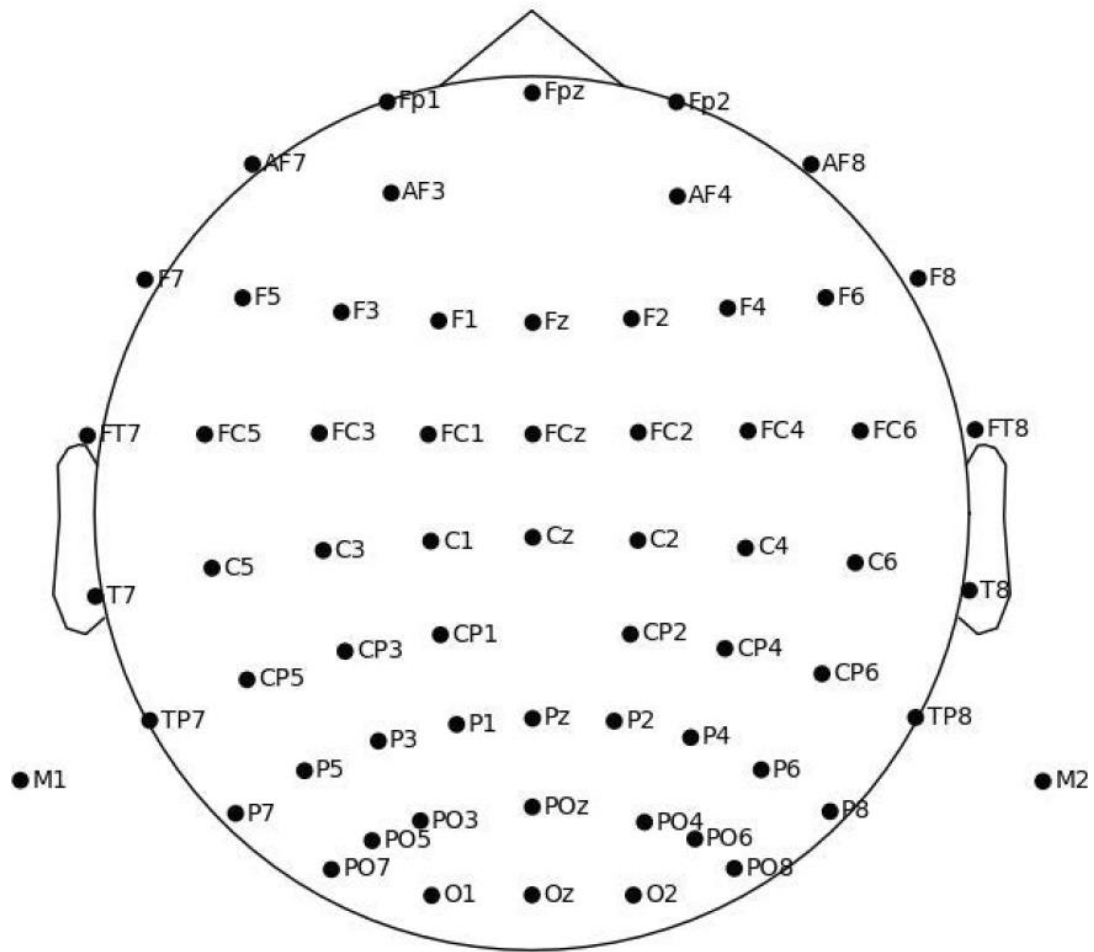


Figure 6-1. Channel locations

Motion data were captured using the Vicon system with an 8-camera motion capture system (T20, Vicon, Oxford Metrics Ltd, Oxford, UK). Before the experiment, 16 retro-reflective markers used for motion capture were attached to the lower limbs of the participants. Positions of attaching the markers were followed by the plug-in lower limb marker set in the Vicon tutorial (Figure 6-2).

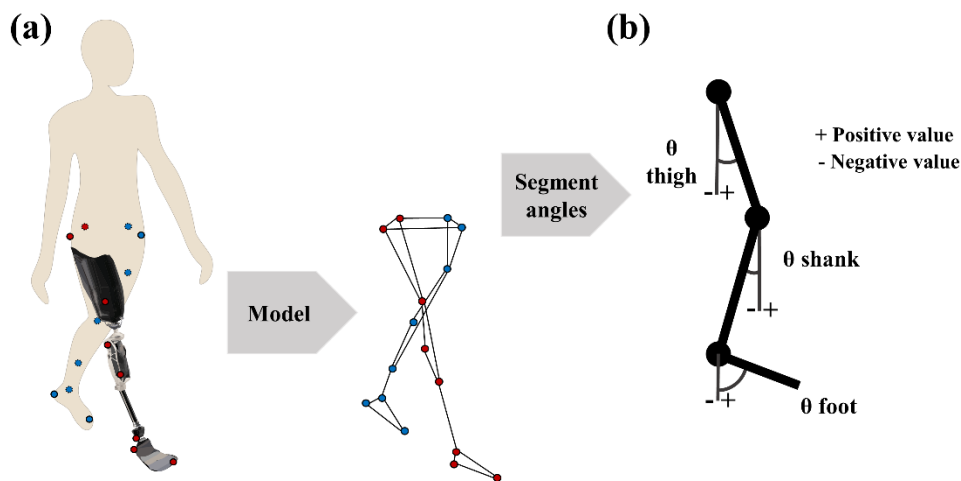


Figure 6-2. Marker positions (a) and Model definition (b)

During the pre-experiment session, participants first changed into lab suits and walked on the treadmill (Zebris Medical GmbH, Germany) to get familiar with the treadmill walking and confirm their preferred walking speed. They were required to wear a safety belt with adequate tightness that was neither too loose to lose safety effectiveness nor too tight that would impede them from walking on the treadmill. They walked on the treadmill until they confirmed their preferred walking speed. Then, they walked at this speed for two 2-minute walking sessions. In the experimental session, participants walked on another treadmill (Unisen Inc., Tustin, California, USA) wearing an EEG cap on the head and with Vicon reflective markers on their lower limbs. The treadmill was placed in the centre of the experiment room. A specially designed frame was utilised, from which a safety tether was suspended overhead. This setup was to prevent falls while experiments were conducted using a treadmill. They were instructed to walk on the treadmill for 5 minutes. The data was captured for three times during a session

of 5-minutes walking with each recording lasting for 1-minute (Figure 6-3).

Participants first performed a static standing trial, from which the marker data would be used for model scaling in the subsequent simulation session. The EEG signals during the quiet standing session were also recorded. After that, the participants were asked to walk at their preferred speed on a treadmill. The data collection started when the participants were able to smoothly walk on the treadmill. The EEG and Vicon synchronisation was performed via an external synchronisation trigger. Special precautions were applied to minimise the noises during data collection. Participants were asked to fix their gaze on a poster with a target point in front of them while walking. This setting avoids big movements of the head therefore minimising the muscle artefacts in EEG signals. The amplifier was fixed on the specially designed frame higher than the location where the safety belt was suspended. The cables from the EEG cap were securely fastened to the back of the participants and connected to the EEG amplifier, which was fixed on the top of the frame.

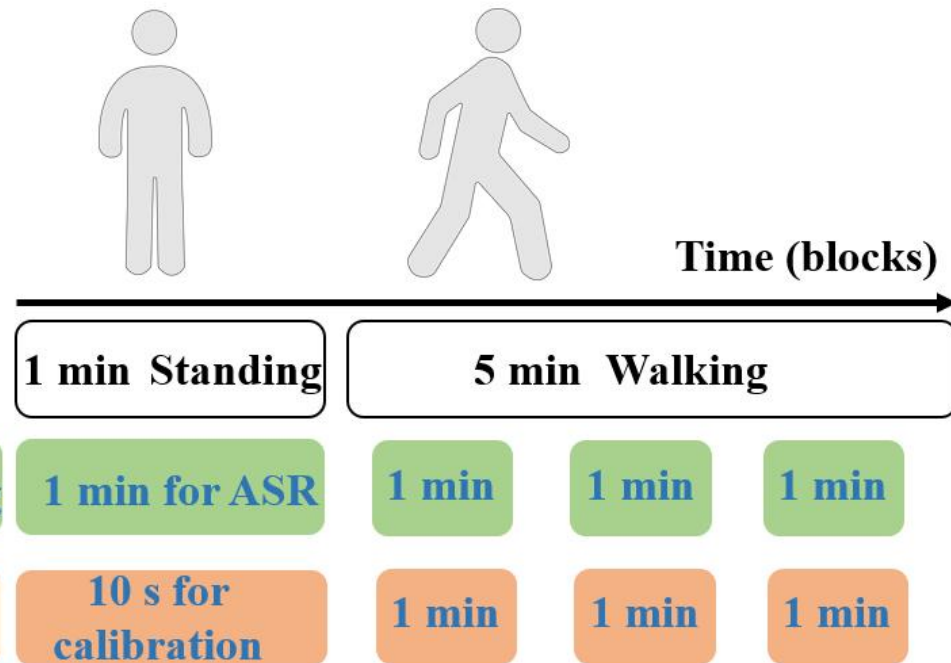
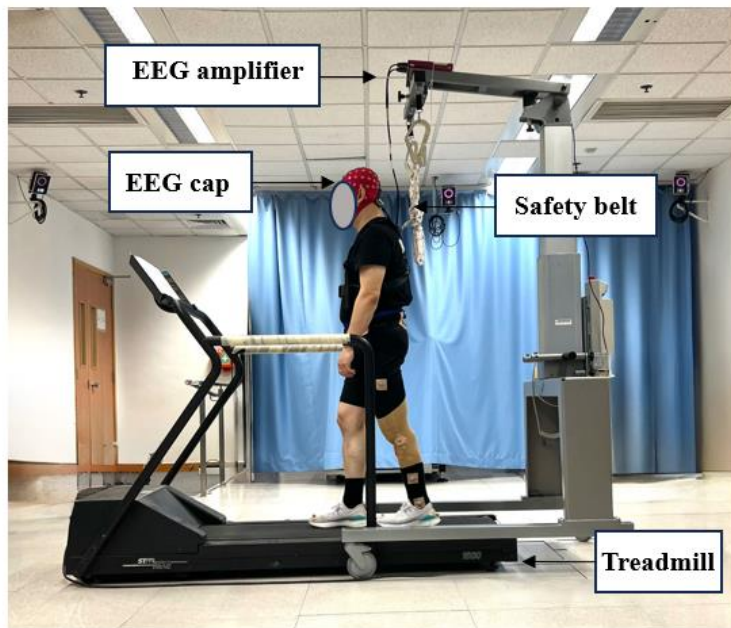


Figure 6-3. Experiment settings and protocol

## **Data processing**

### ***Coordination***

The motion data captured by the Vicon system were then analysed in the Vicon Nexus software and the thigh, shank, and foot segment angles in the sagittal plane were exported for further analysis. The marker coordinates of the heel and toe in both left and right limbs were applied to define the gait events. The heel strike, and toe off were defined by the height of the two markers on both limbs. After the definition of the gait events, the segment angles were chopped into each GCs and normalised into 101 points. Then the phase angles and the CRP in thigh- shank and shank-foot couplings were calculated following the calculation of the CRP analysis.

The Hilbert transform was used to calculate CRP. Segment angles ( $\theta$ ) underwent normalisation (eq1) and were interpreted as a time series signal (eq2), with  $i$  and  $t$  denoting the respective data points. A house written script using MATLAB was utilised to execute the Hilbert transformation on the data in steps (eq3) and (eq4), with  $j$  representing the imaginary component. The phase angle (eq5) was calculated using the MATLAB 'unwarp' function. Although the arctan function produced phase angles within  $\pm 90^\circ$ , a full  $360^\circ$  range was necessary for polarised coordinates. The “unwarp” tool was utilised to maintain the prior value and to avoid limiting it to the  $\pm 90^\circ$  range. The CRP angles for target coupling were calculated by using the PA of the distal segment minus the proximal segment (eq6). In cases where CRP angles exceeded  $\pm 180^\circ$ , they were adjusted to fall within this range by  $\pm 360^\circ$ . Then the CRP values obtained were applied to compute the DP and MARP using the equations (eq7) and (eq8). The DP and MARP assess the variability of the coordination and the general coordination



patterns, respectively [162]. MARP close to  $0^\circ$  signifies an in-phase coordination pattern, whereas increasing distance from  $0^\circ$  indicates an out-of-phase pattern within the coupled segments. Regarding the DP, a notably big (or small) value of DP suggests inconsistent (or limited) motion coordination [63].

$$\bar{\theta} = \theta - \min(\theta) - \left( \frac{\max(\theta) - \min(\theta)}{2} \right), \quad (\text{eq1})$$

$$\theta(t) = \bar{\theta}_{(i)}, i = 1, 2, \dots, n, \quad (\text{eq 2})$$

$$H(t) = H(\theta(t)) = \theta(t) * \frac{1}{\pi t}, \quad (\text{eq 3})$$

$$\zeta(t) = \theta(t) + jH(t), \quad (\text{eq 4})$$

$$\phi_{rp} = \arctan \left[ \frac{H(t_i)}{\theta(t_i)} \right], i = 1, 2, \dots, n, \quad (\text{eq 5})$$

$$\phi_{CRP} = \phi_{rp-distal} - \phi_{rp-proximal}, \quad (\text{eq 6})$$

$$MARP = \sum_{i=1}^n \frac{|\phi_{i th-crps}|}{n}, i = 1, 2, \dots, n, \quad (\text{eq 7})$$

$$DP = \frac{\sum_{i=1}^n |SD_i|}{n}, i = 1, 2, \dots, n \quad (\text{eq 8})$$

In CRP curves, a positive (negative) slope signifies that the distal (proximal) segment is leading the movement. CRP in shank-foot coupling and thigh-shank coupling were computed using the angles of the foot, shank, and thigh segments.

### ***EEG***

For the EEG signals, the pre-processing and all subsequent analyses were performed using in-house Matlab scripts, EEGLAB (version 2020) toolbox [218] and Python mne module[219]. EEG signals were first re-sampled into 250 Hz. Then, the gait events recorded in the last step were labelled in the EEG signals. There are four events: lhs (left heel strike), lto (left toe off), rhs (right heel strike), and rto (right toe off). To remove line noises in the EEG signals, a Zapline\_plus tool was applied first[220]. The EEG signals were high-pass filtered at 2 Hz and low-pass filtered at 80 Hz. Subsequently, the quiet standing EEG was extracted and applied in an ASR function to remove the movement noises in the EEG signals during walking [221]. The ASR method learned from the standing baseline signals to modify its model, and then was applied to walking EEG signals to remove walking-induced artifacts. The underlying assumption is that signals unrelated to the brain contribute significantly to variance in EEG data and can be identified by their abnormal statistical characteristics in the principal component analysis (PCA) subspace. In a mathematical sense, this involves iterative PCA computations on covariance matrices to identify artifacts through their statistical properties in the component subspace. Next, a blind source separate (BSS) method was applied to remove noise from the EMG using the 'autobssemg' function with the default setting in EEGLAB [218]. After the removal of noises, the bad channels were rejected by using the clean\_raw data function with a minimum threshold correlation of 0.85 for nearby channels [218]. Then M1 and M2 channels were

removed, then the other channels of EEG signals were re-referenced by common average (Figure 6-4).

The AMICA (adaptive mixture independent component analysis) was then applied by setting the iteration at 5000 times[222]. The resulting ICA components were then dipoles fit and an independent components (IC) label tool trained by deep learning was applied to automatically find the brain activity components[223]. The components with a 50% possibility of being brain activities were left and then projected back to sensor levels. The EEG signals after noise removal were then epoched and normalised in to the GCs using the time-warp function. There are five gait events applied to normalise the GC. For each side of the limb, it follows the order: heel strike (0%), contralateral toe off (16%), contralateral heel strike (50%), toe off (66%), and next heel strike (100%).

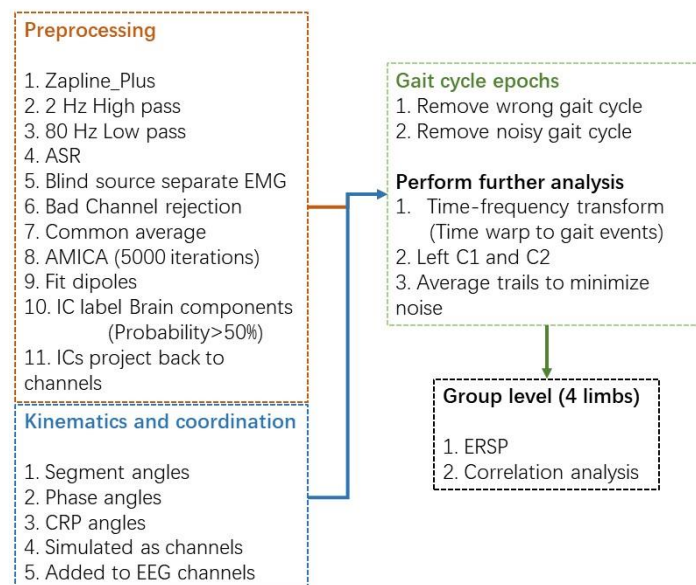


Figure 6-4. Data processing flow

According to the cortical map, the brain regions that control the lower limb movements are located under channels C1 and C2 [224]. As movement is always controlled by the

contralateral side of the brain, in this study we choose the C1 and C2 to represent the target brain activity channels to control the right and left lower limbs.

The gait ERSP (event related spectral perturbation) of the two channels was calculated using Morlet-wavelets to decompose the signals from 2 Hz to 60 Hz during the GC. The baseline was set as the average power of each GC. Next, four bands alpha (8-13 Hz), beta (14-30 Hz), low gamma (31-45 Hz), and mid gamma (46-60 Hz) were selected and averaged based on the frequency range. Alpha waves (8-13 Hz) are associated with relaxation and focused attention, beta waves (14-30 Hz) with alertness and cognitive tasks, low gamma waves (31-45 Hz) with sensory processing and learning, and mid gamma waves (46-60 Hz) with advanced cognitive functions and memory. Pearson correlation between the four bands ERSP power series and the 16 time series of the lower limb motion data were obtained. The correlations between the brain and the movement envelopes were then divided into stance and swing phases (16 envelopes \* 4 bands \* 2 phases).

## Statistical analysis

The statistical analysis of the data in this study was conducted in Python. For the EEG data, each point at the time frequency plot was compared among four limbs (101 times \* 57 frequencies). The normality of the data was tested using the Shapiro-Wilk test. Then the normally distributed data were tested using one-way ANOVA and Bonferroni methods to determine the p values of main effects and post-hoc comparisons, respectively. For data without normal distribution, the Krustal-Wallis test and Dunn's test were to determine the p values of main effects and post-hoc comparisons, respectively. The p values are then adjusted by the false discovery rate (FDR). Regarding the correlation analysis, the Pearson correlation analysis was performed on each subject between the 8 kinematics and coordination curves and 4 bands in neural dynamics. The obtained correlation was transformed into a Z score using Fisher's transformation. The averaged Z score was then transformed back. Only the correlation with statistical significance was plotted. For the CRP curves in this study, the SPM was involved to test the effects of the four limbs' coordination patterns. Due to the general linear model applied in SPM, the normality test was skipped [163].

### 6.4 Results

#### Coordination pattern

Figure 6-5 shows the “time warped” coordination patterns of the coupling of thigh-shank segments and shank-foot segments. After time warping, the main effects of limb demonstrated differences among the four limbs in the thigh-shank and shank-foot couplings. However, the multiple comparisons revealed no significant differences. Regarding the details of the coordination patterns. In the coupling of thigh-shank segments, the four limbs start the coordination by a shank-leading pattern. Then they switch to a thigh-leading pattern before the contralateral toe off and remain in this coordination pattern until the end of stance. In the swing phase, they apply back to a shank-leading pattern till the end of the GC. Regarding the coupling of shank-foot segments, four limbs start the gait by applying a shank-leading pattern. They switch to a foot-leading pattern by the end of the stance phase. The right and left limbs

demonstrate a sharp shank-leading pattern at around 20% of the GC, but this feature is not significant.

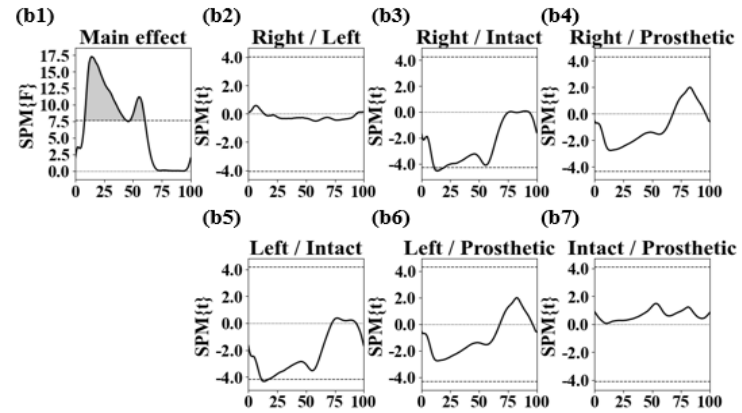
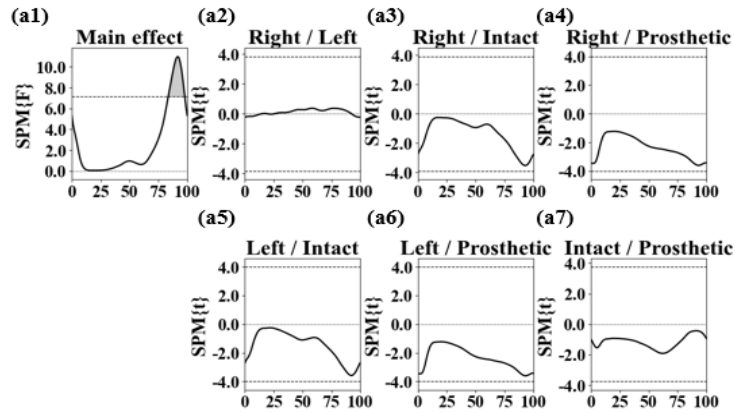
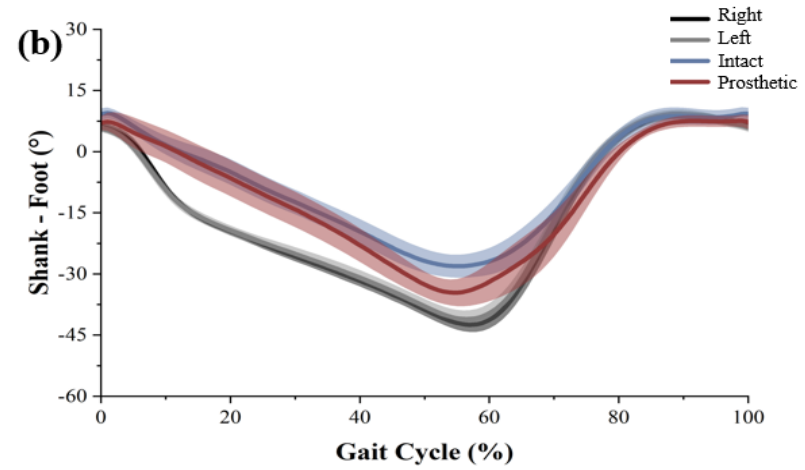
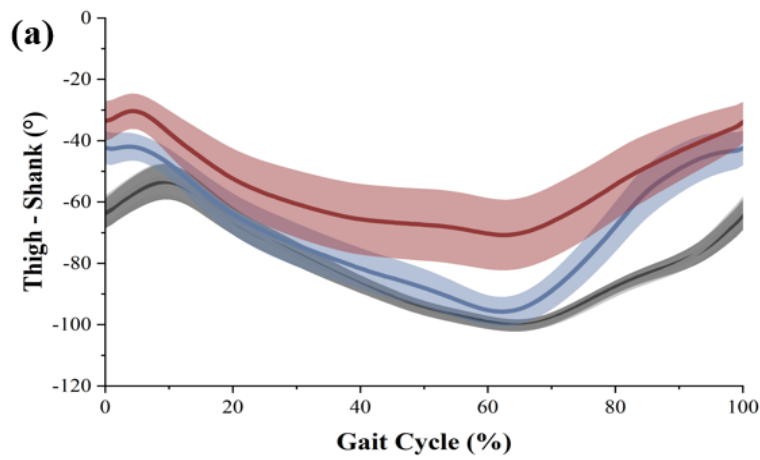


Figure 6-5. Coordination profiles of the thigh-shank (a) and shank-foot (b) couplings. The bottom sub-plots are the SPM results, the shaded parts indicated significance between the compared pairs.

### **ERSP and connectivity**

The utilisation of EEG processing facilitated the identification of significant (0.5 dB) fluctuations in gait-related spectral power perturbations within certain frequency bands in the brain's lower limb motor regions of four limbs during walking (Fig. 6). The comparisons between limbs were calculated for four pairs: right limb minus left limb, right limb minus intact limb, right limb minus prosthetic limb, and intact limb minus prosthetic limb. The adjusted p values ( $p < 0.05$ ) were masked for significance in each comparison plot (Figure 6-6). During the GC of the right limb, the ERSP for the right limb exhibited desynchronisation in the toe-off of the contralateral side and its own toe-off occurrences in the alpha and beta bands. Synchronisation was observed in the mid-stance phase in the alpha, beta, and gamma bands. For the GC of the left limb, the same synchronisation was observed during the mid-stance in alpha, beta, and gamma bands. Desynchronisation was only observed at the toe-off of the left limb, which is the end of the stance phase. Synchronisation was observed in alpha, beta, and gamma bands, while desynchronisation was observed in alpha and beta bands. Regarding the intact limb, the only obvious synchronisation was observed right after the toe-off of the prosthetic limb. Synchronisation was observed in alpha, beta, and gamma bands. For the prosthetic limb, desynchronisation was observed before mid-stance around the toe-off of the intact limb. Synchronisation was observed at the end of the GC. Synchronisation and desynchronisation were observed in the alpha, beta, and gamma bands.



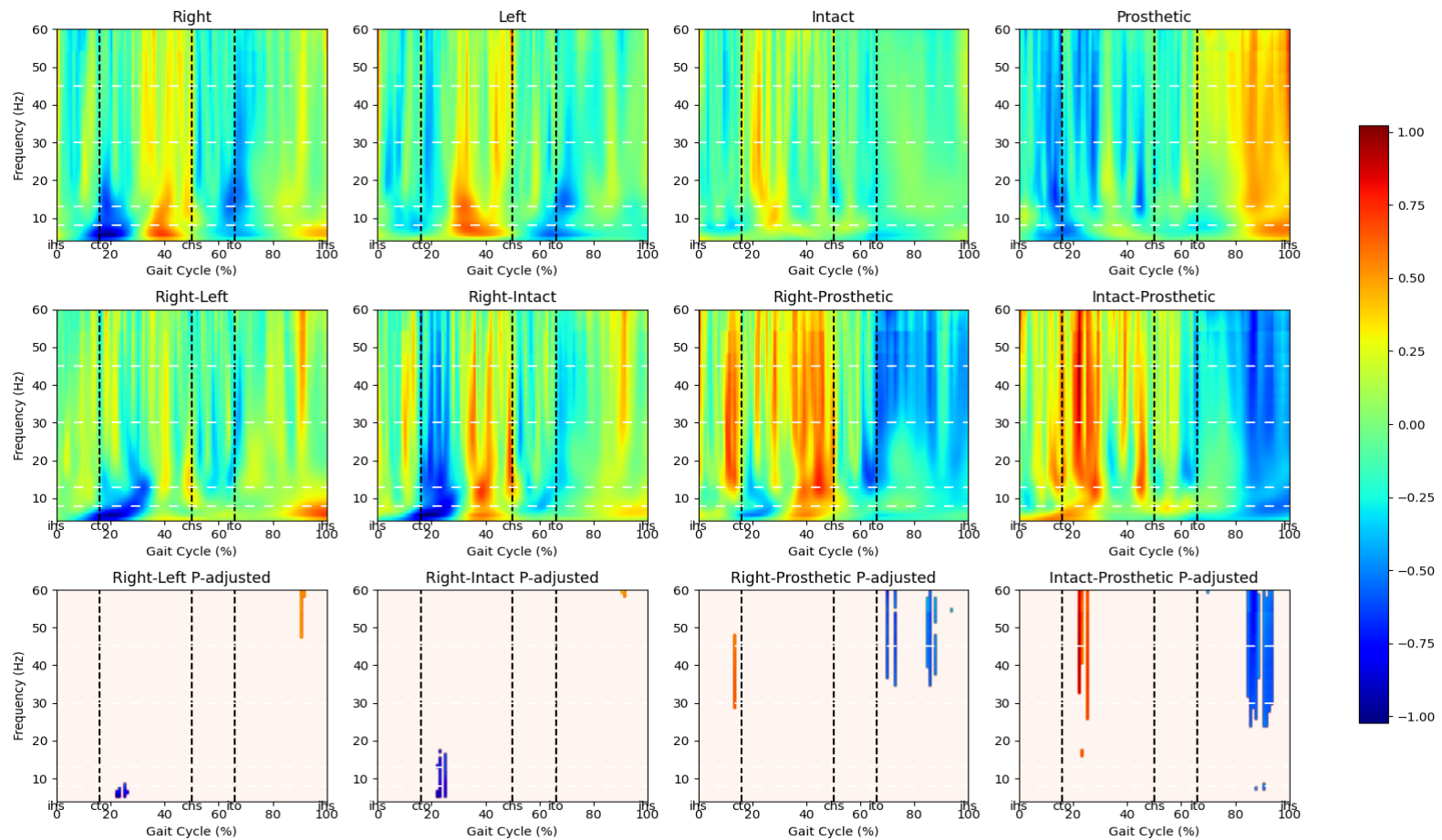


Figure 6-6. ERSP for the four limbs. The plot in the first row are the mean ERSP for the four limbs. The middle row indicate the differences among the four pairs in the sub-plot name. The bottom four plots are the differences with masked significance. The alpha level is 0.05, p values are adjusted as mentioned the statistical analysis.

Differences in the ERSP of the four limbs were compared. The right limb showed significant desynchronisation in the alpha band at 25% of the GC than the left and intact limbs. Significantly stronger synchronisations on the right limb were observed in the gamma band at around 90% of the GC than in the left and intact limbs. When comparing the prosthetic limb with the right and intact limbs, significant differences were observed in the gamma band. The two limbs showed significantly stronger activation than the prosthetic limb during the stance phase. This significant activation in the right limb occurred during the double support phase, while it occurred in the intact limb during the single support phase of the stance. The prosthetic limb exhibited significantly higher power in the swing phase than the two limbs.

The correlations between brain activities and the lower limb coordination were evaluated during stance (0-66%) and swing (67-100%) phases (Figure 6-7). All the significant correlations were positive. No significant connectivity in the correlations between the brain and motion were found in the right, left, and prosthetic limbs in the stance and swing phases. Significant correlations were only found in the intact limb during both stance and swing phases. Specifically, significant strong correlations were found in both stance and swing phases in the correlations between phase angles and ERSP in beta and gamma bands. For correlations between segment angles and brain activities, significant correlations were only found in the thigh segment angles among four bands. During the stance phase in the alpha band, significant positive correlations were also found in the phase angles. For the correlation between two CRP curves and brain activities, significant positive correlations were only found in the two gamma bands during the stance phase in the CRP shank-foot curves.

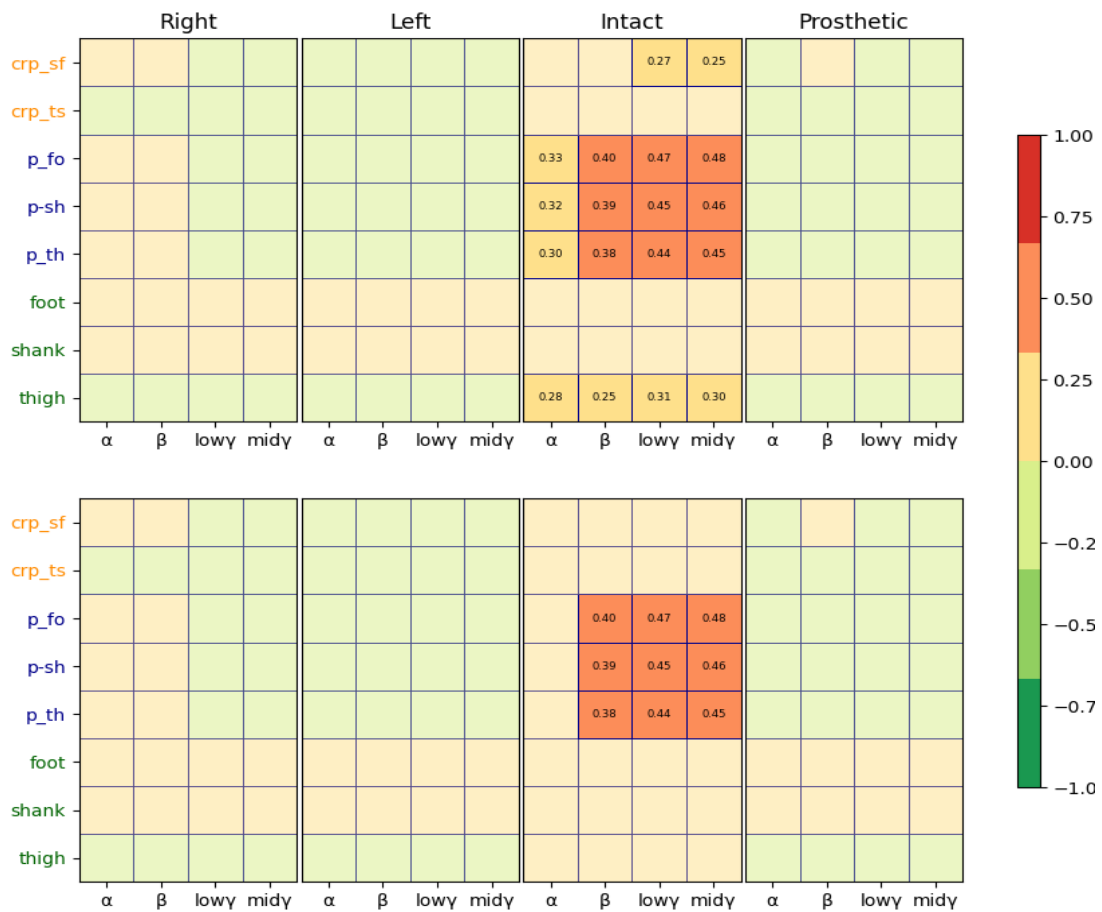


Figure 6-7. Connectivity between the neural dynamics and the coordination parameters. Abbreviations are as follows, crp\_sf: CRP in shank-foot coupling; crp-ts: CRP in thigh-shank coupling; p\_fo: PA (phase angle) of foot segment; p\_sh: PA of shank segment; p\_th: phase angle of thigh segment; foot: foot segment angle; shank: shank segment angle; thigh: thigh segments angle.

## 6.5 Discussion

In this study, the activities of the brain foot control region during gait in individuals with uTFA were observed. The connectivity between the neural dynamics and coordination patterns was evaluated. Hypothesis was supported that during the GC of the intact side, the contralateral side of the brain foot control region showed a strong correlation with the phase angles of the intact limb, while there were no significant correlations found in the prosthetic, right, and left limbs. This might suggest that the brain exhibited more activation in controlling the intact limb to compensate for the limb loss of the prosthetic side.

To understand the effectiveness of the DST in revealing CNS control mechanisms, the coordination patterns and their association with the neural dynamics were investigated. The study revealed significant strong correlations between the phase angles of lower limbs and the contralateral foot region were found. This suggests a high level of neural activation in controlling the intact limb during gait. Consequently, there seems to be a stronger voluntary activation of the intact limb compared to other limbs during walking. It should be noted that during the gait of individuals with uTFA, the intact limb compensates for the weaker force generation of the prosthetic limb by generating larger forces than other limbs. Phase angles were transformed by the basic segment angles using the Hilbert transformation, and it was built based on the theory that the changes in phase angles might suggest changes in the brain dynamics in controlling movement. The strong correlation between neural dynamics and phase angles of the intact limb might suggest that the voluntary motion control mechanism could be reflected by the phase angles. This finding is in accordance with the dynamic system theory, which indicates that the control mechanism from CNS could be reflected using changes in the

phase plane.

Strong correlations were found in higher frequency bands. This is in line with previous studies that explored the dynamics of corticospinal motor control during walking or imagination, which revealed increased modulations in the beta and gamma frequencies [215, 225]. Considering the functions of the modulations in the two bands [225], the involvement in walking might contribute to coordinating muscles and dealing with processing information of the environment during walking.

It is reasonable to assume that a lack of correlation between neural dynamics and coordination patterns of the prosthetic limb could be a result of limb loss. Because the residual limb of individuals with uTFA retains only a minor portion of the thigh segment's musculoskeletal structure, it may lead to incomplete neural control pathways. Another important parameter in dynamic system theory is the CRP. Minor correlations were found between the CRP and neural dynamics. In DST, changes in CRP are suggested to be the intervention of motion control outside the lower limb system. The minor correlation between the CRP and neural dynamics is reasonable, as the ankle joint (consisting of shank-foot segments) of the intact limb intentionally generated force during the stance phase compared to other limbs. This intentional strong voluntary movement might induce synchronisation in neural dynamics and phase angles. This might result in a minor correlation between neural dynamics and CRP, especially considering that the relationship isn't strictly linear, given that CRP is derived from two phase angles.

During walking, the CPG might govern the lower limb of AB individuals, and the CRP method might be effective in evaluating control strategy changes in CNS. The right and

left limbs of the AB individuals exhibited no correlation in the neural dynamics and coordination patterns. The underlying cause may be attributed to the predominance of the CPG located in the spinal cord. Rhythmic movement can start without the continuous control of the brain motor area, possibly causing unsynchronised neural dynamics and coordination patterns. The existence of CPG has been doubted since no direct observation has been made due to ethical considerations. However, it is a fact that CPG can be observed in vertebrate animals such as cats [226, 227]. Studies in spinal cord injuries indicate that epidural electrical stimulation targeting the distinct dorsal root entrance zones of the lumbosacral spinal cord permits the control of unique leg motor patterns [228-231]. Studies using CPG patterns to modify the control algorithm received promising outcomes in optimising the control of exoskeletal [232, 233]. Our findings might support the existence of CPG, and the CRP tools might have the potential to distinguish motion control between neural dynamics or CPG.

In prosthetic gait rehabilitation, a question is whether a prosthetic limb should have similar performance and movement patterns as the intact limb to make gait more symmetrical. Our previous study on walking gait coordination of individuals with uTFA reported differences in the stance and swing phases between two lower limbs. After time-warping, the gait events are fixed at the same percentage of the GC. The CRP curves indicated similar coordination patterns after time-warping. It seems that as long as the two lower limbs have similar stance and swing phases, the coordination patterns could be similar. However, it is not reasonable to force the two lower limbs of individuals with uTFA to generate similar movement patterns. Taking AB individuals as an example, it can be observed that they typically demonstrate symmetrical gait patterns, potentially governed by CPG to control their similar lower limbs. In this study,

findings suggested that the intact limb might be strongly connected to the CNS while the prosthetic limb was not. Additionally, the prosthetic limb is an artificial item without biological tissues to connect to the human body. Thus, a good prosthetic gait rehabilitation target might be the gait patterns of experienced individuals with uTFA, rather than directly forcing the prosthetic limb to mimic the performance of the intact limb.

Limitations should be noted before interpreting the findings of this study. Firstly, this study combined the artifacts removing methods from previous mobile EEG study, such as the application of AMICA and the use of a standing baseline recording with ASR to eliminate mobile artifacts. However, there is no best or perfect method of removing artifacts during movements, as this field is has not yet developed an EEG cap with the ability to remove movement artifacts mentioned in previous study [234]. Secondly, this study investigated EEG at the sensor level, which, while offering valuable insights, has inherent limitations in spatial resolution and the ability to accurately localise the sources of neural activity [235]. Investigating high-density EEG at the cortical level using source localisation might provide more comprehensive and precise information about the spatial distribution and origin of brain activity during walking [236]. Thirdly, in the kinematics data, only the sagittal plane data were included as the kinematics of stereotyped walking on a treadmill is mainly located in the sagittal plane. Including other planes might enhance the understanding of the gait during walking and the association with brain activities. Fourthly, it should be noted that the correlation in this study did not indicate any causality relationship. Fifthly, the EMG was not recorded during the experiment due to the prosthetic socket effects, this impede this experiment to observe the cortical muscle correlation. Finally, there are confounding factors (such

as amputation cause, age and duration of training, walking velocity) that might influence the results.

In summary, findings might suggest the existence of CPGs to dominant the ambulation in non-disabled individuals. But in individuals with uTFA, the CNS becomes more active when controlling the intact limb during walking compared with the prosthetic limb and two lower limbs in non-disabled individuals. This phenomenon might suggest the strategy for compensation of the biological limitations of the prosthetic limb by intentional activation of the intact limb. Differences between the prosthetic limb and other limbs existed throughout the neuromusculoskeletal system. Due to these differences, the prosthetic gait rehabilitation training and development of prosthesis might not necessarily aim for a symmetrical gait resembling the intact limb. Instead, the focus should be on optimising the treatment or performance to suit the individual's distinct abilities and circumstances.



## CHAPTER VII CONCLUSION

This dissertation reports a series of studies that were designed to comprehensively investigate the gait of individuals with uTFA in terms of coordination. Restoring the movement ability of the prosthetic limb to generate smooth gait patterns is the main aim of prosthetic gait rehabilitation and prosthesis design. Motion control was believed to originate from the CNS and was executed by musculoskeletal systems. This interdisciplinary study conducted three independent sub-studies from biomechanics to neuroscience to investigate how the movement of the lower limb were coordinated and their association with the neural dynamics.

The first study explored the lower-limb coordination of individuals with uTFA during walking, using CRP analysis to examine kinematic data from fourteen participants. Despite observing distinct coordination traits in different phases, a similar coordination pattern in thigh-shank coupling was found in both the uTFA and AB groups. Notably, in shank-foot coupling, intact limbs of individuals with uTFA displayed a brief foot-leading pattern during mid-stance as a compensatory strategy for the reduced force generation by prosthetic limbs. These insights contribute valuable information for improving prosthetic gait rehabilitation and development.

The second study investigated the sprinting patterns of individuals with uTFA to enhance prosthetic design and gait rehabilitation. Seven participants with uTFA sprinted on a 40meter runway, and their lower limb spatial-temporal parameters, joint angles, and segment angles were analysed using CRP analysis. Significant differences were found in stance time, stance phase percentage, ankle joint angles, and CRP of shank-foot coupling, attributed to structural differences between the lower limbs. Despite

these differences, no significant variation was observed in overall thigh-shank coupling coordination. The findings highlight the unique compensation strategies employed by individuals with uTFA to achieve symmetrical coordination between the lower limbs during sprinting.

The third study examined the connection between neural dynamics and coordination patterns in individuals with uTFA, aiming to enhance understanding of gait generation and aid prosthetic gait rehabilitation. The study, involving twelve individuals with uTFA and age-matched AB participants, utilised a 64-channel EEG cap to record brain activities alongside motion data. Post-analysis revealed a significant correlation between coordination patterns and neural dynamics on the intact limb during both stance and swing phases. However, no such correlation was found in the prosthetic and two limbs of AB individuals. These findings underscore the effectiveness of the CRP method in unveiling central nervous system activities. The results suggested that while the intact limb might be directly dominated by the brain, the CPG might control the lower limbs of AB individuals. This finding cautions against forcing the prosthetic limb to mimic the intact limb's movement, given the differing origins of their gait pattern generators.

In conclusion, these findings collectively emphasise the importance of understanding the diverse coordination patterns and neural dynamics in individuals with uTFA. The research suggests a cautious approach to prosthetic design, advocating against forcing prosthetic limbs to mimic intact limb movements due to the differing origins of their gait pattern generators. The findings obtained from this study have the potential to substantially advance the field of prosthetic gait rehabilitation and prosthesis

development, paving the way for more tailored and effective interventions for individuals with uTFA.

## REFERENCES

1. Edition, P., *Prosthetics and orthotics-Vocabulary-Part 1: General terms for external limb prostheses and external orthoses*. 1989.
2. Organization, W.J.W.H., *Priority assistive products list*. 2016.
3. Cordella, F., et al., *Literature Review on Needs of Upper Limb Prosthesis Users*. 2016.  
**10.**
4. Casler, P., *Atlas of Limb Prosthetics: Surgical, Prosthetic and Rehabilitation Principles*, John H. Bowker, John W. Michael (Eds.), Mosby-Year Book, St. Louis, Missouri (1992), 930 pp. \$155.00. 1993, Elsevier.
5. Söderberg, B., *Partial foot amputations*. 2001, Sweden: Centre for Partial Foot Amputees.
6. Organization, W.H., *World report on disability 2011*. 2011: World Health Organization.
7. Crowe, C.S., et al., *Prosthetic and orthotic options for lower extremity amputation and reconstruction*. 2019. **6**: p. 4.
8. MacKenzie, E.J., et al., *Factors influencing the decision to amputate or reconstruct after high-energy lower extremity trauma*. *J Trauma*, 2002. **52**(4): p. 641-9.
9. Boulton, A.J., et al., *Diagnosis and management of diabetic foot complications*. 2018.
10. Lusardi, M.M., M. Jorge, and C.C. Nielsen, *Orthotics and prosthetics in rehabilitation-e-book*. 2013: Elsevier Health Sciences.
11. Gailey, R.S. and S.M. Clemens, *Sacrifice, Science, and Support: A History of Modern*

- Prosthetics*, in *Full Stride: Advancing the State of the Art in Lower Extremity Gait Systems*, V. Tepe and C.M. Peterson, Editors. 2017, Springer New York: New York, NY. p. 35-54.
12. Steinberg, N., et al., *Fall incidence and associated risk factors among people with a lower limb amputation during various stages of recovery—a systematic review*. Disability and rehabilitation, 2019. **41**(15): p. 1778-1787.
  13. Harandi, V.J., et al., *Gait compensatory mechanisms in unilateral transfemoral amputees*. Med Eng Phys, 2020. **77**: p. 95-106.
  14. De Marchis, C., et al., *Characterizing the Gait of People With Different Types of Amputation and Prosthetic Components Through Multimodal Measurements: A Methodological Perspective*. Front Rehabil Sci, 2022. **3**: p. 804746.
  15. Kobayashi, T., et al., *Effects of walking speed on magnitude and symmetry of ground reaction forces in individuals with transfemoral prosthesis*. J Biomech, 2022. **130**: p. 110845.
  16. Gard, S.A., *Use of quantitative gait analysis for the evaluation of prosthetic walking performance*. JPO: Journal of Prosthetics and Orthotics, 2006. **18**(6): p. P93-P104.
  17. Lee, I.C., et al., *Perceiving amputee gait from biological motion: kinematics cues and effect of experience level*. Sci Rep, 2020. **10**(1): p. 17093.
  18. Jarvis, H.L., et al., *Temporal spatial and metabolic measures of walking in highly functional individuals with lower limb amputations*. Archives of physical medicine and rehabilitation, 2017. **98**(7): p. 1389-1399.

19. Schaarschmidt, M., et al., *Functional gait asymmetry of unilateral transfemoral amputees*. Human Movement Science, 2012. **31**(4): p. 907-917.
20. Michaud, S.B., S.A. Gard, and D.S. Childress, *A preliminary investigation of pelvic obliquity patterns during gait in persons with transtibial and transfemoral amputation*. J Rehabil Res Dev, 2000. **37**(1): p. 1-10.
21. Orekhov, G., et al., *Knee joint biomechanics in transtibial amputees in gait, cycling, and elliptical training*. PLoS One, 2019. **14**(12): p. e0226060.
22. Heitzmann, D.W.W., et al., *Benefits of an increased prosthetic ankle range of motion for individuals with a trans-tibial amputation walking with a new prosthetic foot*. Gait & Posture, 2018. **64**: p. 174-180.
23. Kobayashi, T., et al., *Effects of walking speed on magnitude and symmetry of ground reaction forces in individuals with transfemoral prosthesis*. Journal of biomechanics, 2021: p. 110845.
24. Hisano, G., et al., *Unilateral above-knee amputees achieve symmetric mediolateral ground reaction impulse in walking using an asymmetric gait strategy*. Journal of Biomechanics, 2021. **115**: p. 110201.
25. Nolan, L., et al., *Adjustments in gait symmetry with walking speed in trans-femoral and trans-tibial amputees*. Gait Posture, 2003. **17**(2): p. 142-51.
26. Hof, A.L., et al., *Control of lateral balance in walking. Experimental findings in normal subjects and above-knee amputees*. Gait Posture, 2007. **25**(2): p. 250-8.
27. Zmitrewicz, R.J., et al., *The effect of foot and ankle prosthetic components on braking*

- and propulsive impulses during transtibial amputee gait.* Arch Phys Med Rehabil, 2006. **87**(10): p. 1334-9.
28. Makimoto, A., et al., *Ground Reaction Forces During Sprinting in Unilateral Transfemoral Amputees.* J Appl Biomech, 2017. **33**(6): p. 406-409.
  29. Russell Esposito, E. and R.H. Miller, *Maintenance of muscle strength retains a normal metabolic cost in simulated walking after transtibial limb loss.* PLoS One, 2018. **13**(1): p. e0191310.
  30. Gholizadeh, H., et al., *Transtibial prosthesis suspension systems: Systematic review of literature.* Clinical Biomechanics, 2014. **29**(1): p. 87-97.
  31. Morriën, F., M.J.D. Taylor, and F.J. Hettinga, *Biomechanics in Paralympics: Implications for Performance.* Int J Sports Physiol Perform, 2017. **12**(5): p. 578-589.
  32. Winter, D.A., et al., *Biomechanical walking pattern changes in the fit and healthy elderly.* Phys Ther, 1990. **70**(6): p. 340-7.
  33. Ziegler-Graham, K., et al., *Estimating the prevalence of limb loss in the United States: 2005 to 2050.* Arch Phys Med Rehabil, 2008. **89**(3): p. 422-9.
  34. Jacquelin Perry, M., *Gait analysis: normal and pathological function.* New Jersey: SLACK, 2010.
  35. Gailey, R., et al., *Review of secondary physical conditions associated with lower-limb.* Journal of Rehabilitation Research & Development, 2008. **45**(1-4): p. 15-30.
  36. Whittle, M.W., *Gait analysis: an introduction.* 2014: Butterworth-Heinemann.
  37. Buongiorno, D., et al., *A linear approach to optimize an EMG-driven*

- neuromusculoskeletal model for movement intention detection in myo-control: A case study on shoulder and elbow joints*. *Frontiers in neurorobotics*, 2018. **12**: p. 74.
38. Taylor, W., et al., *An intelligent non-invasive real-time human activity recognition system for next-generation healthcare*. *Sensors*, 2020. **20**(9): p. 2653.
39. Minassian, K. and U.S. Hofstoetter, *Spinal cord stimulation and augmentative control strategies for leg movement after spinal paralysis in humans*. *CNS neuroscience & therapeutics*, 2016. **22**(4): p. 262-270.
40. Asano, Y., K. Okada, and M. Inaba, *Design principles of a human mimetic humanoid: Humanoid platform to study human intelligence and internal body system*. *Science Robotics*, 2017. **2**(13): p. eaaq0899.
41. Fleming, A., et al., *Myoelectric control of robotic lower limb prostheses: a review of electromyography interfaces, control paradigms, challenges and future directions*. *Journal of neural engineering*, 2021. **18**(4): p. 041004.
42. Higuchi, T., *Visuomotor control of human adaptive locomotion: understanding the anticipatory nature*. *Frontiers in psychology*, 2013. **4**: p. 277.
43. De Groote, F. and A. Falisse, *Perspective on musculoskeletal modelling and predictive simulations of human movement to assess the neuromechanics of gait*. *Proceedings of the Royal Society B*, 2021. **288**(1946): p. 20202432.
44. Kerkman, J.N., et al., *Network structure of the human musculoskeletal system shapes neural interactions on multiple time scales*. *Sci Adv*, 2018. **4**(6): p. eaat0497.
45. Ye, B., et al., *Recent Advances in the Application of Natural and Synthetic Polymer-*



*Based Scaffolds in Musculoskeletal Regeneration*. Polymers (Basel), 2022. **14**(21).

46. Zehr, E.P. and J. Duysens, *Regulation of arm and leg movement during human locomotion*. Neuroscientist, 2004. **10**(4): p. 347-61.
47. Grillner, S., *Biological pattern generation: the cellular and computational logic of networks in motion*. Neuron, 2006. **52**(5): p. 751-66.
48. Dimitrijevic, M.R., Y. Gerasimenko, and M.M. Pinter, *Evidence for a spinal central pattern generator in humans*. Ann N Y Acad Sci, 1998. **860**: p. 360-76.
49. Rossignol, S., R. Dubuc, and J.P. Gossard, *Dynamic sensorimotor interactions in locomotion*. Physiol Rev, 2006. **86**(1): p. 89-154.
50. Makin, T.R., et al., *Reassessing cortical reorganization in the primary sensorimotor cortex following arm amputation*. Brain, 2015. **138**(Pt 8): p. 2140-6.
51. Kikkert, S., et al., *Motor correlates of phantom limb pain*. Cortex, 2017. **95**: p. 29-36.
52. Lotze, M., et al., *Does use of a myoelectric prosthesis prevent cortical reorganization and phantom limb pain?* Nat Neurosci, 1999. **2**(6): p. 501-2.
53. Flor, H., L. Nikolajsen, and T. Staehelin Jensen, *Phantom limb pain: a case of maladaptive CNS plasticity?* Nat Rev Neurosci, 2006. **7**(11): p. 873-81.
54. Belda-Lois, J.M., et al., *Rehabilitation of gait after stroke: a review towards a top-down approach*. J Neuroeng Rehabil, 2011. **8**: p. 66.
55. van Emmerik, R.E. and E.E. van Wegen, *On the functional aspects of variability in postural control*. Exerc Sport Sci Rev, 2002. **30**(4): p. 177-83.

56. Carpenter, B.J.J.o.N. M., and E. Neurology, *The Co-ordination and Regulation of Movements*. 1968. **27**(2): p. 348.
57. Turvey, M.T., *Coordination*. American psychologist, 1990. **45**(8): p. 938.
58. Morecki, A., et al., *Cybernetic systems of limb movements in man, animals and robots*. 1984: E. Horwood , Halsted Press [distributor] , Polish Scientific Publishers.
59. Stergiou, N., *Innovative analyses of human movement*. 2004: Human Kinetics Publishers.
60. Kelso, J.S., *Dynamic patterns: The self-organization of brain and behavior*. 1995: MIT press.
61. Davids, K., et al., *Movement systems as dynamical systems*. Sports medicine, 2003. **33**(4): p. 245-260.
62. Glazier, P.S. and K. Davids, *Constraints on the complete optimization of human motion*. Sports Medicine, 2009. **39**(1): p. 15-28.
63. Hu, M., et al., *Current Application of Continuous Relative Phase in Running and Jumping Studies: A Systematic Review*. Gait & Posture, 2021.
64. Winogrodzka, A., et al., *Rigidity and bradykinesia reduce interlimb coordination in Parkinsonian gait*. Archives of Physical Medicine and Rehabilitation, 2005. **86**(2): p. 183-189.
65. Kurz, M.J., et al., *The effect of anterior cruciate ligament recontruction on lower extremity relative phase dynamics during walking and running*. Knee Surgery, Sports Traumatology, Arthroscopy, 2005. **13**(2): p. 107-115.

66. Volman, M.C.J. and R.H. Geuze, *Relative phase stability of bimanual and visuomanual rhythmic coordination patterns in children with a developmental coordination disorder*. Human Movement Science, 1998. **17**(4-5): p. 541-572.
67. Stergiou, N., et al., *A dynamical systems investigation of lower extremity coordination during running over obstacles*. Clinical Biomechanics, 2001. **16**(3): p. 213-221.
68. Harrison, A., W. Ryan, and K. Hayes, *Functional data analysis of joint coordination in the development of vertical jump performance*. Sports Biomechanics, 2007. **6**(2): p. 199-214.
69. Marin, L., et al., *Level of gymnastic skill as an intrinsic constraint on postural coordination*. Journal of sports sciences, 1999. **17**(8): p. 615-626.
70. Seifert, L., et al., *Inter-limb coordination in swimming: effect of speed and skill level*. Human movement science, 2010. **29**(1): p. 103-113.
71. Seth, A., et al., *OpenSim: Simulating musculoskeletal dynamics and neuromuscular control to study human and animal movement*. PLoS Comput Biol, 2018. **14**(7): p. e1006223.
72. Hochberg, L.R., et al., *Reach and grasp by people with tetraplegia using a neurally controlled robotic arm*. Nature, 2012. **485**(7398): p. 372-5.
73. Chang, Y., et al., *Changes in spatiotemporal parameters and lower limb coordination during prosthetic gait training in unilateral transfemoral amputees*. International Journal of Precision Engineering and Manufacturing, 2022. **23**(3): p. 361-373.
74. Lathouwers, E., et al., *Continuous relative phases of walking with an articulated*

- passive ankle-foot prosthesis in individuals with a unilateral transfemoral and transtibial amputation: an explorative case-control study.* BioMedical Engineering OnLine, 2023. **22**(1): p. 14.
75. Xu, Z., et al., *Lower Limb Inter-Joint Coordination of Unilateral Transfemoral Amputees: Implications for Adaptation Control.* Applied Sciences, 2020. **10**(12): p. 4072.
76. Scott Kelso, J.A. and B. Tuller, *A dynamical basis for action systems.* Handbook of cognitive neuroscience, 1984: p. 321-356.
77. Clark, J.E. and S.J. Phillips, *A longitudinal study of intralimb coordination in the first year of independent walking: a dynamical systems analysis.* Child development, 1993. **64**(4): p. 1143-1157.
78. Kugler, P.N., J.A.S. Kelso, and M.T. Turvey, *1 on the concept of coordinative structures as dissipative structures: I. theoretical lines of convergence,* in *Advances in psychology.* 1980, Elsevier. p. 3-47.
79. Haddad, J.M., et al., *Relative phase coordination analysis in the assessment of dynamic gait symmetry.* J Appl Biomech, 2010. **26**(1): p. 109-13.
80. Rangaprakash, D., et al., *Hemodynamic response function (HRF) variability confounds resting-state fMRI functional connectivity.* Magn Reson Med, 2018. **80**(4): p. 1697-1713.
81. Logothetis, N.K., *What we can do and what we cannot do with fMRI.* Nature, 2008. **453**(7197): p. 869-78.
82. Cherry, S.R., et al., *Total-Body PET: Maximizing Sensitivity to Create New Opportunities*

- for Clinical Research and Patient Care. J Nucl Med, 2018. 59(1): p. 3-12.*
83. Smith-Bindman, R., et al., *Radiation dose associated with common computed tomography examinations and the associated lifetime attributable risk of cancer. Arch Intern Med, 2009. 169(22): p. 2078-86.*
  84. Cohen, M.X., *Where Does EEG Come From and What Does It Mean? Trends Neurosci, 2017. 40(4): p. 208-218.*
  85. Gwin, J.T., et al., *Electrocortical activity is coupled to gait cycle phase during treadmill walking. Neuroimage, 2011. 54(2): p. 1289-96.*
  86. Jiang, N., et al., *A brain-computer interface for single-trial detection of gait initiation from movement related cortical potentials. Clin Neurophysiol, 2015. 126(1): p. 154-9.*
  87. Malcolm, B.R., et al., *The aging brain shows less flexible reallocation of cognitive resources during dual-task walking: A mobile brain/body imaging (MoBI) study. Neuroimage, 2015. 117: p. 230-42.*
  88. Seeber, M., et al., *EEG beta suppression and low gamma modulation are different elements of human upright walking. Front Hum Neurosci, 2014. 8: p. 485.*
  89. Teixeira, S., et al., *Integrative parietal cortex processes: neurological and psychiatric aspects. J Neurol Sci, 2014. 338(1-2): p. 12-22.*
  90. De Pauw, K., et al., *The efficacy of the Ankle Mimicking Prosthetic Foot prototype 4.0 during walking: Physiological determinants. Prosthetics and Orthotics International, 2018. 42(5): p. 504-510.*
  91. Bamdad, M., H. Zarshenas, and M.A. Auais, *Application of BCI systems in*

- neurorehabilitation: a scoping review*. Disability and Rehabilitation: Assistive Technology, 2015. **10**(5): p. 355-364.
92. Holdefer, R.N. and L.E. Miller, *Primary motor cortical neurons encode functional muscle synergies*. Experimental Brain Research, 2002. **146**: p. 233-243.
93. Sporns, O., et al., *Dynamic expression of brain functional systems disclosed by fine-scale analysis of edge time series*. Network Neuroscience, 2021. **5**(2): p. 405-433.
94. Hussain, L., et al., *Symbolic time series analysis of electroencephalographic (EEG) epileptic seizure and brain dynamics with eye-open and eye-closed subjects during resting states*. Journal of physiological anthropology, 2017. **36**(1): p. 1-12.
95. Thompson, W.H. and P. Fransson, *On stabilizing the variance of dynamic functional brain connectivity time series*. Brain Connectivity, 2016. **6**(10): p. 735-746.
96. Zhao, M., et al., *Assessing Neurokinematic and Neuromuscular Connectivity During Walking Using Mobile Brain-Body Imaging*. Front Neurosci, 2022. **16**: p. 912075.
97. Latash, M.L., J.P. Scholz, and G. Schöner, *Toward a new theory of motor synergies*. Motor control, 2007. **11**(3): p. 276-308.
98. Kelso, J.A.S., *Dynamic patterns: The self-organization of brain and behavior*. 1995: MIT press.
99. Schmidt, R., et al., *Dynamical aspects of learning an interlimb rhythmic movement pattern*. Journal of Motor Behavior, 1992. **24**(1): p. 67-83.
100. Kelso, J., *Relative timing in brain and behavior: Some observations about the generalized motor program and self-organized coordination dynamics*. Human

- Movement Science, 1997. **16**(4): p. 453-460.
101. Kelso, J. and M. Ding, *Fluctuations, intermittency, and controllable chaos in biological coordination*. Variability and motor control, 1993: p. 291-316.
  102. Kelso, J., J. Buchanan, and S. Wallace, *Order parameters for the neural organization of single, multijoint limb movement patterns*. Experimental brain research, 1991. **85**(2): p. 432-444.
  103. Hamill, J., et al., *A dynamical systems approach to lower extremity running injuries*. 1999. **14**(5): p. 297-308.
  104. Burgess-Limerick, R., B. Abernethy, and R.J. Neal, *Relative phase quantifies interjoint coordination*. Journal of biomechanics, 1993. **26**(1): p. 91-94.
  105. Lamb, P.F. and M.J.C.B. Stöckl, *On the use of continuous relative phase: Review of current approaches and outline for a new standard*. 2014. **29**(5): p. 484-493.
  106. Bailey, J.P., et al., *Understanding the influence of perceived fatigue on coordination during endurance running*. 2018: p. 1-15.
  107. Bailey, J.P., et al., *Effects of treadmill running velocity on lower extremity coordination variability in healthy runners*. Human movement science, 2018. **61**: p. 144-150.
  108. Frank, N.S., J.P. Callaghan, and S.D.J.F.S. Prentice, *Lower limb kinematic variability associated with minimal footwear during running*. 2013. **5**(3): p. 171-177.
  109. Hannigan, J., L.-S.J.G. Chou, and posture, *Sex differences in lower extremity coordinative variability during running*. 2019. **70**: p. 317-322.
  110. Hein, T., et al., *Using the variability of continuous relative phase as a measure to*

- discriminate between healthy and injured runners*. 2012. **31**(3): p. 683-694.
111. Miller, R.H., et al., *Continuous relative phase variability during an exhaustive run in runners with a history of iliotibial band syndrome*. 2008. **24**(3): p. 262-270.
112. Morgan, J., et al., *Influence of Aging on Lower Extremity Sagittal Plane Variability During 5 Essential Subphases of Stance in Male Recreational Runners*. 2019. **49**(3): p. 171-179.
113. Prejean, B.J. and M.D.J.F.S. Ricard, *A quantification of lower-limb coordinative variability during running with different levels of midsole cushioning*. 2019. **11**(2): p. 93-104.
114. Seay, J.F., R.E. Van Emmerik, and J.J.C.b. Hamill, *Low back pain status affects pelvis-trunk coordination and variability during walking and running*. 2011. **26**(6): p. 572-578.
115. Seay, J.F., R.E. Van Emmerik, and J.J.E.j.o.s.s. Hamill, *Trunk bend and twist coordination is affected by low back pain status during running*. 2014. **14**(6): p. 563-568.
116. Abbasi, A., et al., *A comparison of coordination and its variability in lower extremity segments during treadmill and overground running at different speeds*. 2020.
117. Argaud, S., et al., *Age-related differences of inter-joint coordination in elderly during squat jumping*. PloS one, 2019. **14**(9).
118. Blache, Y., et al., *Asymmetry of inter-joint coordination during single leg jump after anterior cruciate ligament reconstruction*. International journal of sports medicine, 2017. **38**(02): p. 159-167.
119. Castro, M.A., et al., *Ankle sprain influence on inter-joint coordination during jump of*



- basketball players*. *Gait & Posture*, 2009. **30**: p. S128-S129.
120. Dierks, T.A. and I.J.C.B. Davis, *Discrete and continuous joint coupling relationships in uninjured recreational runners*. 2007. **22**(5): p. 581-591.
121. Floría, P., et al., *Effects of running experience on coordination and its variability in runners*. 2018. **36**(3): p. 272-278.
122. Gidley, A.D., D.E. Lankford, and J.P.J.J.o.s.s. Bailey, *The construction of common treadmills significantly affects biomechanical and metabolic variables*. 2020. **38**(19): p. 2236-2241.
123. Gittoes, M.J. and C.J.J.o.A.B. Wilson, *Intralimb joint coordination patterns of the lower extremity in maximal velocity phase sprint running*. 2010. **26**(2): p. 188-195.
124. Heiderscheit, B.C., J. Hamill, and R.E. Van Emmerik, *Q-angle influences on the variability of lower extremity coordination during running*. *Medicine and science in sports and exercise*, 1999. **31**(9): p. 1313.
125. Krajewski, K.T., et al., *Inter-Segmental coordination during a unilateral 180 jump in elite rugby players: Implications for prospective identification of injuries*. 2020. **10**(2): p. 427.
126. Pupo, J.D., et al., *Stiffness, intralimb coordination, and joint modulation during a continuous vertical jump test*. *Sports biomechanics*, 2013. **12**(3): p. 259-271.
127. Byrne, J.E., et al., *Comparison of gait patterns between young and elderly women: an examination of coordination*. *Perceptual and motor skills*, 2002. **94**(1): p. 265-280.
128. Raffalt, P.C., T. Alkjær, and E.B. Simonsen, *Intra-and inter-subject variation in lower limb coordination during countermovement jumps in children and adults*. *Human*

- movement science, 2016. **46**: p. 63-77.
129. van Emmerik, R.E.A. and R.C. Wagenaar, *Effects of walking velocity on relative phase dynamics in the trunk in human walking*. Journal of biomechanics, 1996. **29**(9): p. 1175-1184.
130. Stergiou, N., et al., *Intralimb coordination following obstacle clearance during running: the effect of obstacle height*. Gait & Posture, 2001. **13**(3): p. 210-220.
131. Gabor, D., *Theory of communication. Part 1: The analysis of information*. Journal of the Institution of Electrical Engineers-Part III: Radio and Communication Engineering, 1946. **93**(26): p. 429-441.
132. Hoitz, F., et al., *The effects of systematically altered footwear features on biomechanics, injury, performance, and preference in runners of different skill level: a systematic review*. Footwear Science, 2020. **12**(3): p. 193-215.
133. Raffalt, P.C., et al., *To walk or to run—a question of movement attractor stability*. 2020.
134. Gheller, R.G., et al., *Effect of different knee starting angles on intersegmental coordination and performance in vertical jumps*. Human movement science, 2015. **42**: p. 71-80.
135. de Castro, F., et al., *Assessment of patterns and variability in lower extremity coordination between genders with different shoe insole stiffness during jump-landing tasks*. 2017. **18**(2): p. 3-14.
136. Winter, D.A., *Biomechanics and motor control of human movement*. 2009: John Wiley & Sons.

137. Nunez, P.L. and R. Srinivasan, *Electric fields of the brain: the neurophysics of EEG*. 2006: Oxford University Press, USA.
138. Teplan, M., *Fundamentals of EEG measurement*. Measurement science review, 2002. **2**(2): p. 1-11.
139. Cohen, M.X., J.F. Cavanagh, and H.A. Slagter, *Event-related potential activity in the basal ganglia differentiates rewards from nonrewards: Temporospacial principal components analysis and source localization of the feedback negativity: Commentary*. Human brain mapping, 2011. **32**(12): p. 2270-2271.
140. Singh, K.D., *Which "neural activity" do you mean? fMRI, MEG, oscillations and neurotransmitters*. Neuroimage, 2012. **62**(2): p. 1121-1130.
141. Nathan, K. and J.L. Contreras-Vidal, *Negligible motion artifacts in scalp electroencephalography (EEG) during treadmill walking*. Frontiers in human neuroscience, 2016. **9**: p. 708.
142. Jacobsen, N.S.J., et al., *A walk in the park? Characterizing gait-related artifacts in mobile EEG recordings*. European Journal of Neuroscience, 2021. **54**(12): p. 8421-8440.
143. Gorjan, D., et al., *Removal of movement-induced EEG artifacts: current state of the art and guidelines*. Journal of neural engineering, 2022. **19**(1): p. 011004.
144. Phadikar, S., et al., *Automatic muscle artifacts identification and removal from single-channel eeg using wavelet transform with meta-heuristically optimized non-local means filter*. Sensors, 2022. **22**(8): p. 2948.
145. Gorjan, D., et al., *Removal of movement-induced EEG artifacts: current state of the art*

- and guidelines*. J Neural Eng, 2022. **19**(1).
146. Safieddine, D., et al., *Removal of muscle artifact from EEG data: comparison between stochastic (ICA and CCA) and deterministic (EMD and wavelet-based) approaches*. EURASIP Journal on Advances in Signal Processing, 2012. **2012**(1): p. 1-15.
  147. Mahmud, S., et al., *MLMRS-Net: Electroencephalography (EEG) motion artifacts removal using a multi-layer multi-resolution spatially pooled 1D signal reconstruction network*. Neural Computing and Applications, 2023. **35**(11): p. 8371-8388.
  148. Motdhare, S.S. and G. Mathur, *An Experimental Analysis on EMG Artifact Removal Methods from EEG Signal Records*. Mathematical Statistician and Engineering Applications, 2022. **71**(1): p. 72-78.
  149. Ichimura, D., et al., *Acquisition of bipedal locomotion in a neuromusculoskeletal model with unilateral transtibial amputation*. Front Bioeng Biotechnol, 2023. **11**: p. 1130353.
  150. Kooiman, V.G.M., et al., *Rhythmic neural activity is comodulated with short-term gait modifications during first-time use of a dummy prosthesis: a pilot study*. J Neuroeng Rehabil, 2020. **17**(1): p. 134.
  151. Bonacci, J., et al., *Neuromuscular adaptations to training, injury and passive interventions: implications for running economy*. Sports Med, 2009. **39**(11): p. 903-21.
  152. Draganski, B., et al., *Neuroplasticity: changes in grey matter induced by training*. Nature, 2004. **427**(6972): p. 311-2.
  153. Shaffer, J., *Neuroplasticity and Clinical Practice: Building Brain Power for Health*. Front Psychol, 2016. **7**: p. 1118.

154. Bellmann, M., et al., *Immediate effects of a new microprocessor-controlled prosthetic knee joint: a comparative biomechanical evaluation*. Arch Phys Med Rehabil, 2012. **93**(3): p. 541-9.
155. Mahncke, H.W., A. Bronstone, and M.M. Merzenich, *Brain plasticity and functional losses in the aged: scientific bases for a novel intervention*. Prog Brain Res, 2006. **157**: p. 81-109.
156. Hara, Y., *Brain plasticity and rehabilitation in stroke patients*. J Nippon Med Sch, 2015. **82**(1): p. 4-13.
157. Beretta, E., et al., *Assessment of gait recovery in children after Traumatic Brain Injury*. Brain Inj, 2009. **23**(9): p. 751-9.
158. Carratalá-Tejada, M., et al., *Reflex Locomotion Therapy for Balance, Gait, and Fatigue Rehabilitation in Subjects with Multiple Sclerosis*. J Clin Med, 2022. **11**(3).
159. Mishra, P., et al., *Performance Evaluation of Jaipur Knee Joint through Kinematics and Kinetics Gait Symmetry with Unilateral Transfemoral Indian Amputees*. J Med Syst, 2019. **43**(3): p. 55.
160. Kobayashi Y, Hida N, Nakajima K, Fujimoto M, Mochimaru M. 2019: AIST Gait Database. 2019.
161. Kadaba, M.P., H.K. Ramakrishnan, and M.E. Wootten, *Measurement of lower extremity kinematics during level walking*. J Orthop Res, 1990. **8**(3): p. 383-92.
162. Hu, M., et al., *Sprinting performance of individuals with unilateral transfemoral amputation: compensation strategies for lower limb coordination*. Royal Society Open

- Science, 2023. **10**(3): p. 221198.
163. Pataky, T.C., M.A. Robinson, and J. Vanrenterghem, *Region-of-interest analyses of one-dimensional biomechanical trajectories: bridging 0D and 1D theory, augmenting statistical power*. PeerJ, 2016. **4**: p. e2652.
  164. Ranaldi, S., et al., *Characterization of prosthetic knees through a low-dimensional description of gait kinematics*. Journal of NeuroEngineering and Rehabilitation, 2023. **20**(1): p. 46.
  165. Kobayashi, T., et al., *Walking characteristics of runners with a transfemoral or knee-disarticulation prosthesis*. Clinical Biomechanics, 2020. **80**: p. 105132.
  166. Yang, J.R., et al., *Differences in gait patterns of unilateral transtibial amputees with two types of energy storing prosthetic feet*. Annals of rehabilitation medicine, 2018. **42**(4): p. 609-616.
  167. Amma, R., et al., *Inter-limb weight transfer strategy during walking after unilateral transfemoral amputation*. Scientific Reports, 2021. **11**(1): p. 4793.
  168. Motomura, Y., et al., *Effect of different knee flexion angles with a constant hip and knee torque on the muscle forces and neuromuscular activities of hamstrings and gluteus maximus muscles*. European Journal of Applied Physiology, 2019. **119**(2): p. 399-407.
  169. Perry, J. and J.M. Burnfield, *Gait analysis. Normal and pathological function 2nd ed*. California: Slack, 2010.
  170. Schneiders, A.G., et al., *A valid and reliable clinical determination of footedness*. Pm&r,

2010. **2**(9): p. 835-841.
171. Ishmael, M.K., et al., *Powered Hip Exoskeleton Reduces Residual Hip Effort without Affecting Kinematics and Balance in Individuals with Above-Knee Amputations During Walking*. IEEE Transactions on Biomedical Engineering, 2022.
172. Hafner, B.J., et al., *Energy storage and return prostheses: does patient perception correlate with biomechanical analysis?* Clinical Biomechanics, 2002. **17**(5): p. 325-344.
173. Bell, J.C., et al., *Transfemoral amputations: the effect of residual limb length and orientation on gait analysis outcome measures*. JBJS, 2013. **95**(5): p. 408-414.
174. Laferrier, J.Z. and R. Gailey, *Advances in lower-limb prosthetic technology*. Physical Medicine and Rehabilitation Clinics, 2010. **21**(1): p. 87-110.
175. Highsmith, M.J., et al., *BIOENERGETIC DIFFERENCES DURING WALKING AND RUNNING IN TRANSFEMORAL AMPUTEE RUNNERS USING ARTICULATING AND NON-ARTICULATING KNEE PROSTHESES*. Technol Innov, 2016. **18**(2-3): p. 159-165.
176. Esquenazi, A., *Gait analysis in lower-limb amputation and prosthetic rehabilitation*. Physical Medicine and Rehabilitation Clinics, 2014. **25**(1): p. 153-167.
177. Reaburn, P., *Training and Nutritional Needs of the Masters Sprint Athlete*, in *Nutrition and Performance in Masters Athletes*. 2014, CRC Press. p. 308-339.
178. Sepp, L.A., *Running Biomechanics for People with a Unilateral Transtibial Amputation Using Running-Specific and Daily-Use Prostheses*. 2019: Colorado School of Mines.
179. Adamczyk, P.G. and A.D. Kuo, *Mechanisms of gait asymmetry due to push-off deficiency in unilateral amputees*. IEEE transactions on neural systems and

- rehabilitation engineering, 2014. **23**(5): p. 776-785.
180. Willwacher, S., et al., *Sprint Start Kinetics of Amputee and Non-Amputee Sprinters*. PLoS one, 2016. **11**(11): p. e0166219-e0166219.
181. Strutzenberger, G., et al., *First and Second Step Characteristics of Amputee and Able-Bodied Sprinters*. Int J Sports Physiol Perform, 2018. **13**(7): p. 874-881.
182. Makimoto, A., et al., *Ground reaction forces during sprinting in unilateral transfemoral amputees*. Journal of applied biomechanics, 2017. **33**(6): p. 406-409.
183. Namiki, Y., et al., *Joint moments during sprinting in unilateral transfemoral amputees wearing running-specific prostheses*. Biology open, 2019. **8**(2): p. bio039206.
184. Sakata, H., et al., *A Limb-specific Strategy across a Range of Running Speeds in Transfemoral Amputees*. Medicine and science in sports and exercise, 2020. **52**(4): p. 892-899.
185. Buckley, J.G., *Sprint kinematics of athletes with lower-limb amputations*. Arch Phys Med Rehabil, 1999. **80**(5): p. 501-8.
186. DiAngelo, D.J., et al., *Performance assessment of the Terry Fox jogging prosthesis for above-knee amputees*. Journal of biomechanics, 1989. **22**(6-7): p. 543-558.
187. Esposito, E.R. and J.M. Wilken, *The relationship between pelvis–trunk coordination and low back pain in individuals with transfemoral amputations*. Gait & posture, 2014. **40**(4): p. 640-646.
188. Mahon, C.E., et al., *Changes in Trunk and Pelvis Motion Among Persons With Unilateral Lower Limb Loss During the First Year of Ambulation*. Arch Phys Med Rehabil, 2020.



- 101(3):** p. 426-433.
189. Arellano, C.J., et al., *Effect of running speed and leg prostheses on mediolateral foot placement and its variability*. PloS one, 2015. **10(1):** p. e0115637.
190. van Sint Jan, S., *Color Atlas of Skeletal Landmark Definitions E-Book: Guidelines for Reproducible Manual and Virtual Palpations*. 2007: Elsevier Health Sciences.
191. Handsaker, J.C., et al., *A kinematic algorithm to identify gait events during running at different speeds and with different footstrike types*. Journal of Biomechanics, 2016. **49(16):** p. 4128-4133.
192. Silverman, A.K., et al., *Compensatory mechanisms in below-knee amputee gait in response to increasing steady-state walking speeds*. Gait & posture, 2008. **28(4):** p. 602-609.
193. Beck, O.N., P. Taboga, and A.M. Grabowski, *Prosthetic model, but not stiffness or height, affects the metabolic cost of running for athletes with unilateral transtibial amputations*. Journal of Applied Physiology, 2017. **123(1):** p. 38-48.
194. Kram, R., *Muscular force or work: what determines the metabolic energy cost of running?* Exercise and sport sciences reviews, 2000. **28(3):** p. 138-143.
195. Yang, J.R., et al., *Differences in Gait Patterns of Unilateral Transtibial Amputees With Two Types of Energy Storing Prosthetic Feet*. Annals of rehabilitation medicine, 2018. **42(4):** p. 609.
196. Harandi, V.J., et al., *Gait compensatory mechanisms in unilateral transfemoral amputees*. Medical Engineering & Physics, 2020. **77:** p. 95-106.

197. Rabuffetti, M., M. Recalcati, and M. Ferrarin, *Trans-femoral amputee gait: Socket–pelvis constraints and compensation strategies*. *Prosthetics and orthotics international*, 2005. **29**(2): p. 183-192.
198. Seay, J.F., R.E.A. Van Emmerik, and J. Hamill, *Trunk bend and twist coordination is affected by low back pain status during running*. *European journal of sport science*, 2014. **14**(6): p. 563-568.
199. Argaud, S., et al., *Age-related differences of inter-joint coordination in elderly during squat jumping*. *Plos one*, 2019. **14**(9): p. e0221716.
200. Baum, B.S., et al., *Correlation of residual limb length and gait parameters in amputees*. *Injury*, 2008. **39**(7): p. 728-733.
201. Wurdeman, S.R., S.A. Myers, and N. Stergiou, *Trans-tibial amputee joint motion has increased attractor divergence during walking compared to non-amputee gait*. *Ann Biomed Eng*, 2013. **41**(4): p. 806-13.
202. Stevens, P.M. and S.R. Wurdeman, *Prosthetic Knee Selection for Individuals with Unilateral Transfemoral Amputation: A Clinical Practice Guideline*. *J Prosthet Orthot*, 2019. **31**(1): p. 2-8.
203. Bonnet, X., et al., *Mechanical work performed by individual limbs of transfemoral amputees during step-to-step transitions: Effect of walking velocity*. *Proc Inst Mech Eng H*, 2014. **228**(1): p. 60-6.
204. Fuenzalida Squella, S.A., A. Kannenberg, and Â. Brandão Benetti, *Enhancement of a prosthetic knee with a microprocessor-controlled gait phase switch reduces falls and improves balance confidence and gait speed in community ambulators with unilateral*

- transfemoral amputation*. *Prosthet Orthot Int*, 2018. **42**(2): p. 228-235.
205. Lathouwers, E., et al., *Continuous relative phases of walking with an articulated passive ankle-foot prosthesis in individuals with a unilateral transfemoral and transtibial amputation: an explorative case-control study*. *Biomed Eng Online*, 2023. **22**(1): p. 14.
206. Viry, S., et al., *Patterns of horse-rider coordination during endurance race: a dynamical system approach*. *PLoS One*, 2013. **8**(8): p. e71804.
207. Hu, M., et al., *Sprinting performance of individuals with unilateral transfemoral amputation: compensation strategies for lower limb coordination*. *R Soc Open Sci*, 2023. **10**(3): p. 221198.
208. Kwakkel, G. and R.C. Wagenaar, *Effect of duration of upper- and lower-extremity rehabilitation sessions and walking speed on recovery of interlimb coordination in hemiplegic gait*. *Phys Ther*, 2002. **82**(5): p. 432-48.
209. Wagner, J., et al., *Distinct  $\beta$  Band Oscillatory Networks Subservicing Motor and Cognitive Control during Gait Adaptation*. *J Neurosci*, 2016. **36**(7): p. 2212-26.
210. Gramann, K., et al., *Toward a new cognitive neuroscience: modeling natural brain dynamics*. *Front Hum Neurosci*, 2014. **8**: p. 444.
211. Pichiorri, F., et al., *Exploring high-density corticomuscular networks after stroke to enable a hybrid Brain-Computer Interface for hand motor rehabilitation*. *J Neuroeng Rehabil*, 2023. **20**(1): p. 5.
212. Oliveira, A.S., et al., *A Channel Rejection Method for Attenuating Motion-Related*

- Artifacts in EEG Recordings during Walking*. Front Neurosci, 2017. **11**: p. 225.
213. Guo, Z., et al., *Multiscale Wavelet Transfer Entropy With Application to Corticomuscular Coupling Analysis*. IEEE Trans Biomed Eng, 2022. **69**(2): p. 771-782.
214. de Vries, I.E., et al., *Functional connectivity in the neuromuscular system underlying bimanual coordination*. J Neurophysiol, 2016. **116**(6): p. 2576-2585.
215. Roeder, L., et al., *Dynamics of corticospinal motor control during overground and treadmill walking in humans*. J Neurophysiol, 2018. **120**(3): p. 1017-1031.
216. Kobayashi, T., et al., *Effects of walking speed on magnitude and symmetry of ground reaction forces in individuals with transfemoral prosthesis*. Journal of Biomechanics, 2022. **130**: p. 110845.
217. Friel, K.M., S. Chakrabarty, and J.H. Martin, *Pathophysiological mechanisms of impaired limb use and repair strategies for motor systems after unilateral injury of the developing brain*. Dev Med Child Neurol, 2013. **55 Suppl 4**: p. 27-31.
218. Delorme, A. and S. Makeig, *EEGLAB: an open source toolbox for analysis of single-trial EEG dynamics including independent component analysis*. Journal of neuroscience methods, 2004. **134**(1): p. 9-21.
219. Gramfort, A., et al., *MEG and EEG data analysis with MNE-Python*. Frontiers in neuroscience, 2013: p. 267.
220. Klug, M. and N.A. Kloosterman, *Zapline-plus: A Zapline extension for automatic and adaptive removal of frequency-specific noise artifacts in M/EEG*. Human Brain Mapping, 2022. **43**(9): p. 2743-2758.

221. Kumaravel, V.P., M. Buiatti, and E. Farella. *Hyperparameter selection for reliable EEG denoising using ASR: A benchmarking study*. IEEE.
222. Palmer, J.A., K. Kreutz-Delgado, and S. Makeig, *AMICA: An adaptive mixture of independent component analyzers with shared components*. Swartz Center for Computational Neuroscience, University of California San Diego, Tech. Rep, 2012.
223. Pion-Tonachini, L., K. Kreutz-Delgado, and S. Makeig, *ICLabel: An automated electroencephalographic independent component classifier, dataset, and website*. NeuroImage, 2019. **198**: p. 181-197.
224. Hashimoto, Y. and J. Ushiba, *EEG-based classification of imaginary left and right foot movements using beta rebound*. Clinical neurophysiology, 2013. **124**(11): p. 2153-2160.
225. Amo Usanos, C., et al., *Induced Gamma-Band Activity during Actual and Imaginary Movements: EEG Analysis*. Sensors (Basel), 2020. **20**(6).
226. Forssberg, H., S. Grillner, and J. Halbertsma, *The locomotion of the low spinal cat. I. Coordination within a hindlimb*. Acta Physiol Scand, 1980. **108**(3): p. 269-81.
227. Guertin, P.A., *Central pattern generator for locomotion: anatomical, physiological, and pathophysiological considerations*. Front Neurol, 2012. **3**: p. 183.
228. Capogrosso, M., et al., *A computational model for epidural electrical stimulation of spinal sensorimotor circuits*. J Neurosci, 2013. **33**(49): p. 19326-40.
229. Wenger, N., et al., *Closed-loop neuromodulation of spinal sensorimotor circuits controls refined locomotion after complete spinal cord injury*. Sci Transl Med, 2014. **6**(255): p. 255ra133.

230. Wenger, N., et al., *Spatiotemporal neuromodulation therapies engaging muscle synergies improve motor control after spinal cord injury*. Nat Med, 2016. **22**(2): p. 138-45.
231. Moraud, E.M., et al., *Mechanisms Underlying the Neuromodulation of Spinal Circuits for Correcting Gait and Balance Deficits after Spinal Cord Injury*. Neuron, 2016. **89**(4): p. 814-28.
232. Takeda, K., et al., *The walking and running control of a human musculoskeletal model using a low-power consumption hardware central pattern generator model*. International Journal of Advanced Robotic Systems, 2022. **19**(1): p. 17298806221080633.
233. Manoonpong, P., U. Parlitz, and F. Wörgötter, *Neural control and adaptive neural forward models for insect-like, energy-efficient, and adaptable locomotion of walking machines*. Front Neural Circuits, 2013. **7**: p. 12.
234. Kline, J.E., et al., *Isolating gait-related movement artifacts in electroencephalography during human walking*. J Neural Eng, 2015. **12**(4): p. 046022.
235. Rodríguez-González, V., et al., *Consistency of local activation parameters at sensor- and source-level in neural signals*. J Neural Eng, 2020. **17**(5): p. 056020.
236. Liu, C., et al., *Comparison of EEG Source Localization Using Simplified and Anatomically Accurate Head Models in Younger and Older Adults*. IEEE Trans Neural Syst Rehabil Eng, 2023. **31**: p. 2591-2602.